Energy Research and Development Division
FINAL PROJECT REPORT

ADVANCED POWER ELECTRONICS INTERFACE INITIATIVE

Smart Grid and Advanced Power Electronics Research and Development

Prepared for: California Energy Commission

Prepared by: National Renewable Energy Laboratory

NREL
NATIONAL RENEWABLE ENERGY LABORATORY

JUNE 2012

CEC-500-2014-006

PREPARED BY:

Primary Author(s):
William Kramer
Sudipta Chakraborty
Mariko Shirazi
Blake Lundstrom
Kevin Harrison

National Renewable Energy Laboratory
15013 Denver West Parkway
Golden, CO 80401

Contract Number: 500-05-027

Prepared for:

California Energy Commission

Steve Ghadiri
Contract Manager

Fernando Pina
Office Manager
Energy Systems Research Office

Laurie ten Hope
Deputy Director
Energy Research and Development Division

Robert P. Oglesby
Executive Director

DISCLAIMER

This report was prepared as the result of work sponsored by the California Energy Commission. It does not necessarily represent the views of the Energy Commission, its employees or the State of California. The Energy Commission, the State of California, its employees, contractors and subcontractors make no warranty, express or implied, and assume no legal liability for the information in this report; nor does any party represent that the uses of this information will not infringe upon privately owned rights. This report has not been approved or disapproved by the California Energy Commission nor has the California Energy Commission passed upon the accuracy or adequacy of the information in this report.

ACKNOWLEDGEMENTS

- The authors gratefully acknowledge Mike Gravely, Steve Ghadiri and Bernard Treanton from the California Energy Commission for their guidance and support.
- We also thank Robert Hansen from the National Renewable Energy Laboratory for his help in building inverter hardware.
- We thank Danny Martin of the National Renewable Energy Laboratory for his help in cost analysis that were performed.

PREFACE

The California Energy Commission Energy Research and Development Division supports public interest energy research and development that will help improve the quality of life in California by bringing environmentally safe, affordable, and reliable energy services and products to the marketplace.

The Energy Research and Development Division conducts public interest research, development, and demonstration (RD&D) projects to benefit California.

The Energy Research and Development Division strives to conduct the most promising public interest energy research by partnering with RD&D entities, including individuals, businesses, utilities, and public or private research institutions.

Energy Research and Development Division funding efforts are focused on the following RD&D program areas:

- Buildings End-Use Energy Efficiency
- Energy Innovations Small Grants
- Energy-Related Environmental Research
- Energy Systems Integration
- Environmentally Preferred Advanced Generation
- Industrial/ Agricultural/ Water End-Use Energy Efficiency
- Renewable Energy Technologies
- Transportation

Advanced Power Electronics Interface (APEI) Initiative: Smart Grid and Advanced Power Electronics Research and Development is the final report for the Advanced Power Electronic Interface (APEI) Initiative project (contract number 500-05-027) conducted by National Renewable Energy Laboratory.]. The information from this project contributes to Energy Research and Development Division's Energy Systems Integration Program.

For more information about the Energy Research and Development Division, please visit the Energy Commission's website at www.energy.ca.gov/ research/ or contact the Energy Commission at 916-327-1551.

ABSTRACT

Integrating renewable energy and distributed generation into the Smart Grid requires power electronic interfaces for energy conversion. A key to successful Smart Grid implementation is to use interoperable, intelligent, and advanced power electronics technology that improves and accelerates the use of distributed energy resource systems. The Advanced Power Electronic Interface initiative developed a standardized, highly integrated power electronics interconnection device that applied to distributed energy and the Smart Grid. This report highlights the project "The Smart Grid and Advanced Power Electronics Research and Development for Mid Power up to 100 kW" and discusses: development of low-power preproduction Advanced Power Electronics Interfaces; design and development of mid-power 50 kilowatt power blocks; development of an advanced controller board and wireless user interface for the power blocks; design and development of a three-phase inverter with power block, and testing and demonstration of selected IEEE 1547, Standard for Interconnecting Distributed Resources with Electric Power Systems and advanced inverter functionalities. The report provides descriptions and laboratory test data on both low-power and mid-power advanced power electronic interfaces, and it describes the benefits of applying systems integration to advanced renewable and distributed energy technology applications for the Smart Grid. The results demonstrated how advanced power electronic systems and controls can support the California Energy Commission's objectives to improve energy cost and value as well as the reliability and quality of California's electricity.

Keywords: California Energy Commission, National Renewable Energy Laboratory, NREL, advanced power electronics interface, APEI, modular power block, PV inverter, Smart Grid, inverter, MPPT, maximum power point tracking, IEEE Std 1547, island detection.

Please use the following citation for this report:

Kramer W, Chakraborty S, Shirazi M, Lundstrom B, Harrison K. (National Renewable Energy Laboratory). 2012. Advanced Power Electronics Interface (APEI) Initiative: Smart Grid and Advanced Power Electronics Research and Development. California Energy Commission. Publication number: CEC-500-2014-006.

TABLE OF CONTENTS

Acknowledgements i

PREFACE ii

ABSTRACT iii

TABLE OF CONTENTS iv

LIST OF FIGURES vi

LIST OF TABLES viii

EXECUTIVE SUMMARY 1

Introduction 1

Project Purpose 1

Project Results 1

Project Benefits 2

CHAPTER 1: Low-Power APEI – US Hybrid 3

1.1 APEI Description 3

1.2 Advanced Control Description 4

1.3 Test Results 5

1.4 Four-Quadrant P-Q Operation Tests 5

1.4.1 Test Configuration 5

1.4.2 Test Results 5

1.4.3 Test Discussion 13

1.5 MPPT and DC Bus Regulation Tests 14

1.5.1 Test Configuration 14

1.5.2 Test Results 14

1.5.3 Test Discussion 20

1.6 Island Detection Tests 20

1.6.1 Test Configuration 20

1.6.2 Test Results 21

1.6.3 Test Discussion 27

1.7 Conclusion 27
CHAPTER 2: Low-Power APEI – UQM Technologies 28
2.1 Development of APEI Prototype 28
2.1.1 UQM AC120-5KL DC-AC Prototype Modification and Delivery 29
2.1.2 NREL Performance Verification Testing 35
2.1.3 NREL Development towards an APEI Prototype 37
2.1.4 Field Testing of APEI Prototypes 45
2.2 Conclusion 46
CHAPTER 3: Mid-Power APEI 47
3.1 Power Block Pre-production Prototype 48
3.2 Advanced Controller Board Prototype 49
3.3 Graphical User Interface 50
3.4 Connector Board 54
3.5 Test Setup 55
3.5.1 Three-Phase Inverter 55
3.5.2 Inverter Test Setup 58
3.6 Test Results 59
3.6.1 Basic Grid-tied Inverter Operation 60
3.6.2 IEEE 1547 Interconnection 63
3.6.3 Advanced Functionalities 66
3.7 Cost Analysis 71
3.8 Field Demonstration 73
3.9 Conclusion 73
CHAPTER 4: Energy Technologies – Moving Forward 75
4.1. Renewable Electricity 75
4.2 Distributed Energy 75
4.3 Energy Storage 76
4.4 Transportation 77

4.5 Smart Grid 77

4.6 Systems Integration 78

REFERENCES 80

GLOSSARY 81

LIST OF FIGURES

Figure 1. US Hybrid APEI Prototype Test Setup at NREL 3
Figure 2. Iref = 0 A 6
Figure 3. Iref = 3.5 Arms @ 0° (P > 0, Q = 0) 7
Figure 4. Iref =3.5 Arms @ 90° (P = 0, Q > 0) 7
Figure 5. Iref =3.5 Arms @ 180° (P < 0, Q = 0) 8
Figure 6. Iref =3.5 Arms @ -90° (P = 0, Q < 0) 8
Figure 7. Iref =20 Arms @ 0° (P > 0, Q = 0) 9
Figure 8. Iref =20 Arms @ 45° (P > 0, Q > 0) 9
Figure 9. Iref =20 Arms @ 90° (P = 0, Q > 0) 10
Figure 10. Iref =20 Arms @ 135° (P < 0, Q > 0) 10
Figure 11. Iref =20 Arms @ 180° (P < 0, Q = 0) 11
Figure 12. Iref =20 Arms @ -135° (P < 0, Q < 0) 11
Figure 13. Iref =20 Arms @ -90° (P = 0, Q < 0) 12
Figure 14. Iref =20 Arms @ -45° (P > 0, Q < 0) 12
Figure 15. Steady-state, RMS waveforms, timescale = 1s/div 15
Figure 16. Steady-state, instantaneous waveforms with zoom, timescale = 1 s/div (full), 10 ms/div (zoom) 16
Figure 17. PV Start-Up, RMS waveforms, timescale = 1s/div 16
Figure 18. PV Start-Up, instantaneous waveforms, timescale = 1 s/div 17
Figure 19. PV Start-Up, RMS waveforms with zoom of complete start-up, timescale = 1 s/div (full), 200 ms/div (zoom) 17
Figure 20. PV Start-Up, inst. waveforms with zoom of complete start-up, timescale = 1 s/div (full), 200 ms/div (zoom) 18
Figure 21. PV Start-Up, inst. waveforms, zoom at closure of PV disconnect, timescale = 1s/div (full), 100 μs/div (zoom) 18
Figure 22. PV Start-Up, inst. waveforms, zoom at closure of PV contactor, timescale = 1s/div (full), 500 μs/div (zoom) 19
Figure 23. PV Start-Up, inst. waveforms, zoom of DC Bus ramp, timescale = 1s/div (full), 100 ms/div (zoom) 19
Figure 24. PV Start-Up, inst. waveforms, zoom MPPT reset, DC-AC enable, and MPPT re-start, timescale = 1s/div (full), 200 ms/div (zoom) 20
Figure 25. Island detection test results – RLC elements cold (initial island frequency slightly less than 60 Hz) 22
Figure 26. Island detection test results – RLC elements hot (initial island frequency slightly greater than 60 Hz) 25

Figure 27. Steady-state waveforms while grid-connected 26
Figure 28. UQM AC120-5KL DC-AC Inverter Prototype Unit 29
Figure 29. UQM AC120-5KL DC-AC Inverter Prototype Specifications 31
Figure 30. The AC120-5KL DC-AC Inverter Prototype with Cooling System 32
Figure 31. Test Setup for UQM Factory Test of Inverter Prototype 32
Figure 32. Electrical Output of the AC120-5KL Prototype Unit over 50 ms during a 1 Hour Thermal Test of the Inverter Running at Full Power 33
Figure 33. Thermal Response of the AC120-5KL Prototype during the 1 Hour Test 34
Figure 34. Electrical Efficiency versus Loading of the AC120-5KL Prototype during the 1 Hour Test 35
Figure 35. Physical Test Setup for NREL Evaluation of UQM Inverter Prototype 36
Figure 36. Oscilloscope Data for the Inverter Operating at PAC = 1.12 kW 36
Figure 37. Oscilloscope Data for the Inverter Operating at PAC = 1.58 kW 37
Figure 38. Oscilloscope Data for the Inverter Operating at PAC = 3.06 kW 37
Figure 39. Controller-in-the-Loop Paradigm 38
Figure 40. Inside of the APEI Unit's Enclosure Showing the Inverter, Isolation Transformer, Cooling Systems, and Auxiliary Power Supply 40
Figure 41. Front View of the APEI Unit's Enclosure, Highlighting the HMI 41
Figure 42. The Grid Interconnection Unit, which Houses the Electrical Protection Devices and Interfaces to the Solar Panels (DC Input) and Electric Power System (AC Output) 42
Figure 43. Blind-mating Plug System that Interfaces the APEI and Grid Interconnection Units. 43
Figure 44. The Rack Support System, which Holds the APEI and Grid Interconnection Units Together 44
Figure 45. The Final Installation of an APEI System (Only 1 APEI Unit is Included in this Installation) 45
Figure 46. Picture of 50 kW power block without controller 48
Figure 47. 50 kW power block with controller mounted on a backplane 49
Figure 48. Advanced controller board for 50 kW power block (a) sbRIO side, (b) connector side 50
Figure 49. (a) NREL developed native iPad application for power block-based inverter system, (b) screen showing system status 51
Figure 50. (a) Password-protected control mode change screen, (b) screen showing different control modes and set points 51
Figure 51. (a) Screen showing various measurements, (b) screen showing data storing options 53
Figure 52. Connector board (a) controller board side, (b) user connector side 54
Figure 53. Front side of the NREL-developed inverter 56
Figure 54. Front side of the inverter cabinet – inside view 57
Figure 55. Back side of the inverter cabinet – inside view 58
Figure 56. Diagram of the inverter test setup at NREL 59
Figure 57. Grid-tied inverter at UPF with different peak current reference set points (a) 0 A pk, (b) 20 Apk, (c) 40 Apk, (d) 60 Apk, (e) 80 Apk, (f) 118 Apk 61
Figure 58. Start-up current transients for different peak current reference set points (a) 0 A pk, (b) 20 Apk, (c) 50 Apk 62

Figure 59. Over frequency trip times for different trip delays (a) trip time 30.2ms for a trip delay of 10ms, (b) trip time 54.3ms for a trip delay of 33ms, (c) trip time 100.1ms for a trip delay of 80ms 64
Figure 60. Under frequency trip times for different trip delays (a) trip time 29.8ms for a trip delay of 10ms, (b) trip time 53.1ms for a trip delay of 33ms, (c) trip time 99.8ms for a trip delay of 80ms 64
Figure 61. Islanded condition without any active island detection (a) zoomed at the time of grid trip, (b) zoomed at the end of window showing island continues 4 seconds after grid trip 65
Figure 62. Detection of island condition using island detection algorithm and subsequent inverter tripping 66
Figure 63. Grid-tied inverter with current reference set at 40 Apk with different phase angles (a) 0°, (b) 45°, (c) 90°, (d) 135°, (e) 180°, (f) -135°, (g) -90°, (h) -45° 68
Figure 64. Inverter's continued operation during a LFRT event (a) response of the inverter, (b) zoomed at the time of step change from 60 Hz to 59.5 Hz (c) zoomed at the time of step change back to 60 Hz 70
Figure 65. NREL-developed inverter material price with varying quantities 72
Figure 66. Estimated single inverter cost breakdown for quantities of one thousand (estimates assume using same parts as in NREL prototype inverters) 72

LIST OF TABLES

Table 1. 4-quadrant PQ operation test summary 13
Table 2. Key Features of the UQM AC120-5KL DC-AC Inverter Prototype Unit 30

EXECUTIVE SUMMARY

Introduction

The Smart Grid is a modern power grid combined with an intelligent and secure two-way digital communication technology for devices associated with the electric utility grid. It has many benefits, including more cost-effective and more efficient energy usage and reduced greenhouse gas emissions. The Smart Grid also has its challenges, such as integrating renewable energy from wind and solar resources into the larger energy mix. Because of this, Smart Grids require advanced technology systems enable their successful implementation. Most devices currently available are designed for specific technologies. For example, ordinary photovoltaic inverter systems, which are photovoltaic electrical power converters, can only connect solar energy to the grid, and they are not usually compatible with other distributed energy resources or renewable energy applications. Making a device that is universal and accepted in multiple applications would reduce overall product cost because of higher production scales.

Project Purpose

The goal of the Advanced Power Electronic Interface initiative was to design power devices for standardized, highly integrated technologies for connecting distributed energy resources to the grid. Development of such intelligent technology devices will improve and accelerate the use of distributed energy resource systems and help successfully implement Smart Grid elements at the distribution level.

The specific objective of this project was to demonstrate the feasibility of operating a basic, single-phase and three-phase photovoltaic inverter that is tied to the grid and can connect different renewable distributed energy resources on the grid. The researchers believed that this advanced power electronic interface was highly reliable, low-cost, modular, scalable, and capable of seamless grid-connection and standalone operation. This objective addressed transmission, distribution, and Smart Grid applications, pre-production and pilot-scale advanced power electronics up to 100 kilowatts (kWs), systems integration, and codes and standards for the Smart Grid.

Project Results

This project successfully used systems integration techniques to develop a single-phase 6.6 kW inverter and a three–phase 50 kW inverter that were low-cost and connected to the grid. The inverter was an advanced power electronic interface that could be used for both industrial and distributed power generation applications. The design included generic control and measurement interfaces that could be used for multiple applications, as well as a field programmable gate array-based controller that could be programmed with user-friendly wireless software development systems. An operator can view real-time measurements of the power block, control the mode of operation and photovoltaic inverter settings, and export customized data through this wireless control and monitoring system.

This application demonstrated how modular power block based power electronics could be seamlessly integrated into a Smart Grid monitoring and control framework. In addition, the system could provide advanced functionality including voltage control and active and reactive power, dynamic voltage regulation, and charge/ discharge operations for grid-tied battery energy storage. This project showed the feasibility of introducing a low-cost, highly reliable power block that could be produced in high volumes for use in many power electronic

applications. This in turn could reduce the production cost for future distributed energy resource products through larger economies of scale.

At the conclusion of this project, the power block and controller board contractors were ready to manufacture their respective advanced power electronic components. Future work could include further hardware and software development and any redesign as necessary to conduct field testing of the mid-power systems before moving the mid-power technology to full-scale production.

Project Benefits

This project demonstrated how advanced power electronic systems and controls can support the California Energy Commission’s objectives to improve energy cost and value as well as the reliability and quality of California's electricity.

Chapter 1:
Low-Power APEI – US Hybrid

US Hybrid (USH) Corporation was one of two companies that were selected for the APEI Initiative RFP. USH leveraged their experience designing, manufacturing, and marketing power electronics for vehicle applications. A functional 6.6 kW DC-AC APEI prototype with low-level control interface was delivered to NREL's Distributed Energy Resources Test Facility (DERTF) in March 2012. The contractor could not deliver a working grid-tied PV inverter. In order to successfully complete NREL's deliverable with CEC to demonstrate a working residential grid-tied PV system, with CEC Project management support, NREL engineers developed proprietary control algorithms that interfaced to the contractor's low-level controls in order to demonstrate that the USH APEI could be controlled as a grid-connected PV Inverter. After receipt of the contractors working APEI prototype and working low-level control interfaces, NREL interfaced NREL's proprietary control algorithms to each of the contractor low-level control interfaces. Laboratory testing of the USH APEI were conducted. This section provides a summary of the APEI technology and laboratory testing. The test results showed that with further development, the US Hybrid's APEI shows excellent potential to operate as a single-phase grid-tied PV inverter without the need of an isolation transformer. Test results show that the APEI has the potential to provide advanced functionality such as VAR, LVRT and voltage support to the grid at the distribution level. In addition the USH APEI design can be used in other applications including fuel cell and grid-tied battery applications.

1.1 APEI Description

The USH 6.6 kW APEI power stage is a two-stage design, with high frequency isolated DC-DC converter front end, center-tapped DC bus, and H-bridge inverter. The isolated DC-DC stage eliminates the need for a line frequency transformer and also provides a DC connection for other DC-based distributed energy resources (DER) such as fuel cells or batteries. The APEI control platform uses analog circuitry to regulate converter currents/ voltages to provide converter protective functions, and a digital signal processor (DSP) that can be used to provide higher-level control functions. The APEI design and topology can provide both high-bandwidth operation (via the analog control loops) and the integration of advanced control algorithms and functionality (via the DSP). In general, the USH prototype APEI is designed to accept an 80 to 150 V DC input and is recommended not to operate over 7.2 kW DC. The AC output is designed to connect to a single-phase 220V AC grid connection and operate at a maximum power of 6.6 kW. The expected operating temperature of the APEI is -25 to 60 °C and expected operating humidity from 0 to 100 percent. A photograph of a prototype US Hybrid Advanced Power Electronic Interface under test at NREL is shown in the figure below:

Figure 1. US Hybrid APEI Prototype Test Setup at NREL

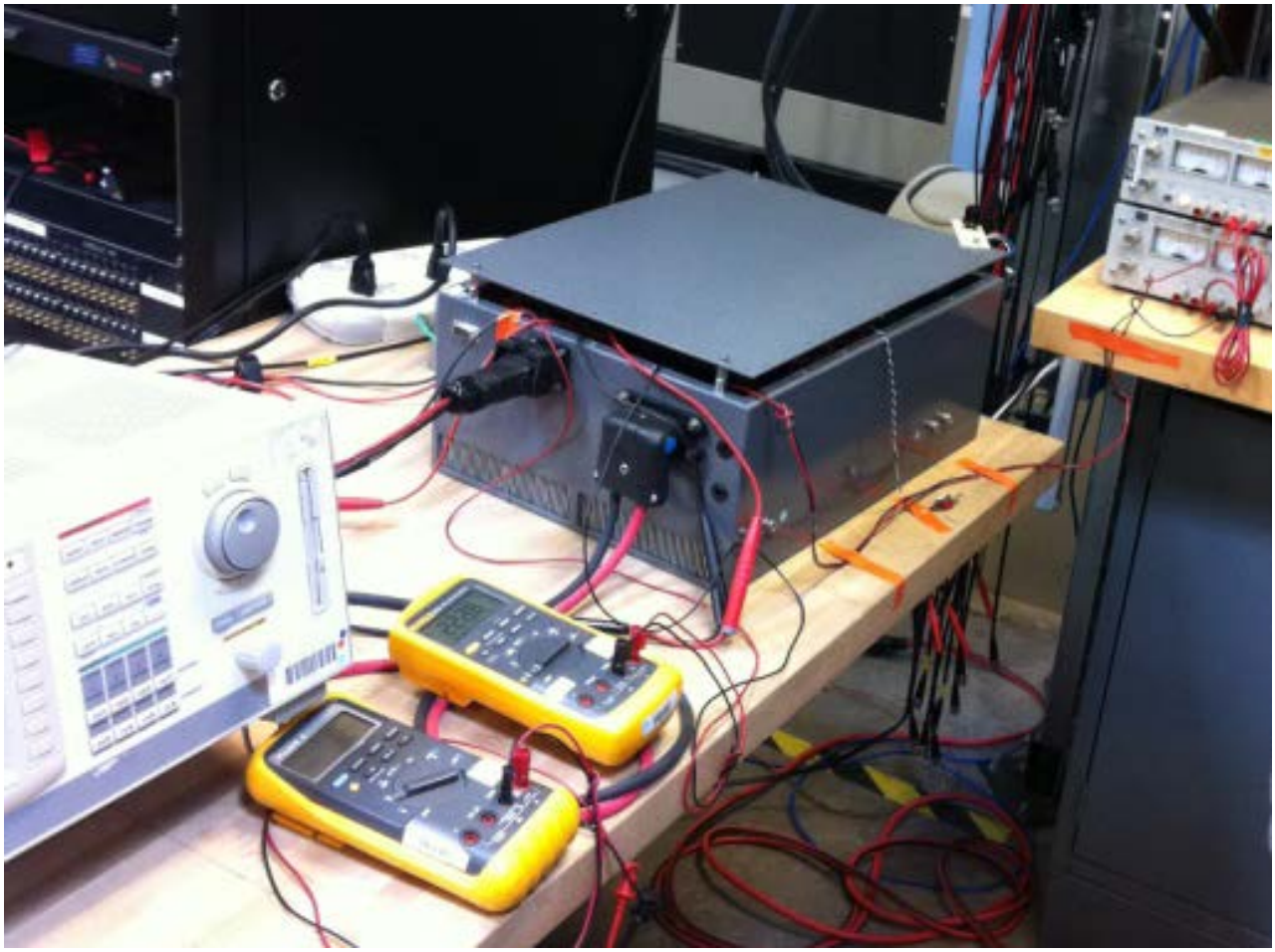

1.2 Advanced Control Description

The low-level (inner) analog control loops in the USH APEI converter directly control the current input to DC-DC stage, and the AC current output of the DC-AC stage, with analog reference waveforms as provided by the DSP via a digital-to-analog converter (DAC). In order to successfully complete NREL's deliverable with CEC to demonstrate a working residential grid-tied PV system, with CEC Project management support, NREL engineers developed proprietary control algorithms that interfaced to the contractor's low-level controls in order to demonstrate that the USH APEI could be controlled as a grid-connected PV Inverter. After receipt of the contractors working APEI prototype and working low-level control interfaces, NREL interfaced NREL's proprietary control algorithms through the contractor provided low-level control interfaces. Specifically, for the DC-DC converter, a proprietary algorithm was used to control MPPT. For the DC-AC converter, NREL proprietary algorithms were used to generate the AC current reference waveform in order to regulate the DC bus at 400 V. NREL also used their digital phase lock loop (PLL) algorithms to generate the reference AC current waveform and an NREL proprietary algorithm control the APEI for full 4-quadrant P-Q (real and reactive power) operation. Finally, additional NREL algorithms were implemented to safely charge the DC bus to its rated voltage at start up to ensure a smooth connection to the grid.

NREL provided NREL's proprietary control algorithms in order to demonstrate the ability of USHybrid's DC-AC platform to provide IEEE Std 1547 compliance. The high level algorithms were implemented in order to actively detect unintentional islanding conditions and to ensure the delivered APEI could disconnect and re-connect to the grid within voltage and frequency ranges as specified in IEEE Std 1547. The disconnect/ connect algorithms that used adjustable set points and time delays for frequency and voltage. In addition, the disconnect algorithms included both fast and slow disconnect settings.

NREL's proprietary algorithms were implemented using the Mathwork's Matlab/ Simulink software tool chain. NREL's Object oriented Simulink code was converted to C-code by NREL using Mathwork's Simulink Coder software and the resultant C code was integrated by NREL into the USH core DSP low-level hardware control using Texas Instruments' Code Composer Studio software. In order to maintain NREL's code as confidential, NREL staff maintained sole control of the software code and software integration efforts were performed by NREL staff on NREL computational resources.

1.3 Test Results

Advanced functionality testing was performed on the USH DC-AC converter in three phases:

- 4-Quadrant P-Q Operation
- MPPT and DC Bus Regulation
- Island Detection

The 4-quadrant P-Q Operation testing was performed to demonstrate the USH APEI hardware capability using NREL's digital PLL and reference current waveform generation. A fourth and final phase testing of the IEEE STD 1547-disconnect/ connect algorithms was planned but not performed due to time constraints. However, these algorithms consist of straightforward comparisons and time delay counters and there are no anticipated challenges to their successful operation using the USHybrid APEI platform.

1.4 Four-Quadrant P-Q Operation Tests

1.4.1 Test Configuration

The 4-quadrant P-Q tests of the USH converter (DC-AC stage) were performed with the DC-DC stage disabled. Instead, an external DC power supply was connected directly to the converter DC bus. The test configuration is described below:

- AreoEnvironment AV-900 regulating DC bus at 380 V (capable of bi-directional current flow)
- Pacific Power Grid Simulator regulating AC bus at 60 Hz, 220 Vrms
- Load bank to provide AC load (since grid simulator not bi-directional)
- NREL PLL locking to sensed VAC, and providing IAC waveform reference based on user-specified amplitude and phase angle

1.4.2 Test Results

Tests were performed at current amplitudes of 3.5 Arms at phase angles of 0°, 90°, 180°, and -90° and 20 Arms and at phase angles of 0°, 45°, 90°, 135°, 180°, -135°, -90°, and -45°. The 3.5

Arms corresponds to 10 percent rated power, while the 20 Arms corresponds to 75 percent rated output power (tests were not performed at 100 percent rated output power due to spikes in AC current command described in the Test Discussion). In addition, one test was performed at a reference current of 0 A. Steady-state waveforms were captured at all operating points showing the DC voltage (*VDC*), AC voltage (*VAC*), AC current waveform command from the DAC (*IAC CMD*), and the actual AC current (*IAC*).

Figure 2 shows the results for reference current of 0 A, Figure 3 - Figure 6 show the results for reference current of 3.5 Arms, and Figure 7 - Figure 14 show the results for reference current of 20 Arms. The timescale for all plots is 10 ms/ div. The y-axis legend and scale is displayed below:

Magenta = *VDC* (50 V/ div)
Red = *VAC* (100 V/ div)
Pink = *IAC CMD* (equivalent 10.6 A/ div)
Orange = *IAC* (10 A/ div)

Figure 2. Iref = 0 A

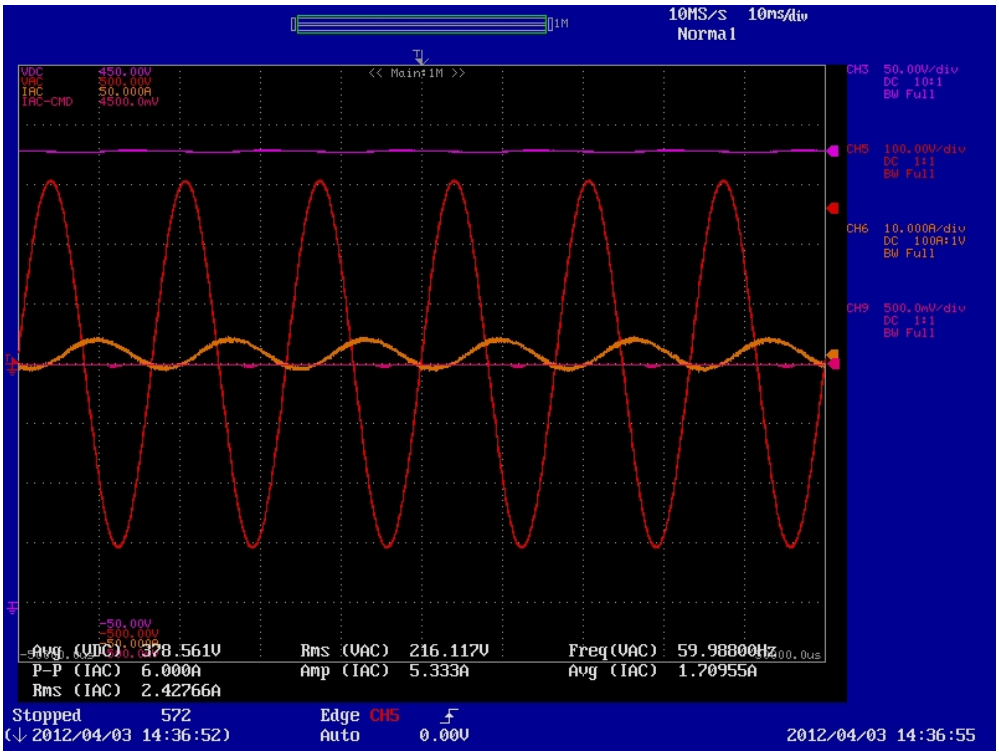

Figure 3. Iref = 3.5 Arms @ 0° (P > 0, Q = 0)

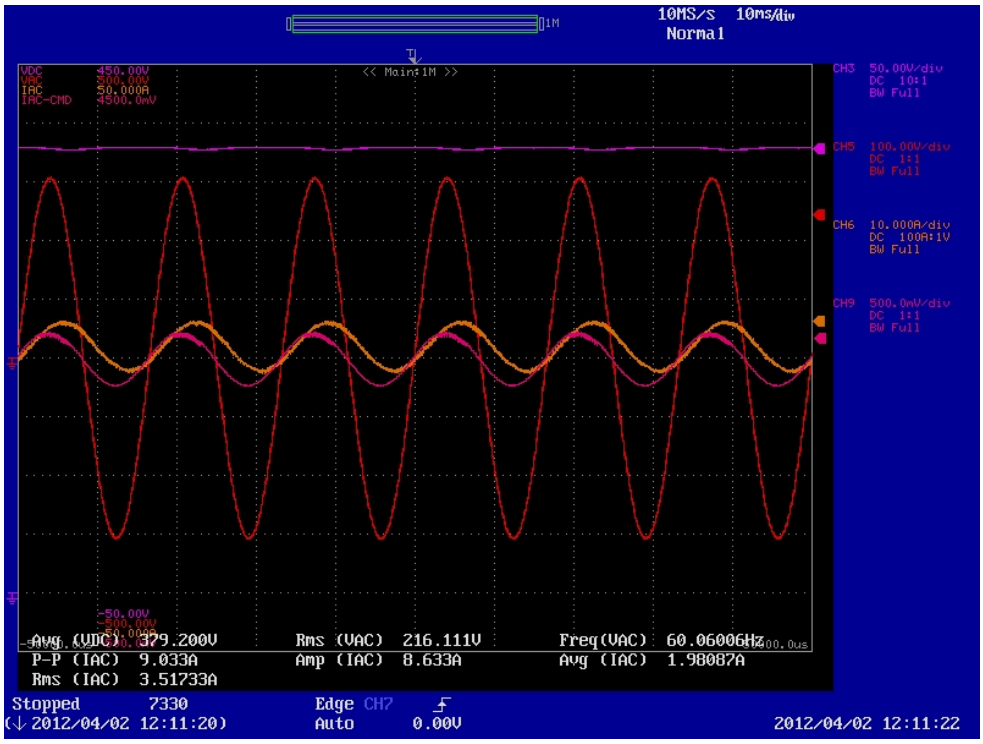

Figure 4. Iref =3.5 Arms @ 90° (P = 0, Q > 0)

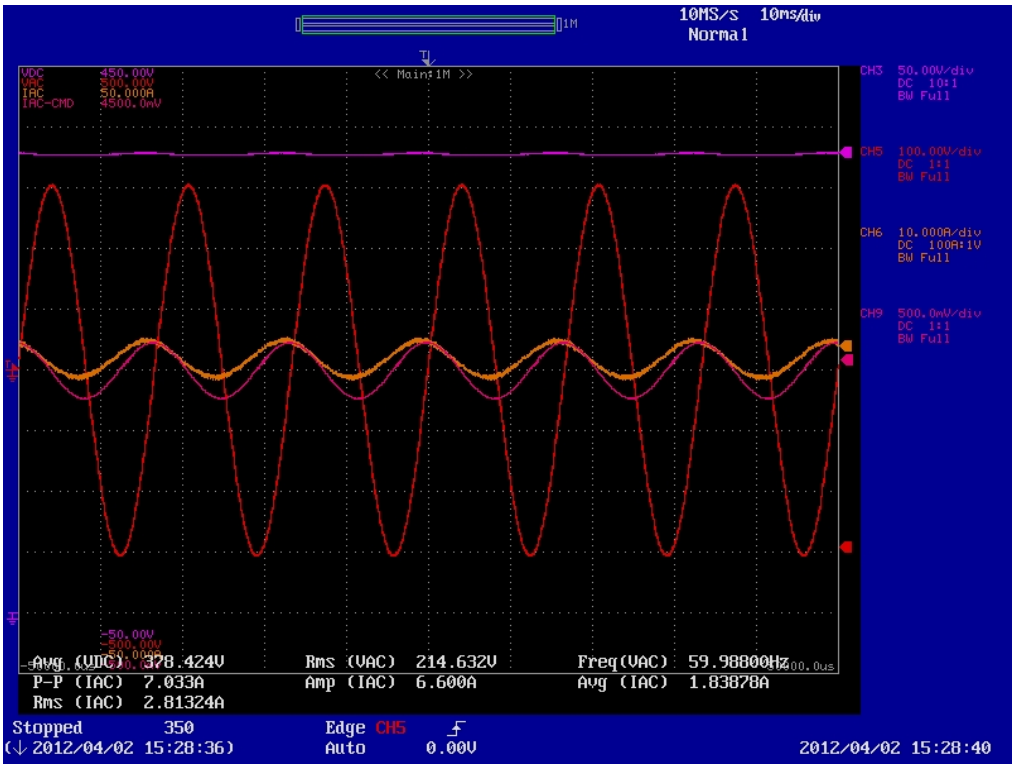

Figure 5. Iref =3.5 Arms @ 180° (P < 0, Q = 0)

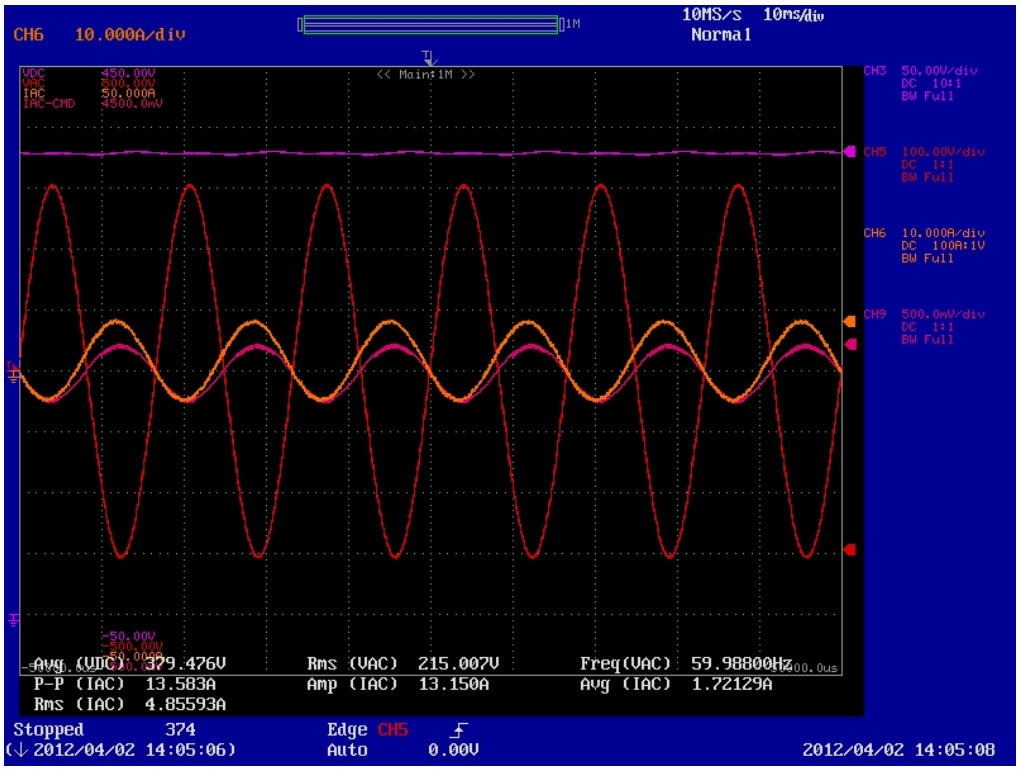

Figure 6. Iref =3.5 Arms @ -90° (P = 0, Q < 0)

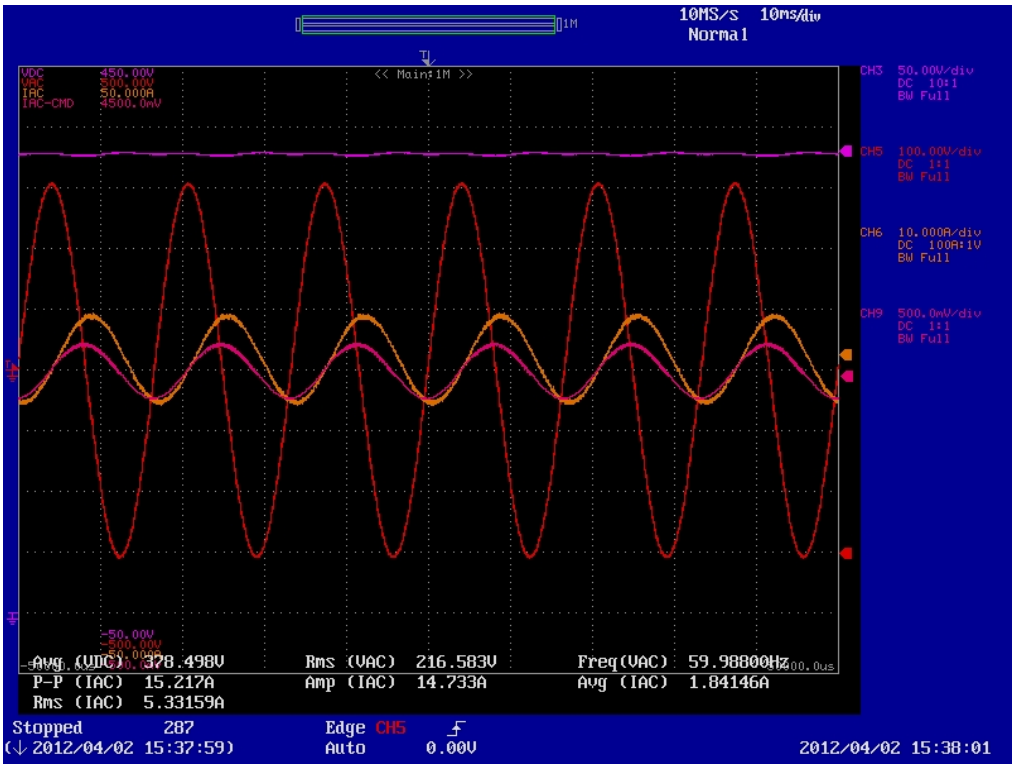

Figure 7. Iref =20 Arms @ 0° (P > 0, Q = 0)

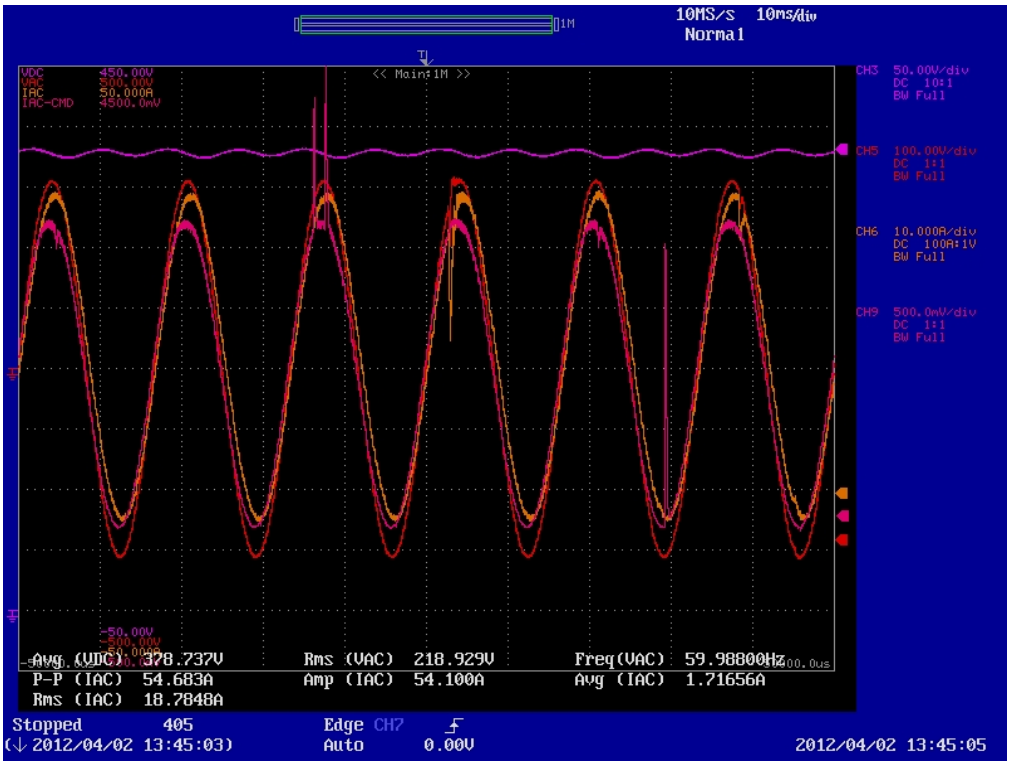

Figure 8. Iref =20 Arms @ 45° (P > 0, Q > 0)

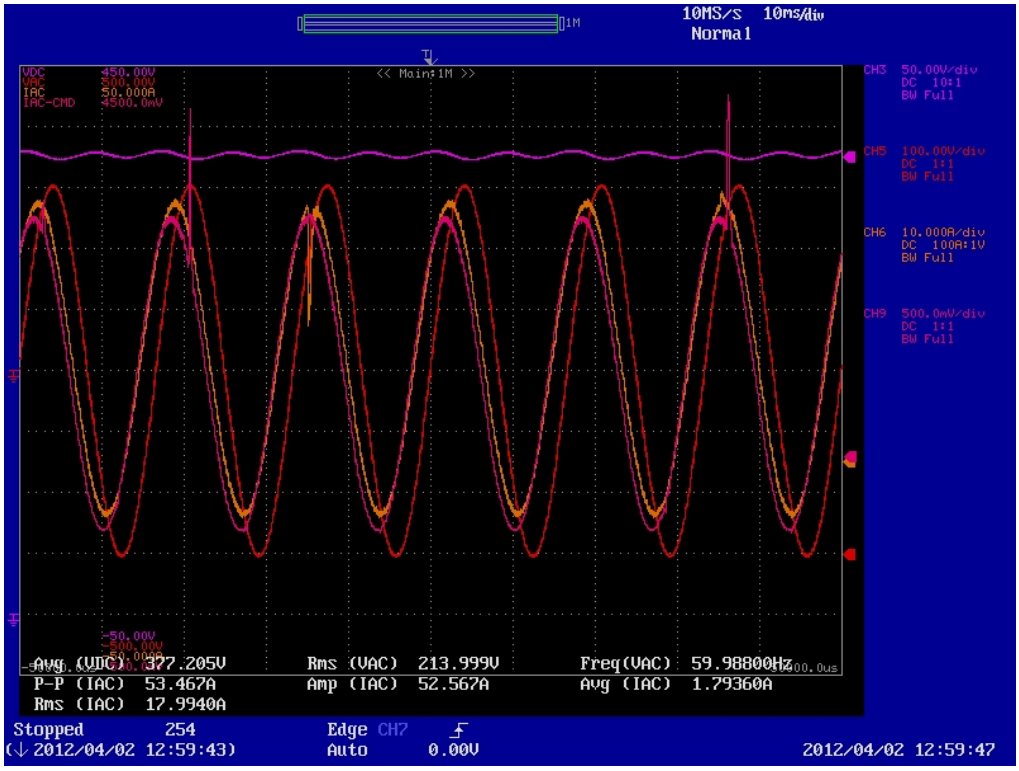

Figure 9. Iref =20 Arms @ 90° (P = 0, Q > 0)

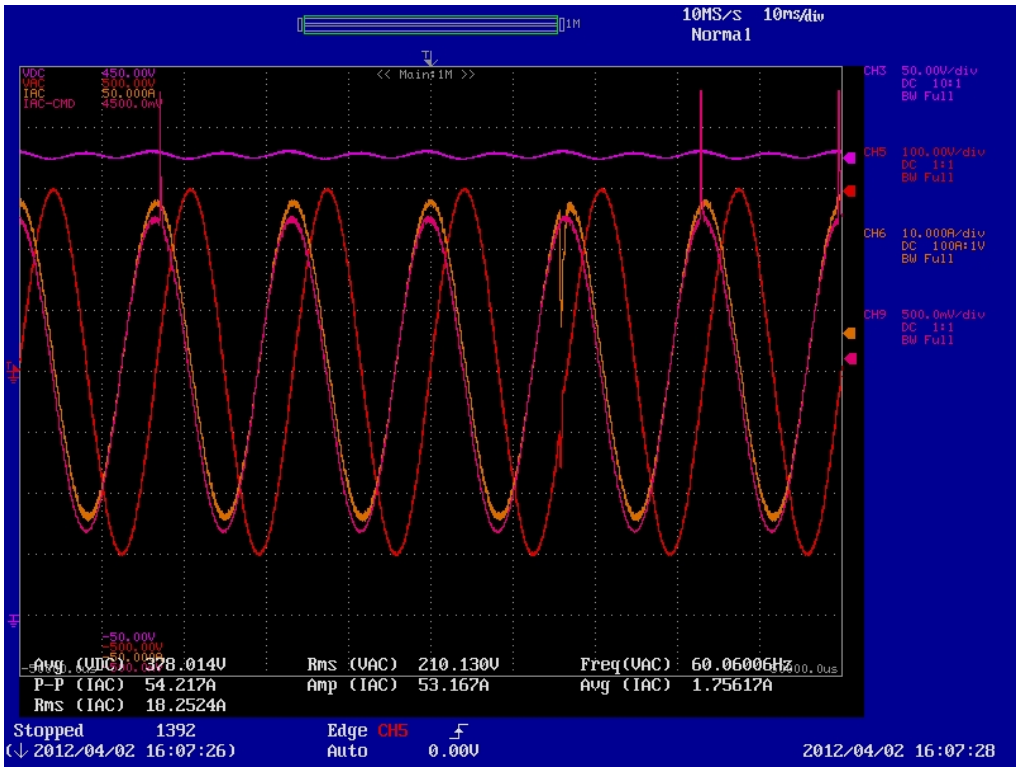

Figure 10. Iref =20 Arms @ 135° (P < 0, Q > 0)

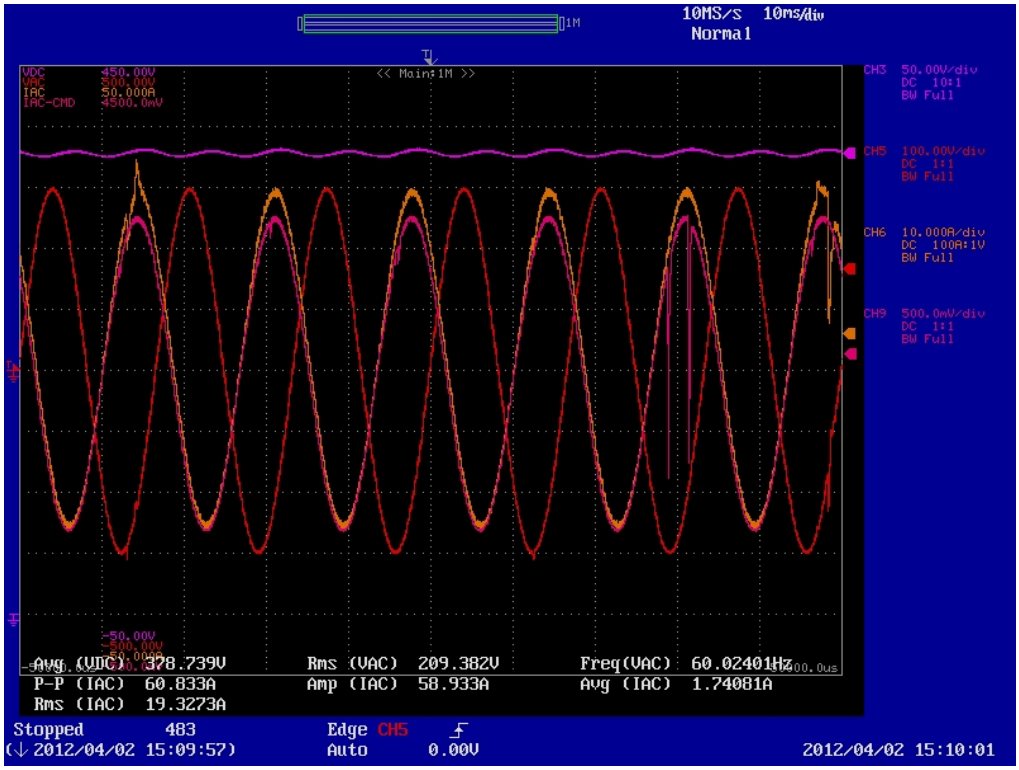

Figure 11. Iref =20 Arms @ 180° (P < 0, Q = 0)

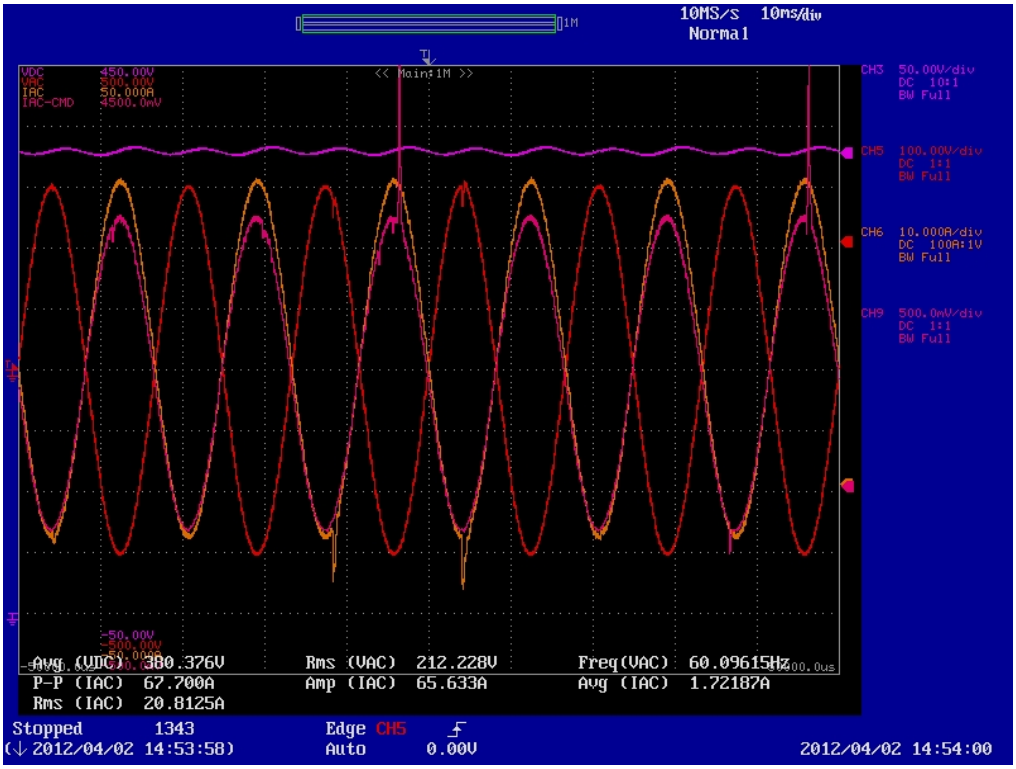

Figure 12. Iref =20 Arms @ -135° (P < 0, Q < 0)

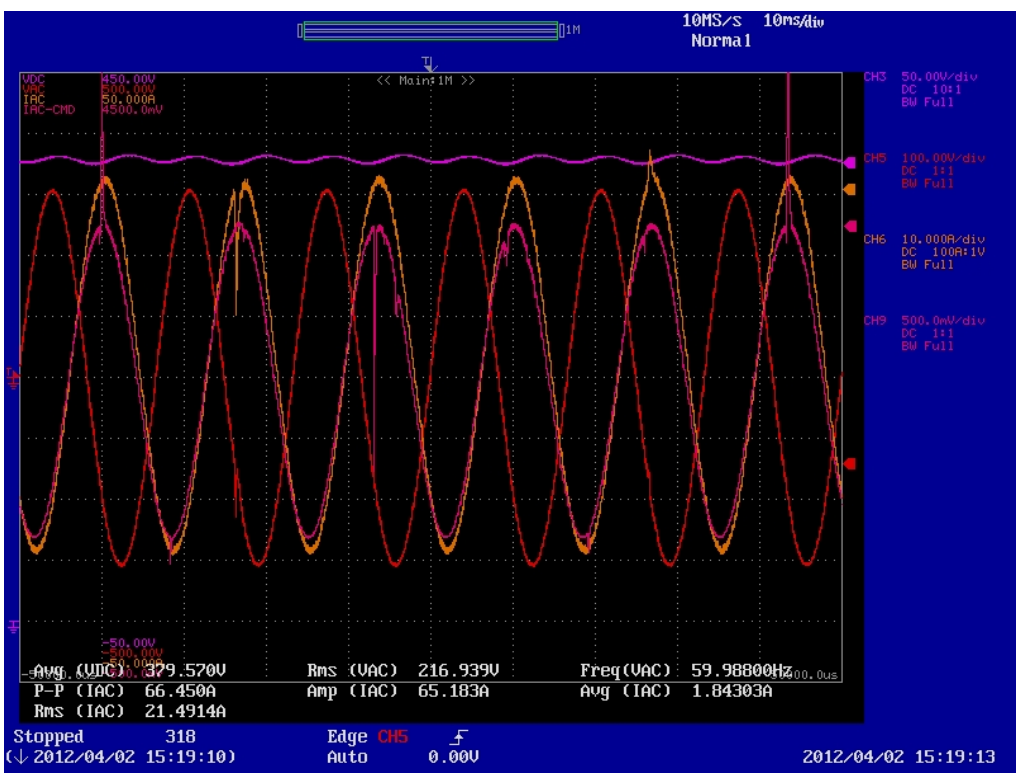

Figure 13. Iref =20 Arms @ -90° (P = 0, Q < 0)

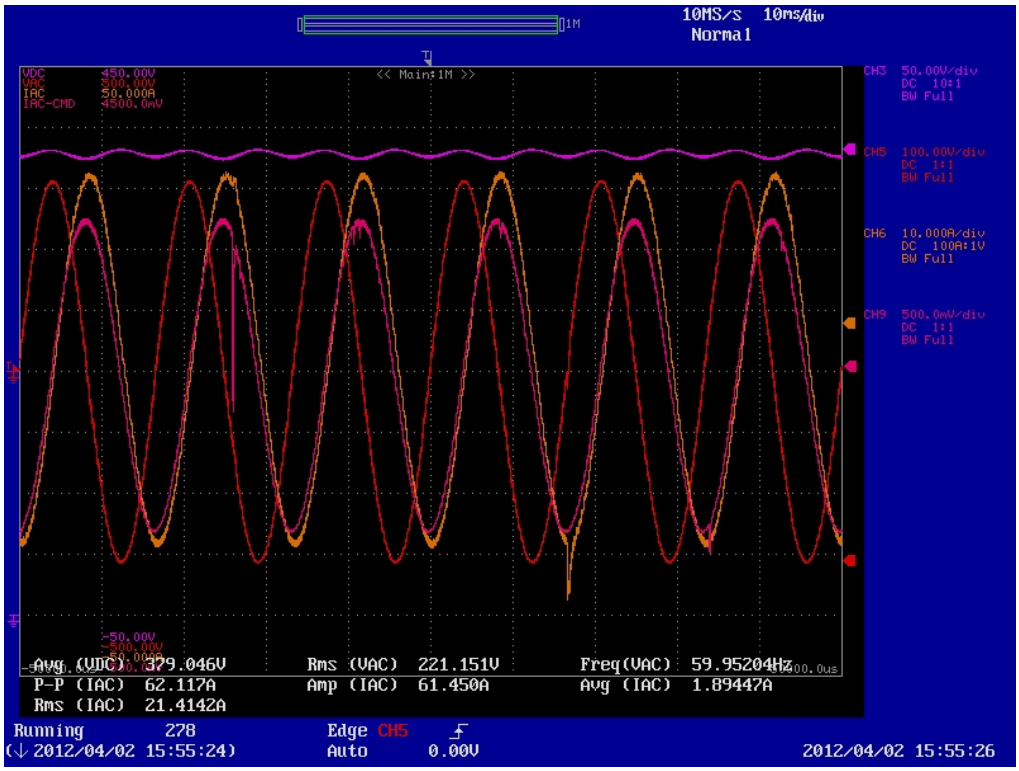

Figure 14. Iref =20 Arms @ -45° (P > 0, Q < 0)

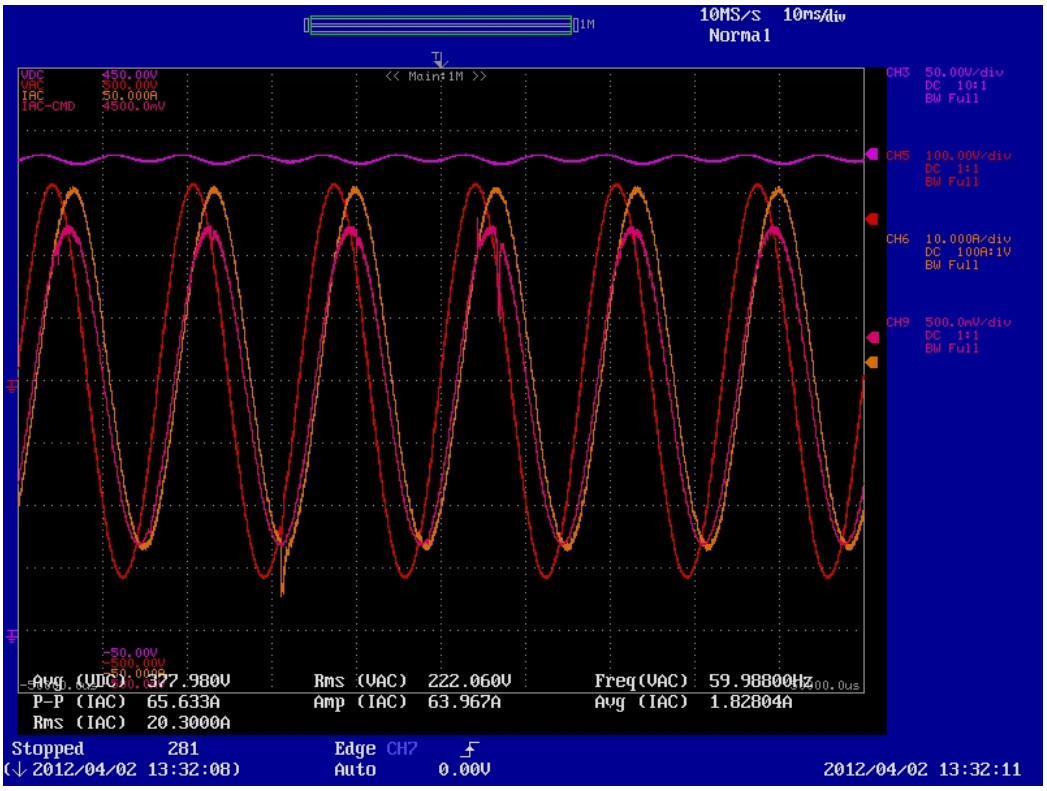

1.4.3 Test Discussion

The results of Figure 2 - Figure 14 are summarized below in Table 2.

Table 1. 4-quadrant PQ operation test summary

Id_ref [A]	Iq_ref [A]	Expected		Measured		
		Iref_magpk [A]	Iref_phase [°]	I_magpk [A]	I_phase [°]	DC offset [A]
0	0	0	0	2.4	-125	1.71
5	0	5	0	4.2	Not meas.	1.98
0	5	5	90	3.1	Not meas.	1.84
-5	0	5	180	6.5	Not meas.	1.72
0	-5	5	-90	7.0	Not meas.	1.84
28.3	0	28.3	0	26.8	-10.2	1.72
20	20	28.3	45	25.3	38.9	1.79
0	28.3	28.3	90	26.0	86.4	1.76
-20	20	28.3	135	27.5	134	1.74
-28.3	0	28.3	180	29.3	180	1.72
-20	-20	28.3	-135	30.2	-138	1.84
0	-28.3	28.3	-90	30.2	-97.2	1.89
20	-20	28.3	-45	28.5	-59.2	1.73

The 4-quadrant PQ operation tests verified the ability of the USH APEI to operate at any arbitrary phase angle using NREL's PLL. This is necessary for proper operation of both the DC bus regulation and the IEEE STD 1547 island detection algorithms. In addition, the results demonstrated the ability of the converter to track the amplitude and phase angle of the commanded current. Most of the observed discrepancy between commanded and actual current magnitude and phase angle can be attributed to excitation of the output filter. However, the tests did illuminate several problems that would need to be addressed in future USH designs in order for the APEI to operate as an Inverter:

- DC offset in actual current output of approximately 1.8 A was observed during testing It should be noted that it is this DC offset, not the inability of the USH APEI to track phase angle, which is responsible for the apparent phase shift in commanded vs. actual output current at low power
- Spikes in AC current waveform command, resulting in spikes in the actual measured output current, were observed. The spikes were likely introduced by board-level noise at higher power levels.

1.5 MPPT and DC Bus Regulation Tests

1.5.1 Test Configuration

The MPPT and DC Bus Regulation tests were performed on the complete system, DC-DC stage and DC-AC stage. The test configuration is described below:

- 5.0 kW PV array connected to PV input (Vmpp~130 V, Impp~40 A, Voc~165 V, Isc~44 A)
- Pacific Power Grid Simulator regulating AC bus at 60 Hz, 220 Vrms
- Load bank providing AC load (since grid simulator not bi-directional)
- NREL DC Bus Regulation PI Loop computing IAC reference magnitude
- NREL PLL locking to sensed VAC to provide IAC reference instantaneous angle
- NREL MPPT computing IPV reference.

The tests were performed under cloudy conditions, thus full power was not available from the PV array.

1.5.2 Test Results

Both instantaneous and RMS waveforms were captured during steady state and start-up conditions. Waveforms were captured showing the DC voltage (*VDC*), PV voltage (*VPV*), and PV current command from the DAC (*IPV CMD*), actual PV current (*IPV*), AC voltage (*VAC*), AC current waveform command from the DAC (*IAC CMD*), actual AC current (*IAC*), DC-AC stage enable command (*DA_EN*), and the DC-DC stage shutdown command (*SS*). Figure 15 and Figure 16 show the steady-state waveforms while Figure 17 and Figure 18 show the PV start-up waveforms. PV start-up refers to the time interval from when PV power is first applied to the converter terminals until steady-state MPPT operation is reached. Figure 19 and Figure 20 show a magnified view of the complete PV start-up. In addition, Figure 21 - Figure 24 show magnified views of the following events:

Closure of external PV disconnect to apply power to converter terminals
Closure of internal PV contactor as commanded by DSP
DC-DC enable and MPPT ramp to initially charge the DC bus
MPPT reset and DC-DC disable once DC bus reaches slightly higher than rated voltage
DC-AC enable and activation of DC bus feedback loop
DC-DC re-enable, MPPT re-start, and ramp to full power

The timescale for all the plots is indicated in the figure captions. The y-axis legend and scale for all the instantaneous waveform figures is displayed below:

Magenta = VDC (50 V/ div)
Yellow = VPV (20 V/ div)
Green = IPV (5 A/ div)
Bright Green = IPV CMD (equivalent 4.6 A/ div)
Red = VAC (100 V/ div)
Pink = IAC CMD (equivalent 10.6 A/ div)
Orange = IAC (10 A/ div)
Blue = DA_EN test point (Enable to DC-AC switches, LOW=shutdown, HIGH=operate)

Bright Yellow = SS test point (DC-DC shutdown to PWM chip, LOW=shutdown, HIGH=operate)

The legend and scale for all the RMS waveform figures is displayed below:

Magenta = VDC (50 V/ div)
Yellow = VPV (20 V/ div)
Green = IPV (5 A/ div)
Bright Green = IPV CMD (equivalent 4.6 A/ div)
Red = VAC (50 Vrms/ div)
Pink = IAC CMD (equivalent 2.1 Arms/ div)
Orange = IAC (2 Arms/ div)
Blue = DA_EN test point (Enable to DC-AC switches, LOW=shutdown, HIGH=operate)
Bright Yellow = SS test point (DC-DC shutdown to PWM chip, LOW=shutdown, HIGH=operate)

Figure 15. Steady-state, RMS waveforms, timescale = 1s/div

Figure 16. Steady-state, instantaneous waveforms with zoom, timescale = 1 s/div (full), 10 ms/div (zoom)

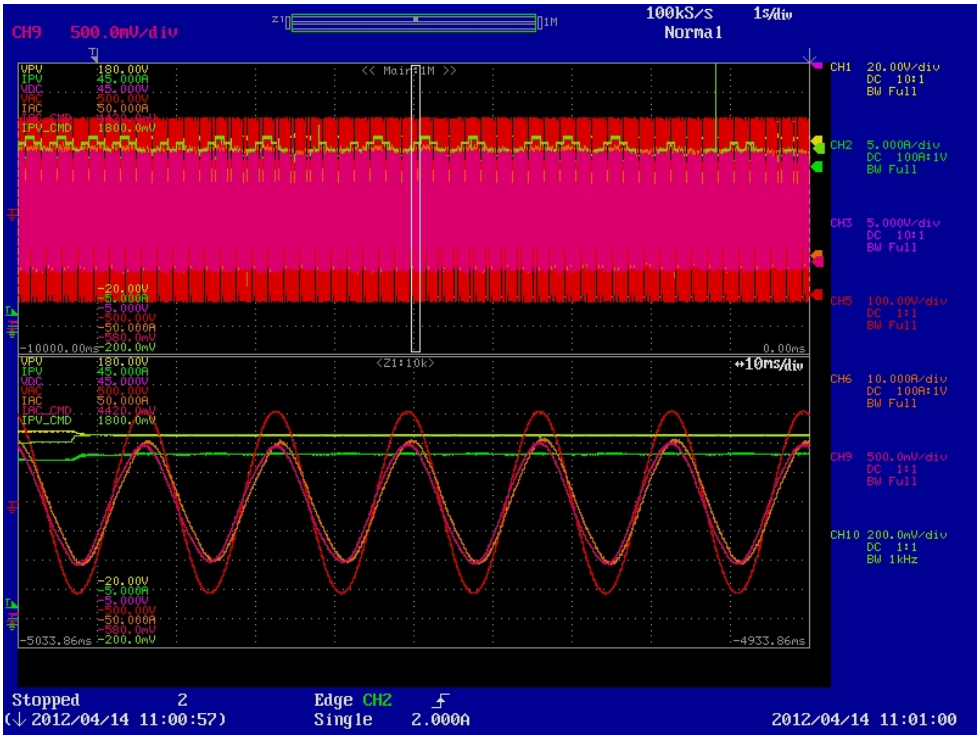

Figure 17. PV Start-Up, RMS waveforms, timescale = 1s/div

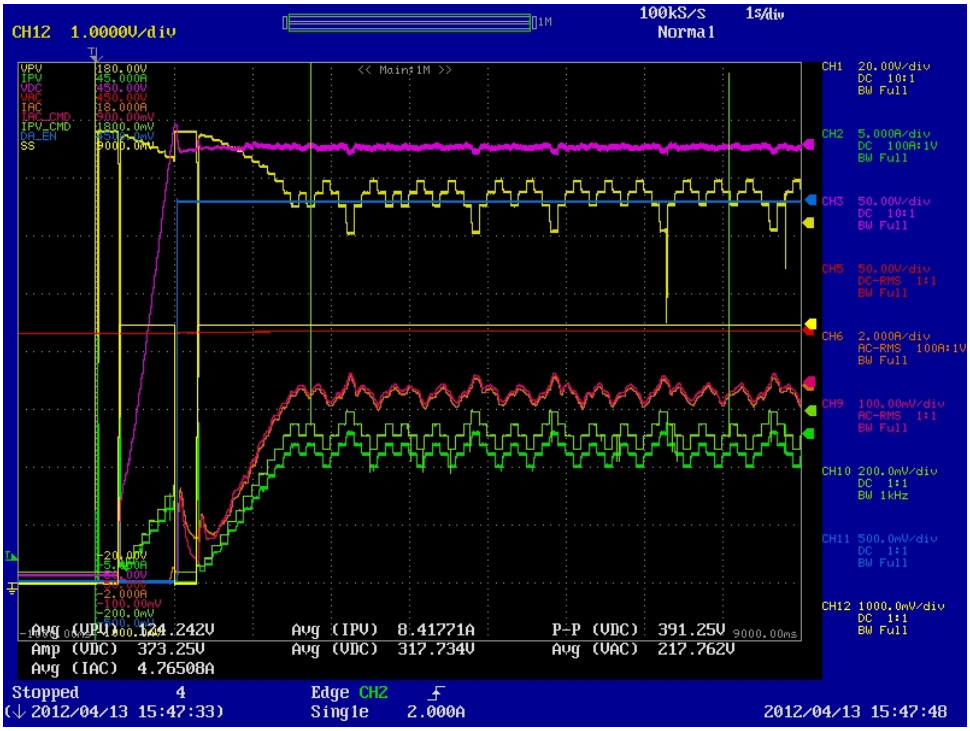

Figure 18. PV Start-Up, instantaneous waveforms, timescale = 1 s/div

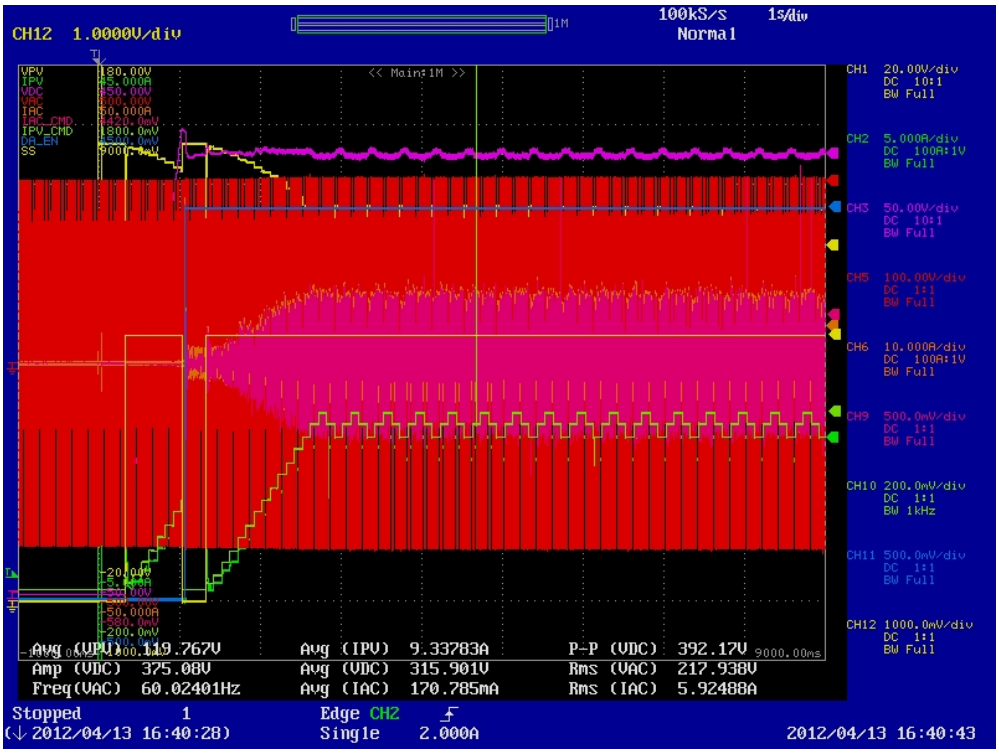

Figure 19. PV Start-Up, RMS waveforms with zoom of complete start-up, timescale = 1 s/div (full), 200 ms/div (zoom)

Figure 20. PV Start-Up, inst. waveforms with zoom of complete start-up, timescale = 1 s/div (full), 200 ms/div (zoom)

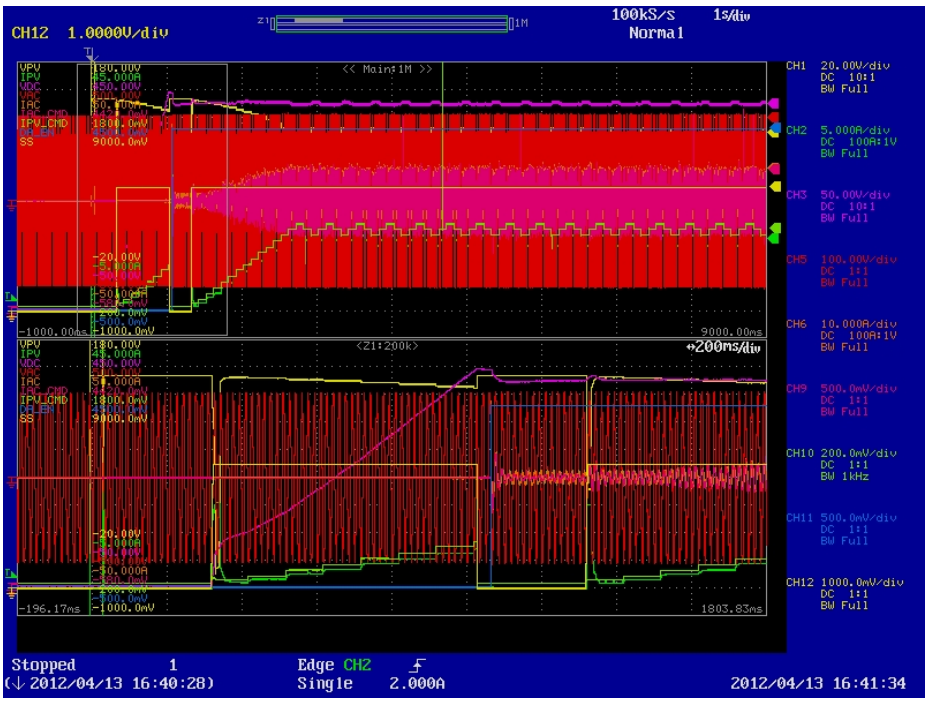

Figure 21. PV Start-Up, inst. waveforms, zoom at closure of PV disconnect, timescale = 1s/div (full), 100 µs/div (zoom)

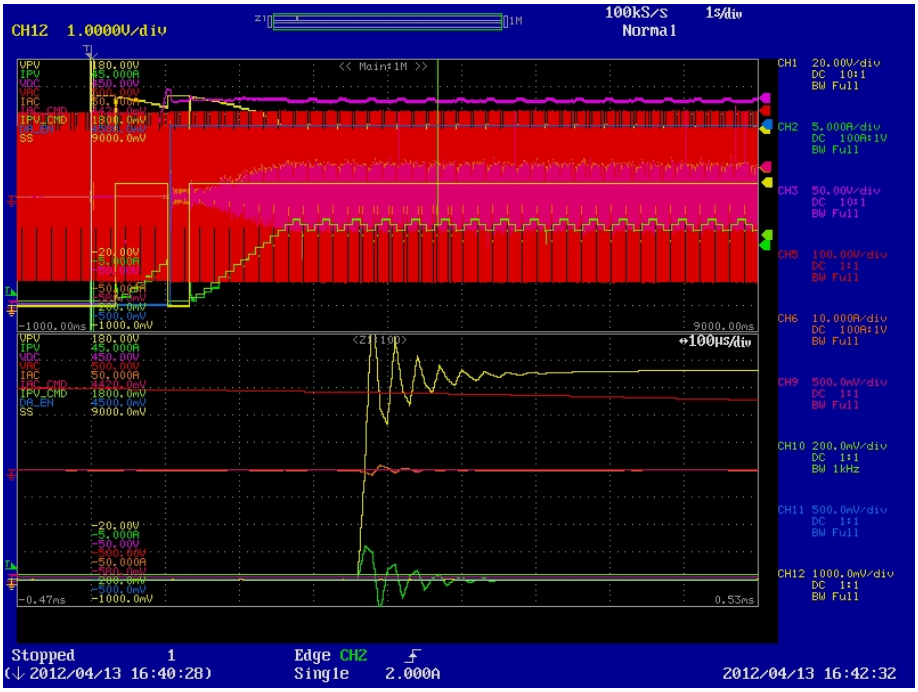

Figure 22. PV Start-Up, inst. waveforms, zoom at closure of PV contactor, timescale = 1s/div (full), 500 µs/div (zoom)

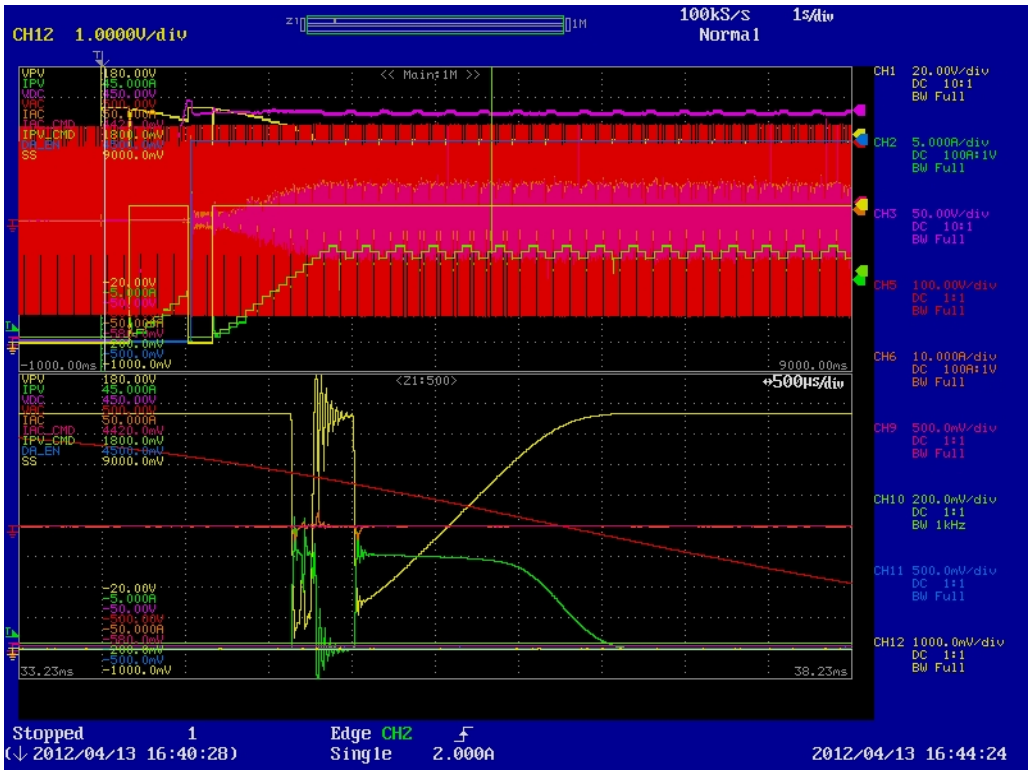

Figure 23. PV Start-Up, inst. waveforms, zoom of DC Bus ramp, timescale = 1s/div (full), 100 ms/div (zoom)

Figure 24. PV Start-Up, inst. waveforms, zoom MPPT reset, DC-AC enable, and MPPT re-start, timescale = 1s/div (full), 200 ms/div (zoom)

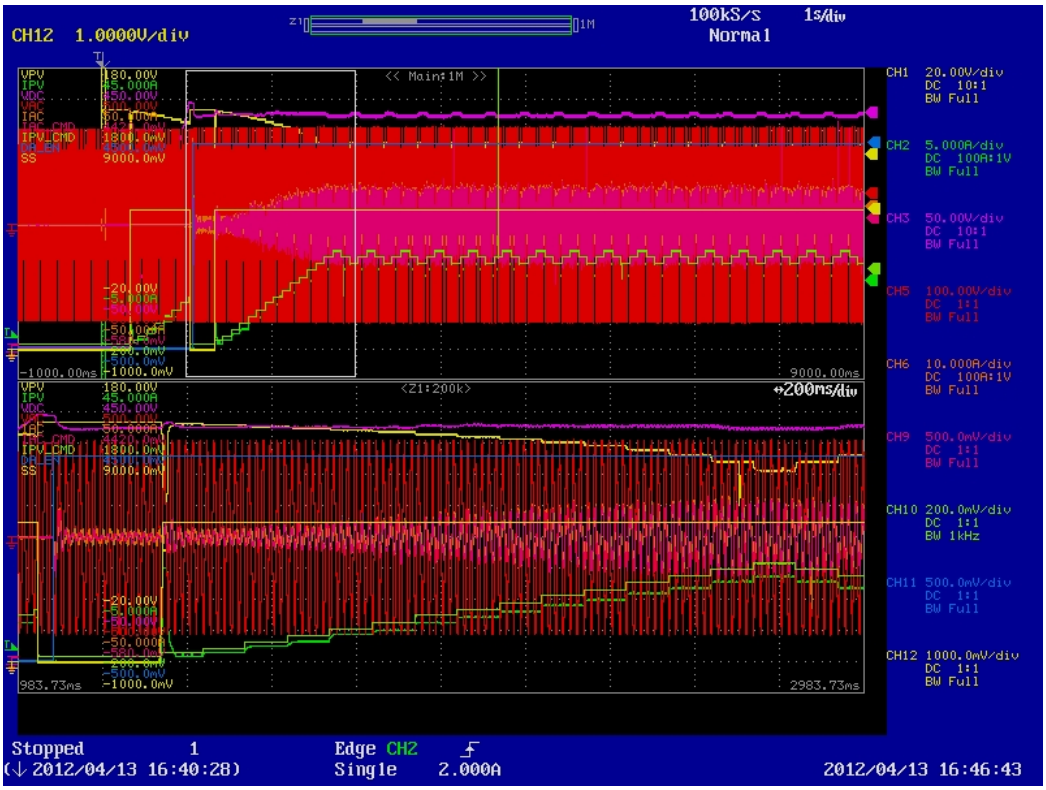

1.5.3 Test Discussion

The MPPT and DC bus regulation tests verified the successful integration of the NREL advanced functionality code with the core USH code. In addition, the tests verified that the US Hybrid APEI could be controlled with NREL's proprietary MPPT and DC bus regulation algorithms. However, evident in the waveforms are the previously observed spikes in AC current waveform command, as well as spikes in PV current command that appear to be introduced by noise inside the converter during higher power operation. As mentioned previously, Finally, DC contactor chatter can be observed in Figure 22, but this should be easily solved using the USH core software.

1.6 Island Detection Tests

1.6.1 Test Configuration

Island testing was performed to demonstrate the performance of the USH APEI using NREL island detection algorithms. The purpose of these algorithms is to detect whether the inverter is still connected to the grid or whether an island has formed. These particular algorithms do so by driving frequency out of bounds when inverter is islanded. Testing was performed by bringing the inverter on-line together with the grid simulator and a resonant load. The load is configured as closely as possible to absorb the same amount of real power as being delivered to the inverter, to have a resonant frequency of 60 Hz, and to have a quality factor of 1. A shunt

trip signal is then sent to the grid simulator circuit breaker to cause an island and the resulting waveforms are captured.

The island detection tests were performed with the DC-DC stage disabled. Instead, an external DC power supply was connected directly to the converter DC bus. The test configuration is described below:

- AreoEnvironment AV-900 regulating DC bus at 380 V
- Pacific Power Grid Simulator regulating AC bus at 60 Hz, 220 Vrms
- RLC load bank to provide AC load, configured to absorb the same amount of real power as being delivered the Inverter, to have a resonant frequency of 60 Hz, and to have a Quality Factor of 1
- NREL PLL locking to sensed VAC, and providing IAC waveform reference with user-specified real power.

1.6.2 Test Results

Island detection test results are shown for two cases: Figure 25 shows results when testing first commenced and resistive-inductive-capacitive (RLC) elements were cold, while Figure 26 shows results after testing for sufficient time for the RLC elements to heat up. In the first case, the resonant frequency of the load is slightly less than 60 Hz while in the latter case the resonant frequency of the load is slightly greater than or equal to 60 Hz. For each case, testing is first performed with island detection disabled, showing that the Inverter remains on-line with output voltage near 60 Hz and 220 Vrms. The test was then repeated with NREL island detection algorithms enabled. Since the purpose of these tests was to demonstrate USH APEI's ability to be controlled using island detection algorithms and not the actual IEEE Std 1547 disconnection compliance, the frequency limits were set at 58 and 62 Hz merely to protect the Inverter. For all cases, the beginning and ending frequencies are recorded in the measurements shown at the bottom of oscilloscope screen-shots. Finally, testing was also performed to verify that the island detection algorithms do not adversely affect normal operation when the inverter is grid-connected. This is demonstrated in Figure 27.

Waveforms were captured showing the DC voltage (*VDC*), AC voltage (*VAC*), AC current waveform command from the DAC (*IAC CMD*), actual AC current (*IAC*), DSP frequency as output via DAC (*DFREQ*), frequency as measured by the oscilloscope (*FREQ_S*), DC-AC stage enable command (*DA_EN*), and the trip signal to the grid simulator (*TRIP*). The timescale for all the plots is indicated in the figure captions. The y-axis legend and scale for all the figures is displayed below:

Magenta = VDC (50 V/ div)
Red = VAC (100 V/ div)
Pink = IAC_CMD (equivalent 10.6 A/ div)
Orange = IAC (10 A/ div)
Green = DFREQ (DSP frequency, equivalent 0.488 Hz/ div)
Light Blue = FREQ_S (Frequency measured by Scope, 0.5 Hz/ div)
Blue = DA_EN (DC-AC Enable)
Light Blue = TRIP (Trip signal to Grid Simulator)

Figure 25. Island detection test results – RLC elements cold (initial island frequency slightly less than 60 Hz)

ISLAND DETECTION DISABLED

1 sec/div

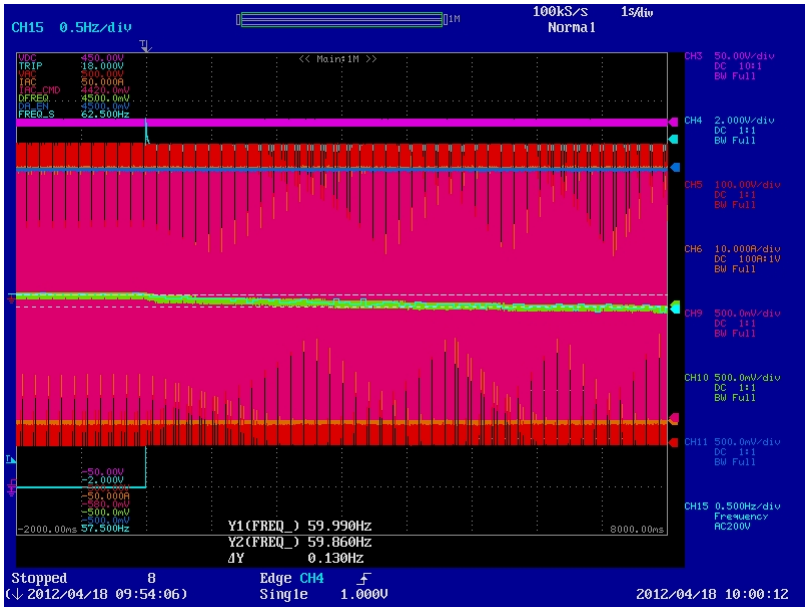

ISLAND DETECTION ENABLED

1 sec/div

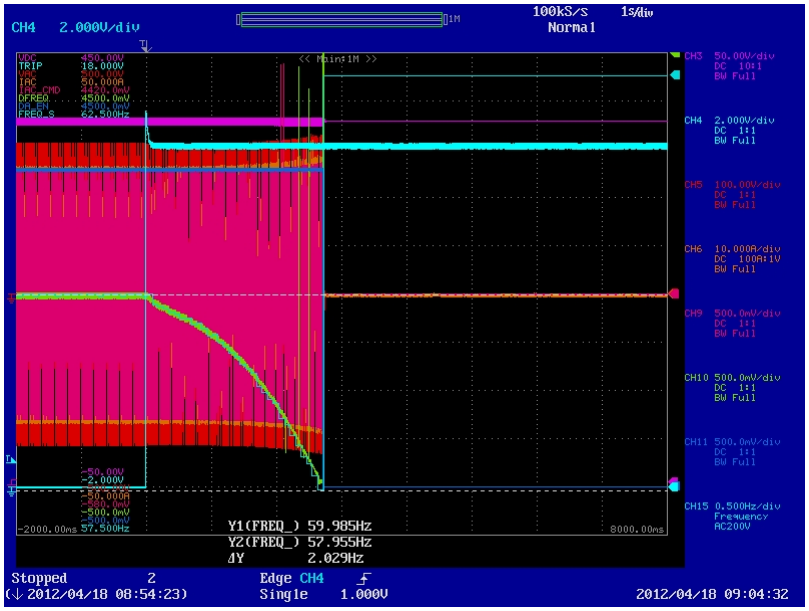

10 ms/div zoom at end of window

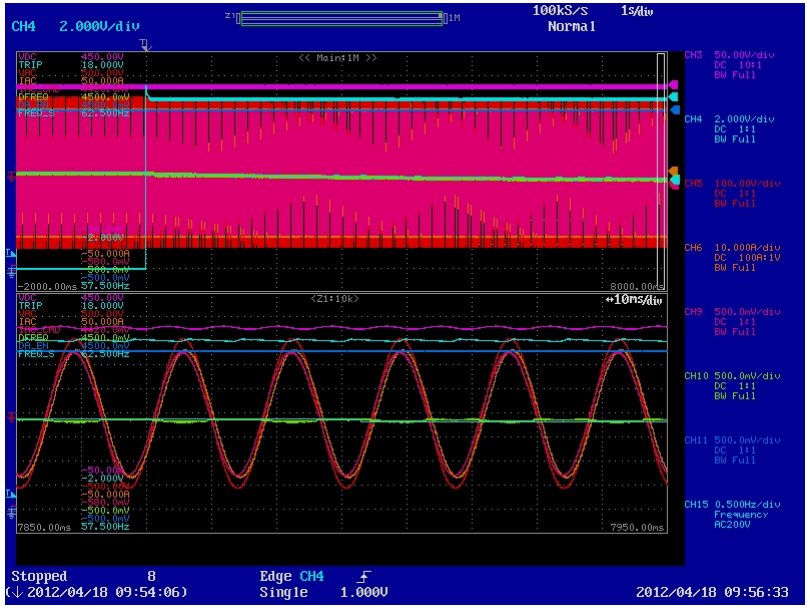

10 ms/div zoom at Inverter disconnection

ISLAND DETECTION DISABLED

1 sec/div

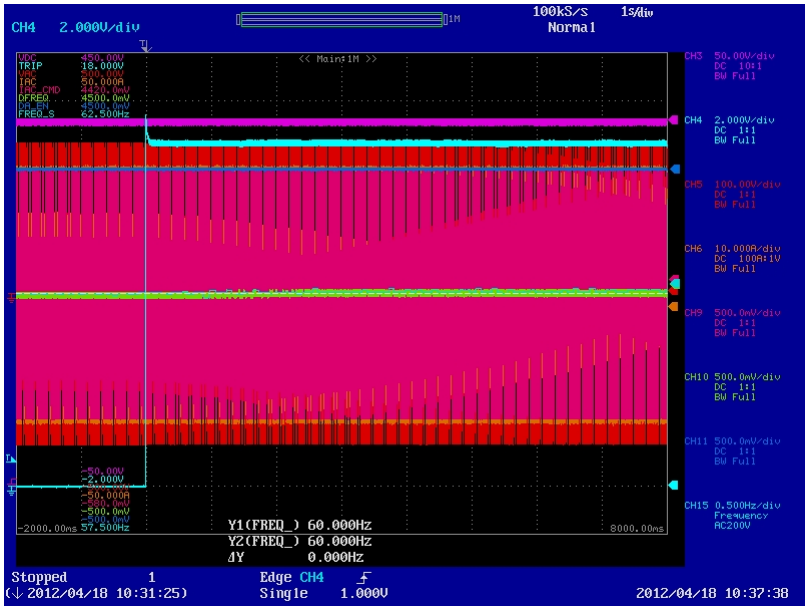

ISLAND DETECTION ENABLED

1 sec/div

Figure 26. Island detection test results – RLC elements hot (initial island frequency slightly greater than 60 Hz)

10 ms/div zoom at end of window

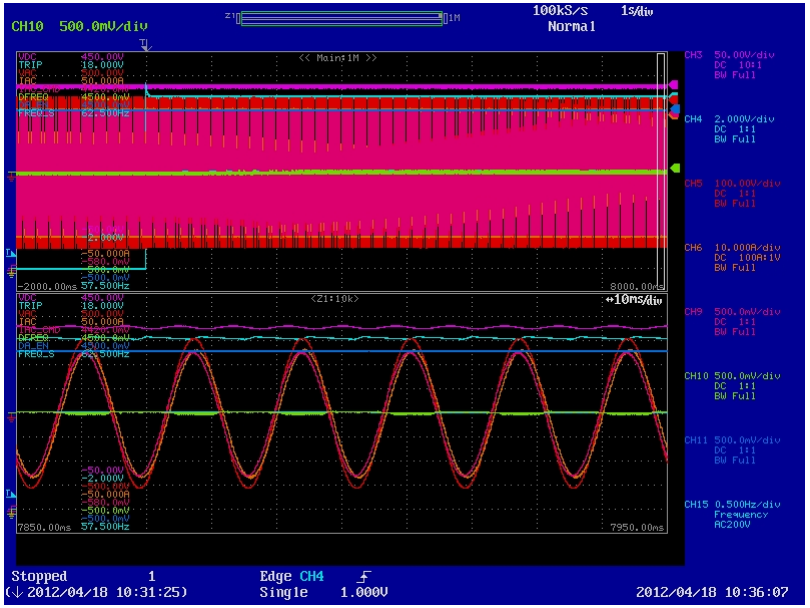

10 ms/div zoom at Inverter disconnection

Figure 27. Steady-state waveforms while grid-connected

ISLAND DETECTION DISABLED

10 ms/div

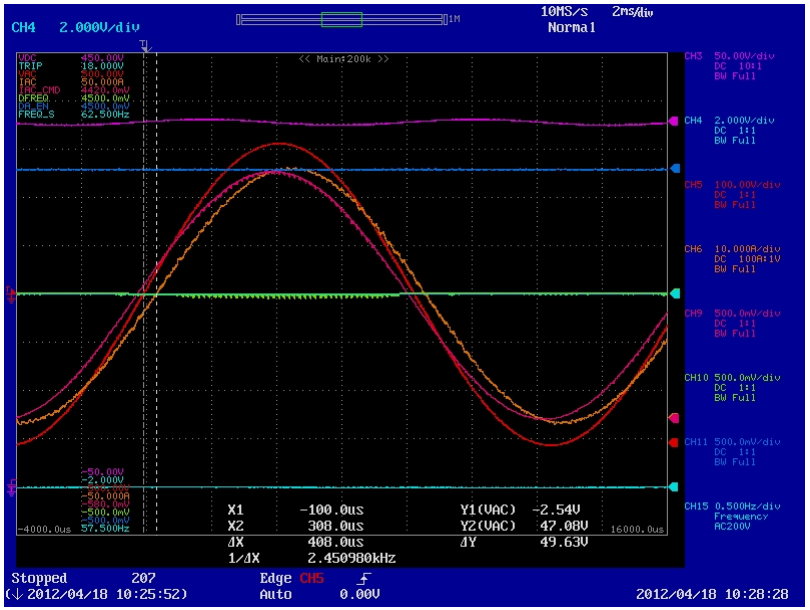

ISLAND DETECTION ENABLED

10 ms/div

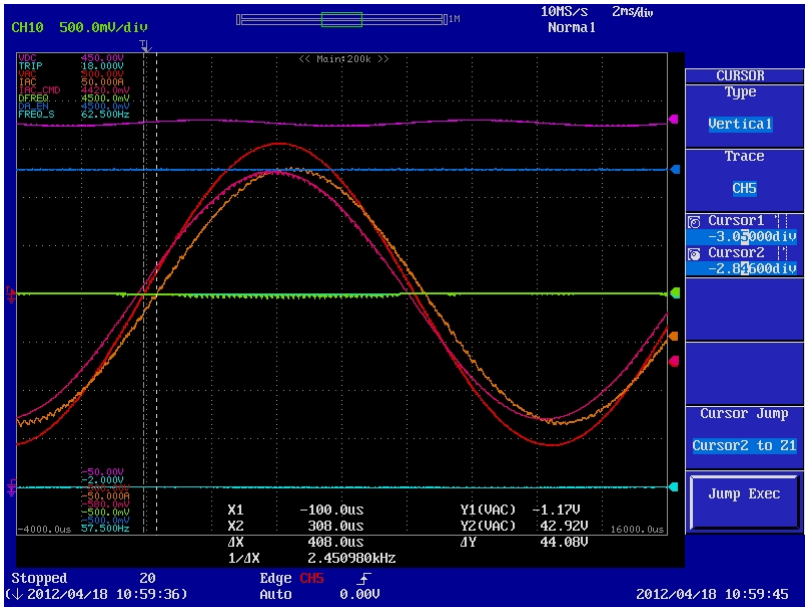

1.6.3 Test Discussion

The island detection tests verified that the USHybrid prototype hardware and low level interface control software could be used with island detection algorithms. Furthermore, the tests show that the specific algorithms implemented are able to successfully detect an islanded condition with matched resonant load without any observable effect on normal grid-connected operation

1.7 Conclusion

Advanced functionality of the USH 6.6 kW APEI prototype was successfully demonstrated by the results shown in this report. In particular, full 4-quadrant operation of the APEI as well as the APEI's ability to operate as a grid-connected PV system. The results are noteworthy not only in demonstrating performance of the APEI, but also in demonstrating the successful integration of separately developed algorithms into the USH core controller. This is a tribute to the cooperation between NREL and USH, along with the support from the Energy Commission, and the outcome is superior advanced power electronics APEI platform that can be used for multiple applications.

Chapter 2:
Low-Power APEI – UQM Technologies

Under task 2.2.1, UQM Technologies Inc. was subcontracted to develop a residential-scale, 5 kW APEI. As with many of the other tasks in this agreement, the principal objective was to develop a highly reliable, low-cost, modular, scalable APEI capable of seamless grid-connection and standalone operation. Employing a building block approach to the interface, designing the unit with "plug and play" ease of installation and operation in mind, implementing advanced circuit topologies that leverage readily-available components that are manufactured in larger quantities and commonly used in other industries, and utilizing robust design practices that emphasize reliability throughout the development of the APEI were key approaches in achieving this objective. UQM proposed a "plug and play" operation that specifically addressed:

- Physical layer design for quick, easy, and safe power terminal "plug-in"
- Control layer design for minimal input and user-friendly "play" operation
- Automatic inter-unit communications, for scaling to higher device power levels, via a well-established and robust communication protocol.

UQM developed an initial prototype that sought to employ these approaches to meet the primary objective of the project. During the testing phase of prototype development, technical difficulties led NREL to renegotiate their contract to develop a single-phase APEI that could also be used for mobile power applications.

This genesis of this new solution was found in a different UQM product that was being developed in parallel with the Energy Commission's APEI. This other product was a DC-AC inverter for automotive applications. The UQM inverter was originally designed for applications that required an islanded mode of operation to produce AC power for power tools from DC batteries on service trucks. Thus, as designed, this inverter didn't meet all of the requirements of a successful APEI prototype, but provided a good foundation as: it was built from both readily-available and very rugged components; had been designed and tested for the higher temperature, potentially wet, vibratory, and non-stationary environment of a service vehicle; had the ability to regulate voltage in islanded mode; and was built to safely provide AC power even under temporary high-current conditions such as those exhibited at the start-up of power tools. UQM didn't have the resources needed to develop this converter into a working grid-tied inverter so NREL took on this task at the request of the Energy Commission Project Manager. UQM provided this inverter unit in a working condition with its software source code and a cooling system and NREL engineers then began work to develop the software necessary for this inverter to meet the APEI prototype requirements, package the inverter into a commercially-ready form, and to test this APEI prototype. The following sections will document the above steps towards development of a working APEI prototype.

2.1 Development of APEI Prototype

Development of a highly reliable, low-cost, modular, and scalable residential-scale APEI capable of seamless grid-connection and standalone operation began with UQM's delivery to

NREL of its AC120-5KL DC-AC inverter. After verifying successful operation of this unit, NREL began development towards a fully functional APEI prototype.

2.1.1 UQM AC120-5KL DC-AC Prototype Modification and Delivery

In fulfillment of their modified contract with NREL, UQM technologies delivered one AC120-5KL DC-AC prototype to NREL. The delivered prototype required further development to meet full requirements. A photograph, key features, and specifications of the inverter prototype, taken from the unit's specification sheet (AC-120-5KL, UQM), are shown in Figure 28, Table 2 and Figure 29 respectively.

Figure 28. UQM AC120-5KL DC-AC Inverter Prototype Unit

Table 2. Key Features of the UQM AC120-5KL DC-AC Inverter Prototype Unit

Key Features	
5 kW continuous power output	Over temperature protection
True sine output – 120 VAC 60 Hz	Internal soft start
Input voltage range of 250 – 425 VDC	Under voltage protection
Compact design	Firmware upgradeable
Power distribution via secondary box	Automatic current limiting
DSP controlled	Environmentally sealed to IP67
Polarized, sealed, interlocked connections	High inrush load cable
Liquid cooling	Brown out protection

Figure 29. UQM AC120-5KL DC-AC Inverter Prototype Specifications

Operating Voltage

Nominal output voltage	120 VAC +/- 1%
Operating voltage input range	250 to 425 VDC
Output current (continuous)	42 Amps RMS
Output current (peak)	140 Amps Peak
Peak output time	2 sec
THD	< 5%
Output frequency	60 Hz +/- 0.02%

Liquid Cooled System

Minimum coolant flow

2 GPM (50/50 water/glycol mix)

Ambient temperature range

-40° C to 105° F

Maximum inlet temperature of coolant

149° F 65° C

Dimensions

Length	17.6 in	447 mm
Width	9.6 in	244 mm
Height	4.0 in	102 mm
Weight	23 lb	10.5 kg

Performance

Power output (continuous)	5 kW
Power output (peak)	16.8 kW
Output efficiency	Up to 92%

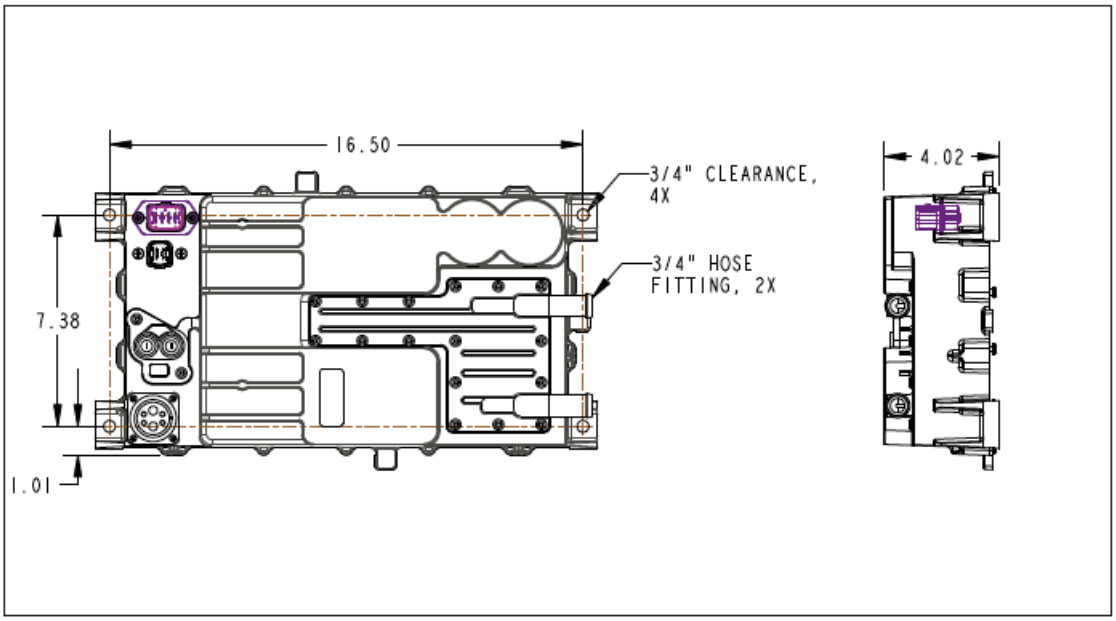

The prototype, as specified above, then required a number of modifications to its hardware in order to be capable of being a viable residential, grid-connected PV inverter. NREL worked with UQM to have UQM implement the following:

1. **Modification of Cooling System**: The AC120-5KL prototype was originally designed to be liquid cooled for use in vehicle applications. Because air-cooling is the industry standard for residential PV inverters, the cooling system had to be modified so that its primary cooling input was air. This was accomplished by designing a pump and radiator system that would deliver cooling fluid to the inverter unit at an appropriate flow rate and temperature to be able to maintain acceptable thermal operation of the inverter unit. The heat transferred to the cooling fluid from the inverter was then rejected using a forced-air-cooled radiator. The inverter prototype with its cooling system is shown in Figure 30.

2. **Modification of Electrical Output**: The AC120-5KL prototype was originally designed to function as an islanded inverter only. Thus, it was not capable of synchronizing with and connecting to the electric power system. In order to provide this key capability, electrical sensors, for use in measuring the grid's voltage and frequency to provide for inverter synchronization, and an electrical contactor, used to allow the inverter to connect or disconnect from the grid when prompted by its control system, were added to the electrical output of the inverter.

Figure 30. The AC120-5KL DC-AC Inverter Prototype with Cooling System

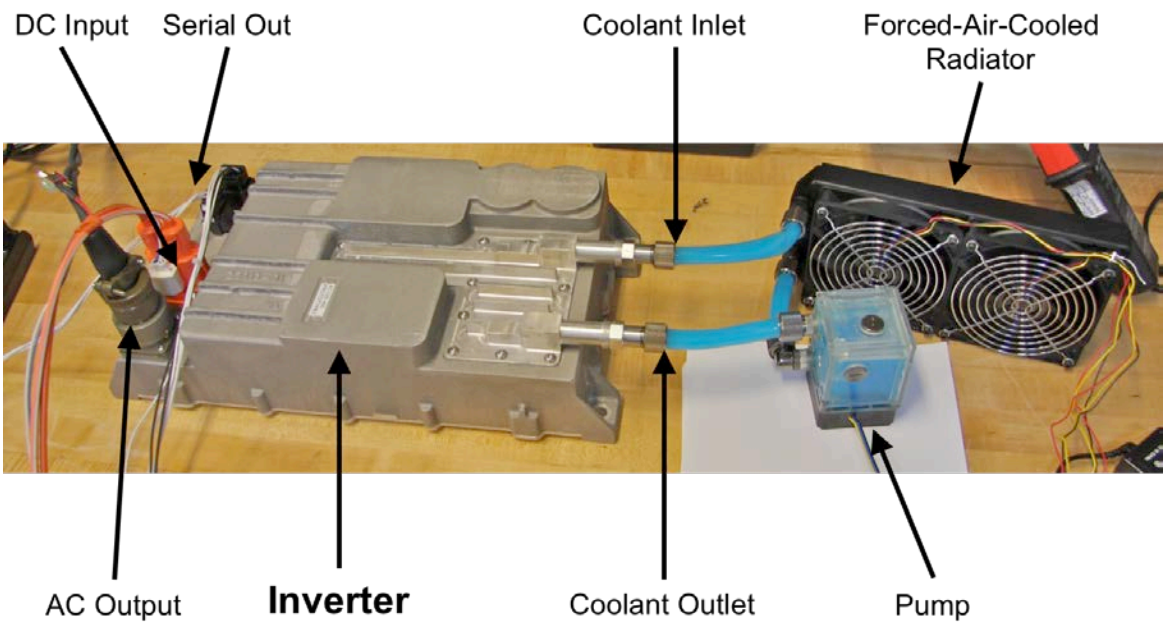

After having made these hardware changes, the prototype was ready for UQM's factory testing. The key test run by UQM to ensure proper operation, electrically and thermally, of the prototype involved connecting the inverter so that it operated in an islanded mode of operation (not connected to the grid) and running the inverter at full-power output (5 kW) continuously for one hour. During this test, electrical parameters of voltage, current, power, and electrical efficiency and thermal parameters of case temperature and power module temperature were measured. All results of the tests conducted showed that the prototype operated safely within its designed limits of electrical and thermal operation. Figure 31 shows the electrical setup for the tests that were performed.

Figure 31. Test Setup for UQM Factory Test of Inverter Prototype

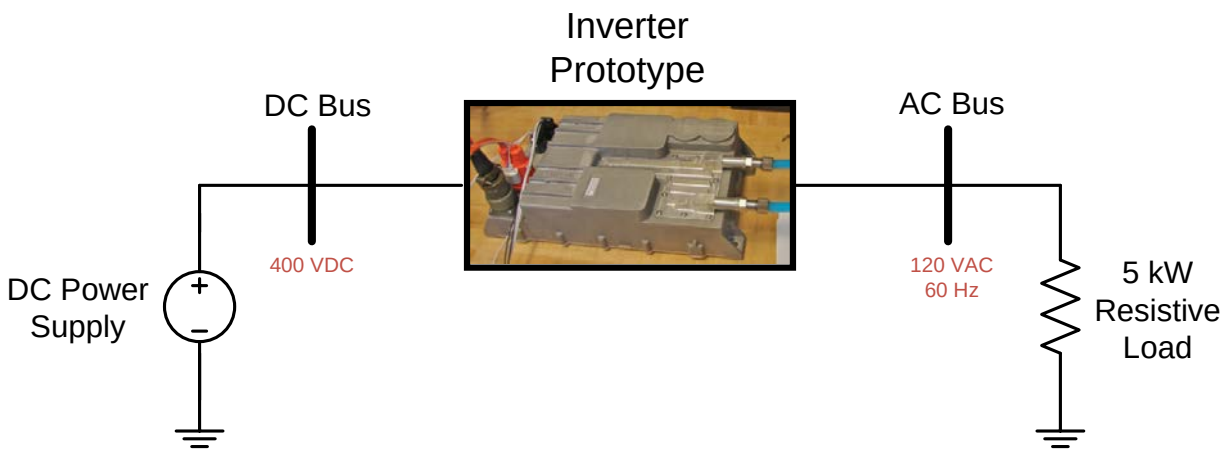

Figure 32 shows the measured AC voltage and current output of the inverter when it was operating at full power. This oscilloscope trace shows the current and voltage exactly 180 degrees out of phase indicating that the inverter was outputting power to the load at unity power factor. At this instant in time, the input DC voltage was 400 VDC, the input power was 5.3 kW, the output power was 4.7 kW, and the efficiency was 89 percent.

Figure 32. Electrical Output of the AC120-5KL Prototype Unit over 50 ms during a 1 Hour Thermal Test of the Inverter Running at Full Power

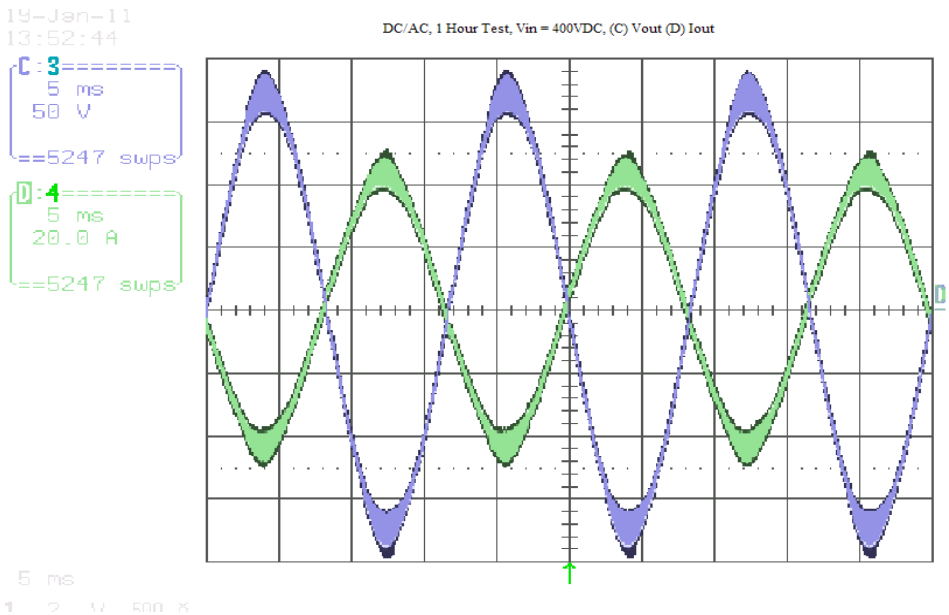

Figure 33 shows the thermal response of the inverter, as measured at the case and the power module, over a 1- hour testing period. The inverter was setup to operate at full power during the test duration. The tests results showed that at a DC input voltage of 400 V, DC input power of 5.3 kW, AC output power of 4.7 kW, and an electrical efficiency of 89 percent. The observed case temperature is higher than the power module temperature throughout the test because the liquid cooling delivered to the unit goes directly to the power module and never interfaces with the case. Both temperatures are within designed operating temperature limits of the unit.

Figure 33. Thermal Response of the AC120-5KL Prototype during the 1 Hour Test

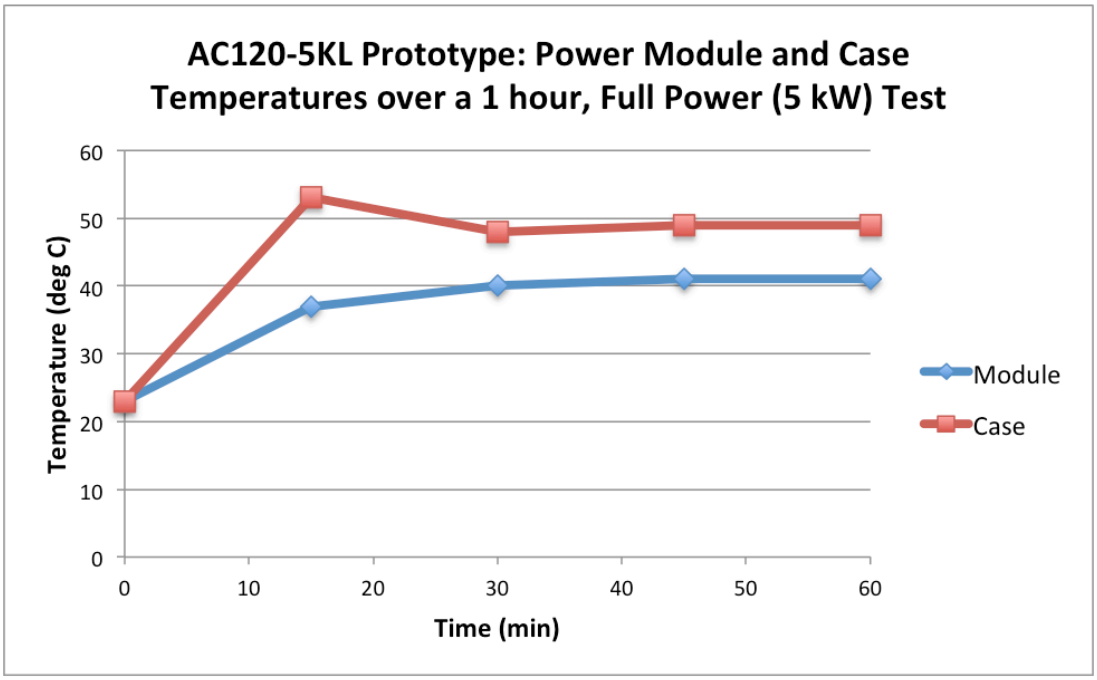

Figure 34 shows the electrical efficiency characteristics of the inverter. The electrical efficiency of the unit (the ratio of ac power output to dc power input) was computed for 11 points from 500 W to 5000 W (full power) at various operating DC voltages. It can be seen that the efficiency of the inverter is approximately 90 percent over its entire range of operation.

Figure 34. Electrical Efficiency versus Loading of the AC120-5KL Prototype during the 1 Hour Test

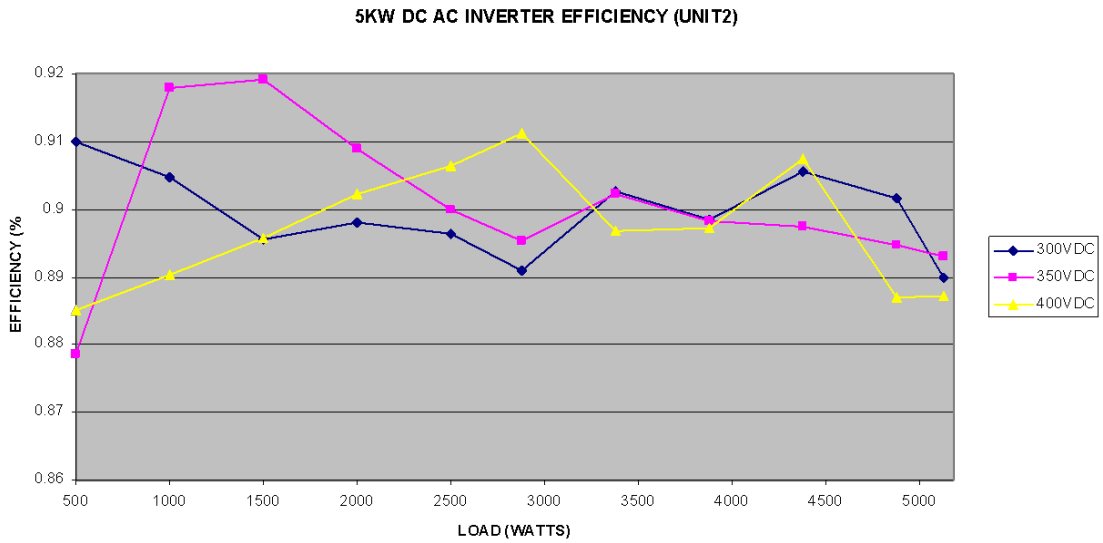

With the completion of the prototype's hardware modifications and the successful completion of testing at UQM, UQM delivered this AC120-5KL DC-AC converter to NREL for further testing and development.

2.1.2 NREL Performance Verification Testing

Upon receipt of the UQM tested AC120-5KL DC-AC prototype, NREL conducted its own independent testing of the inverter's performance. The electrical setup for the test was identical to that shown in Figure 31, but, of course, was conducted at NREL's laboratory. The physical setup for the test is shown below in Figure 35. The objective and evaluation criteria for this test were very similar to those of the UQM factory test: ensure that the inverter operates within its electrical and thermal operation limits.

Figure 36, Figure 37 and Figure 38 show the results of this testing at various output power levels from 1 to 3 kW. It can be seen that the inverter operated as expected with clean output voltage and current waveforms, acceptable DC voltage ripple and AC voltage regulation, and satisfactory unity power factor operation. Throughout this testing, the power module temperature and electrical efficiency were observed to be in the expected ranges and were consistent with results of the UQM factory testing. At this point, the prototype was deemed to be operating correctly and NREL began the design and build of a working APEI prototype using UQM's core technology.

Figure 35. Physical Test Setup for NREL Evaluation of UQM Inverter Prototype

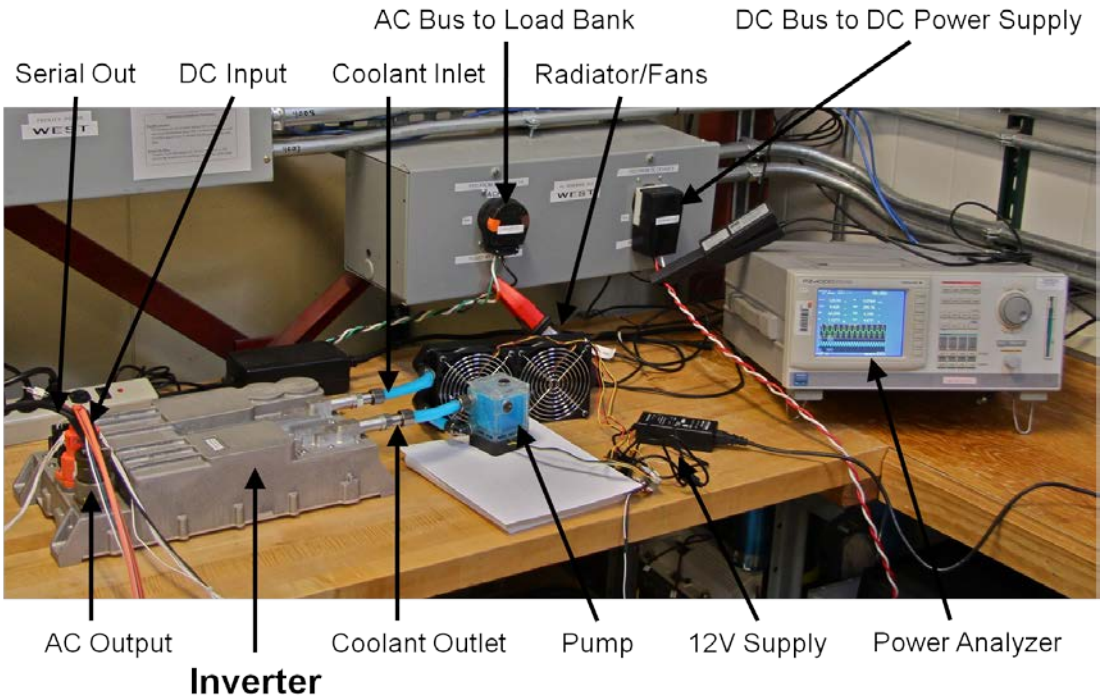

Figure 36. Oscilloscope Data for the Inverter Operating at PAC = 1.12 kW

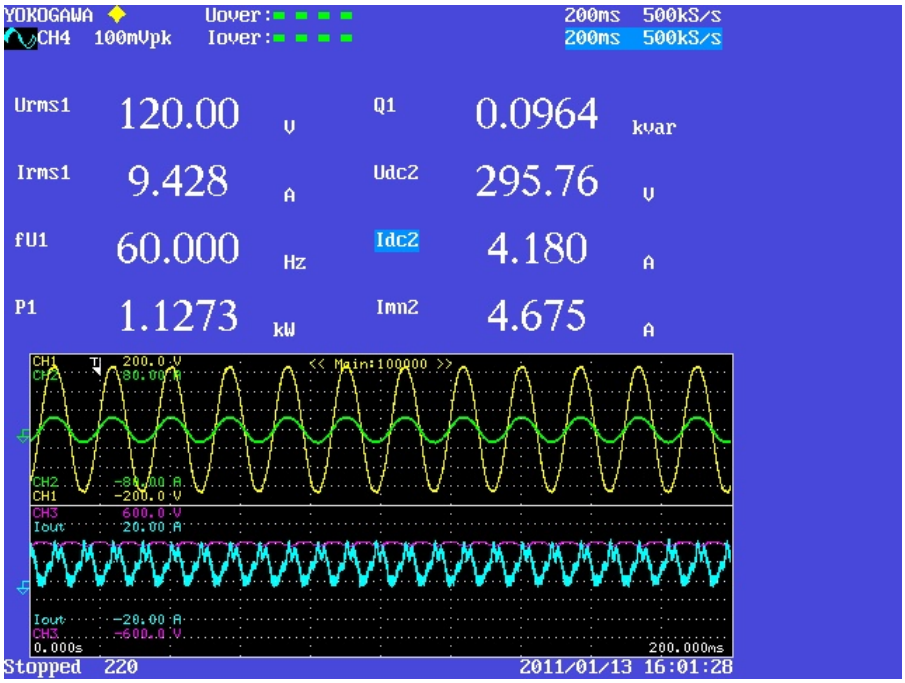

Figure 37. Oscilloscope Data for the Inverter Operating at PAC = 1.58 kW

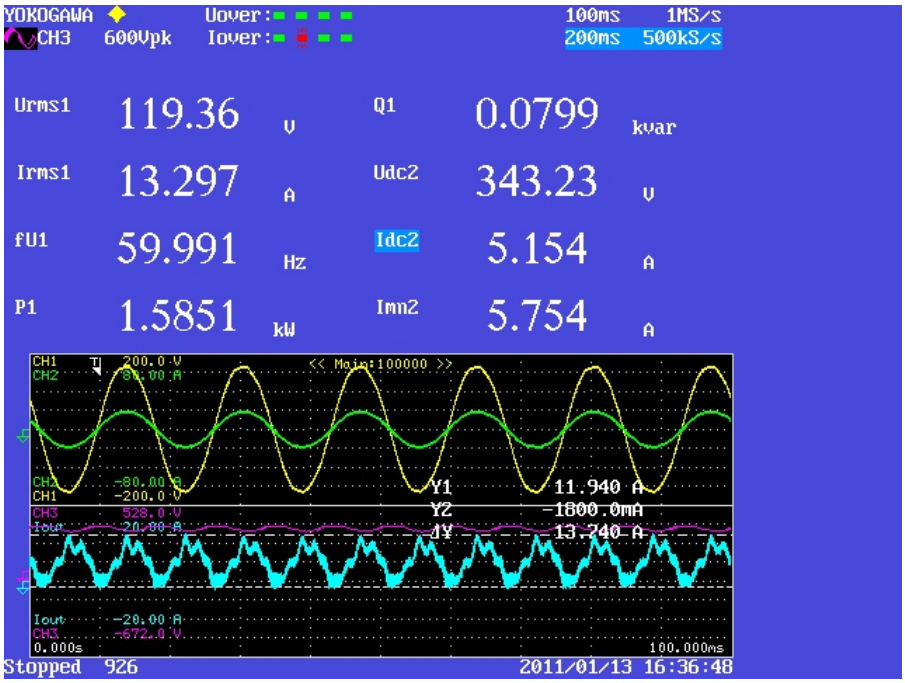

Figure 38. Oscilloscope Data for the Inverter Operating at PAC = 3.06 kW

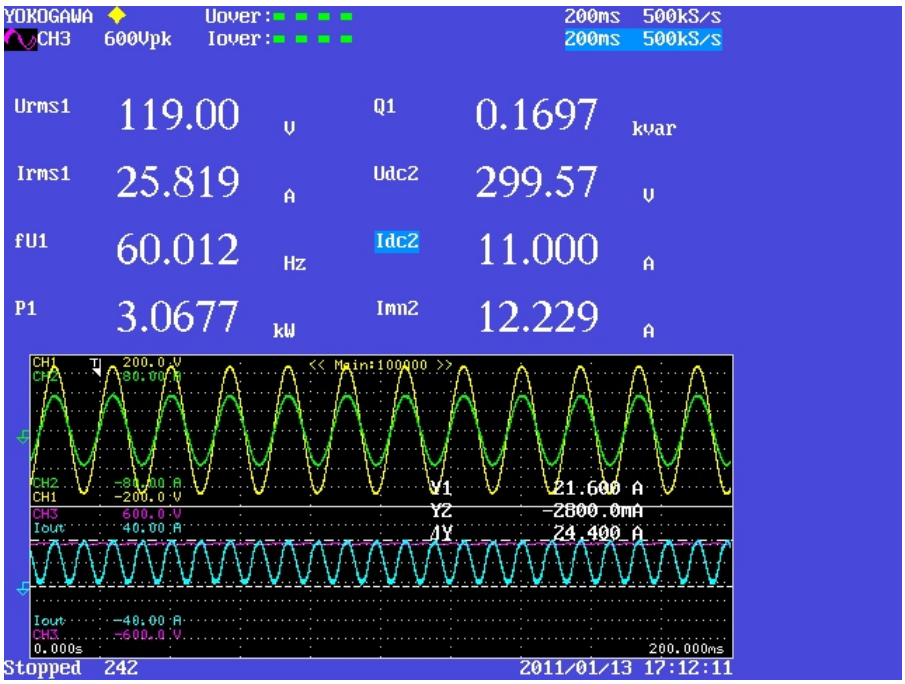

2.1.3 NREL Development towards an APEI Prototype

At this point, a working inverter prototype with features of high reliability, lower cost, and capable of islanded operation was available, but further development was needed to convert

this into a modular, scalable, residential-scale PV APEI capable of seamless grid-connection and standalone operation. The next steps to achieve this final APEI prototype were then to develop the control software necessary for seamless grid-connected operation, interfacing with solar panels instead of relatively-fixed-voltage DC sources, and inter-unit communication to enable future scalability using multiple units and repackaging of the inverter into a hardware form that supported "plug and play" and modular design practices at a residential scale. These two steps were pursued in parallel.

2.1.3.1. Software Controls Development

Software development was conducted in three phases: modeling and simulation, controller-in-the-loop (CIL) testing and refinement, and implementation in the inverter prototype. In the modeling and simulation phase, NREL engineers' adapted NREL proprietary inverter software controls and models that could be used to simulate the UQM inverter prototype. Control algorithms for grid-connected operation were then developed in simulation, tested, and refined until a successful control system could be used to develop a grid-connected inverter using the UQM platform. In order to maintain NREL's code as confidential, NREL staff maintained sole control of the software code and software integration efforts were performed by NREL staff on NREL computational resources.

CIL testing is a method by which the hardware controller for a device, such as this inverter, can be used to control a software model of that device. As such, it is still a model of the final system, but is a much more accurate model as it employs the actual hardware controller. This test setup is achieved through use of a hardware-in-the-loop (HIL) simulator. This simulator deterministically measures and interprets electrical input signals from the controller board, uses these inputs to run an iteration of the inverter software model, and then outputs the measured analog voltages and currents in the software inverter model as an analog electrical signal that can then be measured and used for control purposes by the controller board. This paradigm is shown below in Figure 39.

Figure 39. Controller-in-the-Loop Paradigm

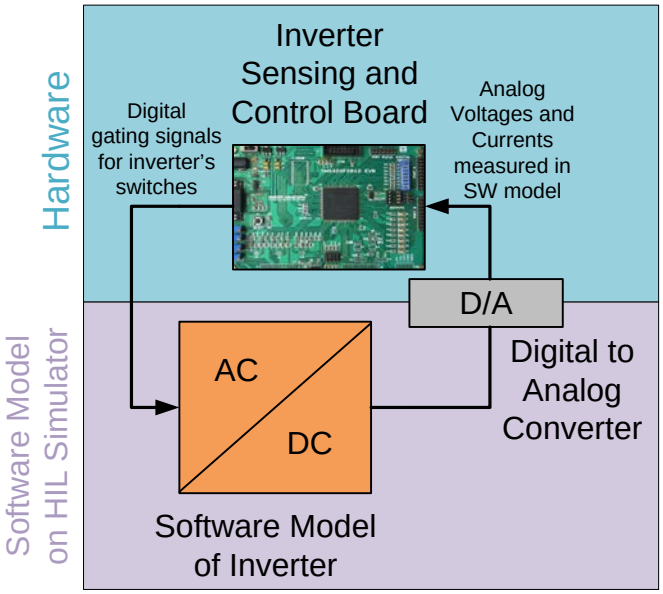

To further develop and refine the software controls developed for the UQM APEI, the control algorithms for grid-connected operation developed during the first phase of software development were placed on the actual UQM hardware control board and then the same inverter software model that was used in phase one was employed in the HIL simulator to complete the CIL paradigm described above. Using this test setup, NREL engineers further refined and tuned the inverter control algorithms.

The third and final phase of software development was then to implement the control algorithms developed and refined in the first two phases in the actual UQM inverter prototype. As NREL engineers began this phase of development, NREL decided to end development of UQM APEI prototype (see the *Field Testing of APEI Prototypes* section later for more details) and so software development ended before being fully implemented in the UQM inverter prototype. Because work on the UQM APEI prototype was halted, no software development for interfacing of the inverter with solar panels in lieu of relatively-fixed-voltage DC sources was completed either.

2.1.3.2 Inverter Repackaging

An enclosure was designed to house the UQM-provided prototype that included the APEI, a cooling system, auxiliary power supply, a human machine interface (HMI), and a number of required safety components to allow for future modularity and scalability. To achieve this goal, NREL engineers designed a hardware package that consists of two interconnected enclosures. The first enclosure, called the APEI Unit, houses the bulk of the APEI components including the inverter unit, an isolation transformer (added for safety and sized specifically for one inverter unit), the inverter and transformer cooling systems, the HMI, and the auxiliary power supply. Photographs of the APEI Unit, which show all of the above-mentioned components, are found in Figure 40 and Figure 41.

Figure 40. Inside of the APEI Unit's Enclosure Showing the Inverter, Isolation Transformer, Cooling Systems, and Auxiliary Power Supply

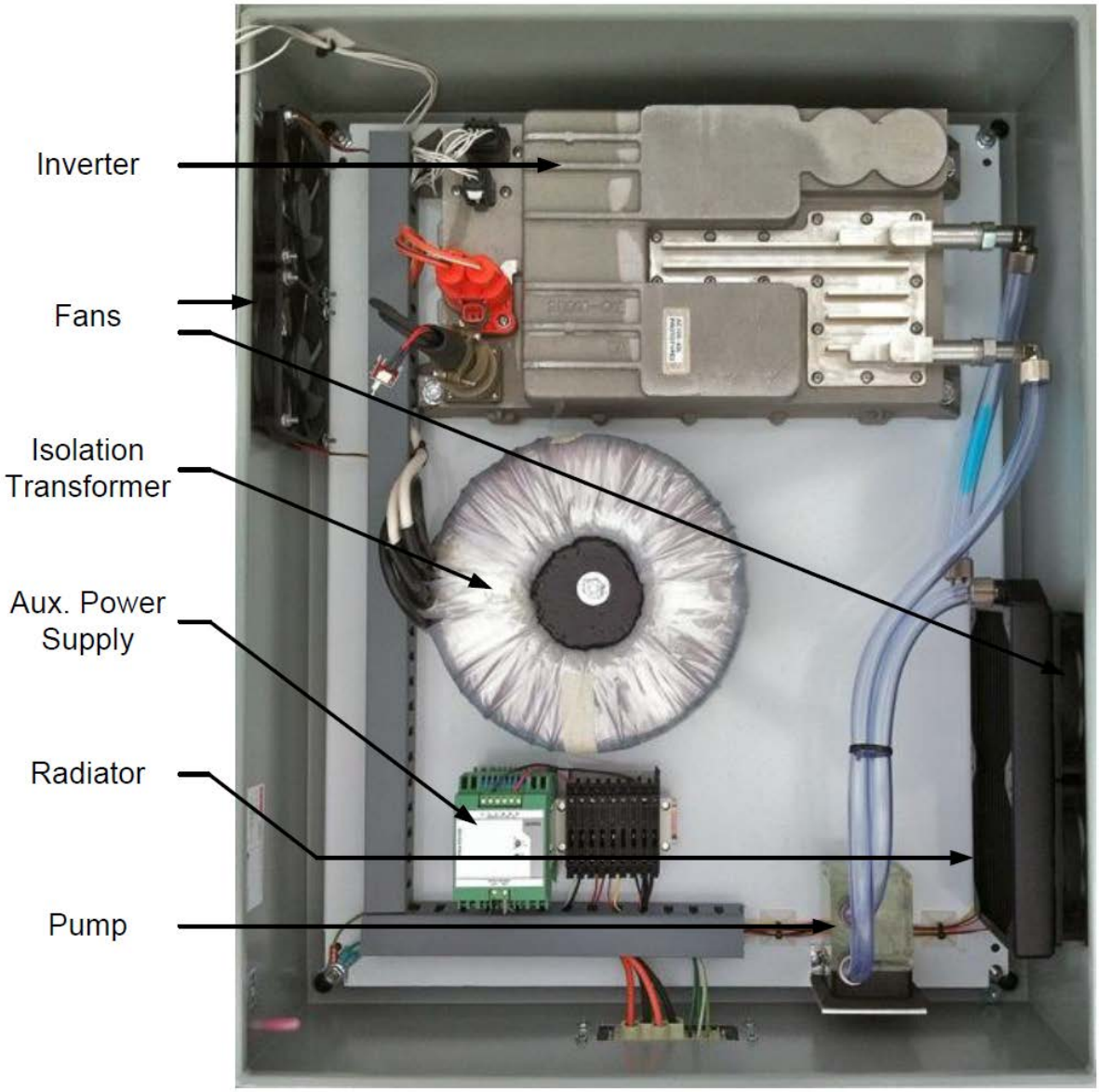

Figure 41. Front View of the APEI Unit's Enclosure, Highlighting the HMI

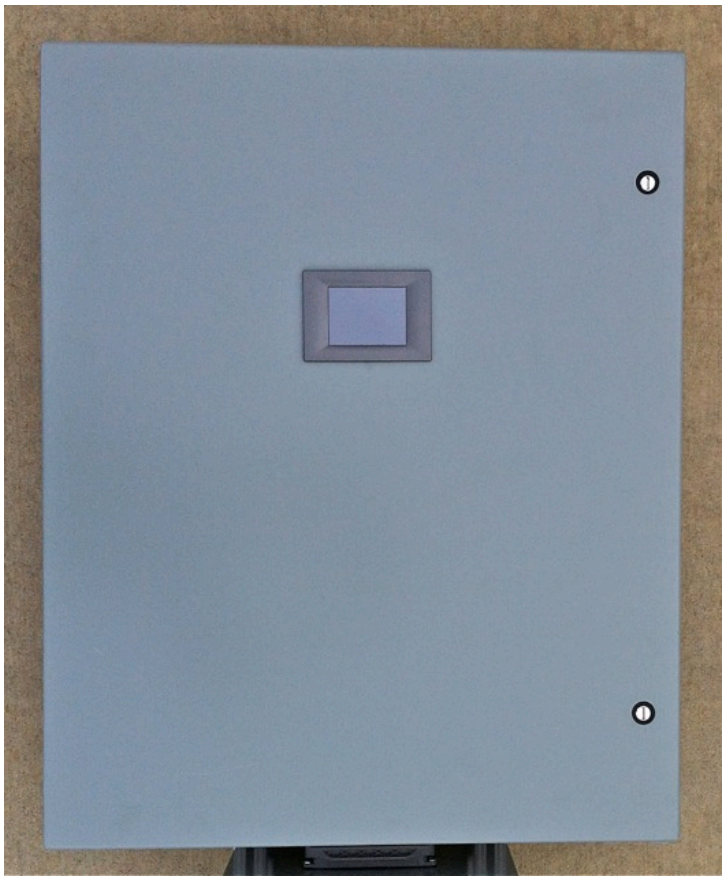

The second enclosure, called the grid interconnection unit (GIU), houses the AC and DC circuit breakers (used for electrical protection of the inverter in the case of an over-current event and for electrical isolation when installation and other electrical work is required) and the wiring interfaces for use in connecting the solar panels (DC input) and electric power system (AC output) to the APEI. A photograph of the GIU is shown below in Figure 42.

Figure 42. The Grid Interconnection Unit, which Houses the Electrical Protection Devices and Interfaces to the Solar Panels (DC Input) and Electric Power System (AC Output)

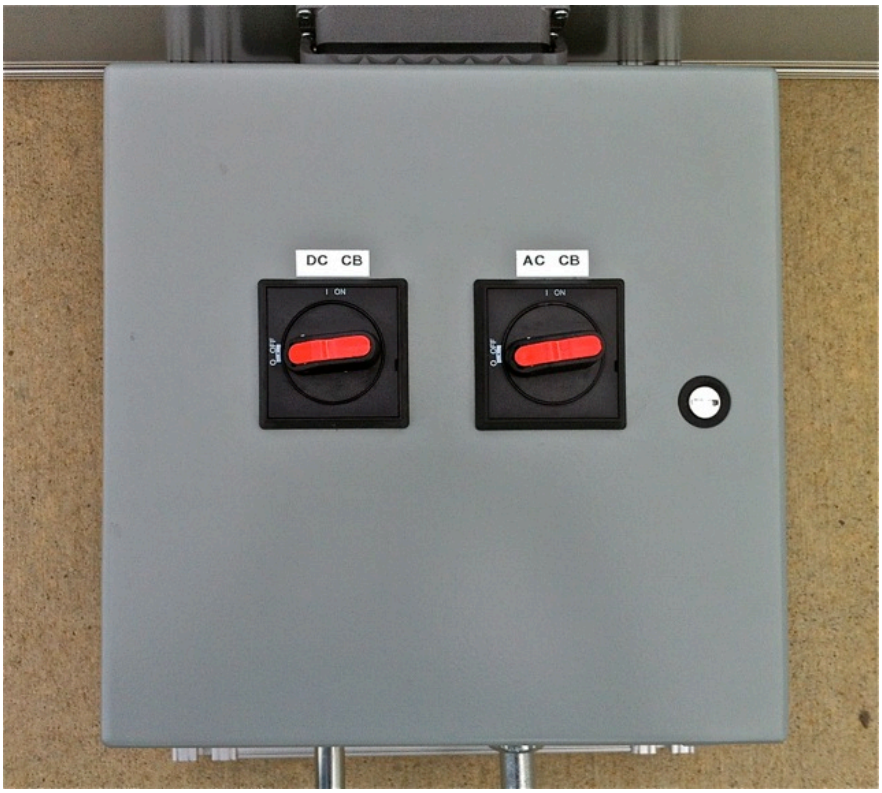

This system allows the main APEI unit to be easily connected (or "plugged" in) and disconnected for rapid installation and service. Also, this system of connection between the APEI unit and the GIU leverages modularity in order to support scalability; the GIU is designed so that it could be easily expanded to allow multiple APEI units to plug into this same enclosure for simple interconnection from one point with the system's DC input and AC output.

Figure 43. Blind-mating Plug System that Interfaces the APEI and Grid Interconnection Units

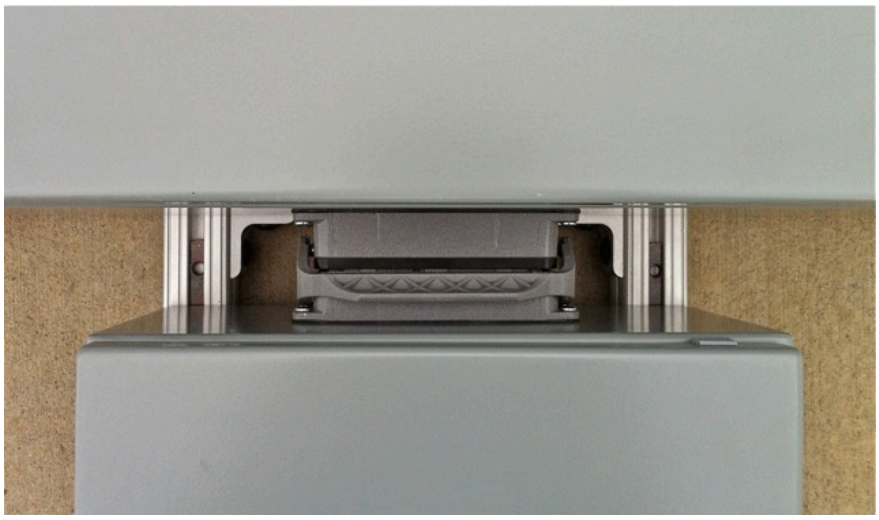

The APEI and grid interconnection units, connected together using this blind-mating plug system, are mounted together on a rack support system. This rack support system holds the APEI and grid interconnection units together and provides for easy installation (no complicated mounting onto a residential structure once the rack support system is in place) of the GIU and as many APEI units are required for the system installation. This rack support system is shown in Figure 44.

Figure 44. The Rack Support System, which Holds the APEI and Grid Interconnection Units Together

The final installed APEI package, including only one APEI unit for this installation, is shown in Figure 45.

Figure 45. The Final Installation of an APEI System (Only 1 APEI Unit is Included in this Installation)

2.1.4 Field Testing of APEI Prototypes

As NREL neared the completion of its APEI prototype development, a plan for field-testing of multiple APEI prototypes was started. The first step in this plan was to work with UQM provide additional AC120-5KL DC-AC Inverter units so that a number of complete APEI prototypes could be prepared for field-testing. When approached about obtaining more units, UQM was unable to provide any further AC120-5KL prototypes or even separate component parts to further develop the technology. As a result, the NREL PI and the CEC project manager agreed to stop development of the UQM APEI prototype.

2.2 Conclusion

Development of the UQM APEI prototype involved successful design and demonstration of a highly reliable, low cost, modular, and scalable APEI capable of standalone operation. This was achieved by building a rugged and scalable power electronic platform that utilizes components common with other industries and includes elements of the plug-and-play design methodology. While the APEI prototype that was developed was not capable of all of the requirements necessary to be a used as a grid-tied it still demonstrated many aspects of a successful APEI design. Field demonstration and further development of the UQM APEI prototype towards a successful design was not possible due to component availability from UQM's suppliers.

Chapter 3: Mid-Power APEI

Successful Smart Grid implementation requires that utilities and electricity customers have advanced technology tools and information needed to participate in the market. Development of interoperable, intelligent technology devices such as advanced power electronics technology will improve and accelerate the use of renewable and distributed energy systems and act as an enabler to the success of Smart Grid implementation (Liserre, 2010).

Currently, most power electronic devices are only developed for specific technology markets. It contains only the components and controls necessary for that application and is not compatible with other renewable energy sources. The short-term advantage of this approach is a least-cost option for the specific application. The long-term disadvantage, however, is that the narrow market opportunity for such a device disqualifies it from the cost advantages that larger economies of scale would realize (Kramer 2008). In other words, making a device that is applicable to more technologies will bring down its overall cost because of higher production. Another disadvantage of the application-specific approach is higher lifetime maintenance costs due to decreased availability of replacement parts and lower expertise of maintenance personnel (Kramer 2008).

To address these problems, engineers at NREL, in collaboration with vendor Semikron USA, designed a configurable, modular 50 kW power block suitable for various renewable and distributed energy applications such as PV, small wind, fuel cells, batteries, and flywheels. Under the previous task (Task 2.3), NREL developed the initial prototypes of the power block and tested it. Under the task 2.4, NREL continued working with the vendor to improve the cost and reliability of the 50 kW power block and developed the preproduction prototype design for the power block.

Additionally, NREL engineers worked with vendor National Instruments to develop a state-of-the-art controller board for these power blocks. The new controller board provided advanced programming capability so that the 50 kW power blocks could be used in various Smart Grid applications. NREL developed a wireless user interface so that the power block-based inverter system can be monitored and controlled through a wireless Apple iPad application. Through the application, an operator can view real-time measurements, control the mode of operation and other settings, and export customized data. This iPad application demonstrated how the modular power block based power electronics could blend into the Smart Grid monitoring and control framework.

NREL designed a three-phase inverter to test these power block and controller board prototypes. NREL was successful to implement grid-tied inverter control algorithms in to the new controller board and conducted various standard interconnection functions for the inverter. In addition, the inverter was operated as active rectifier to validate the functionality of the 50 kW power block in multiple APEI applications. The use of the same power block in various applications is important to reduce cost of production through larger economies of scale.

The outcome of these mid-power APEI subtasks (Task 2.4.2C and 2.4.2D) are: a market-ready design for the 50 kW power block and advanced controller board, the hardware design of a

grid-tied three-phase inverter, available software licenses for control algorithms for the PV inverter and wireless user interface.

3.1 Power Block Pre-production Prototype

From the experience of testing the prototypes developed under Task 2.3, NREL engineers worked closely with the vendor Semikron to finalize the design the 50 kW power block pre-production prototypes in order to improve the performance and cost objectives. The 50 kW power block consists of insulated gate bipolar transistor (IGBT) switches and anti-parallel diodes arranged in three-phase bridges. Other components include gate drivers, DC bus film capacitors, current sensors, a DC voltage sensor, a temperature sensor, a digital controller board, bussing, and connectors — all mounted on an air-cooled heat sink.

Features of this new 50 kW power block include the following:

- The design is based on the commercially successful Semikron IGBT product, which features pressure contact technology, an integrated driver, sensors, and protection. All these inherent features increase the reliability of the power block.
- DC filtering film capacitors are integrated in the power block. The use of a film capacitor improves reliability.
- The DC bus is designed in such a way so that it will be easier to use the blocks in parallel having a common DC-link.
- Output of more than one 50 kW block can be paralleled to have higher power ratings. The design is therefore scalable.
- The main connections to the DC bus and AC terminals are to be made through lugs. A laminated bus bar accessory is designed that will allow the user to bring all power connections to a single side simplifying connections.
- The power block has mounting and cooling for the NREL-National Instruments inverter controller board but flexibility of using various controller boards is incorporated in the design.
- Though designed for 50 kW at 208 VAC, due to high DC input voltage capability (700 V), the power block it can also be used to generate 480 VAC directly. This makes the power block flexible for other applications such as transformer less inverters.
- An open-frame design is utilized to significantly reduce the size and cost. This also enables Semikron to use more off-the-shelf components, thus reducing time to market.

Pictures of the pre-production prototype of the 50 kW power block are shown in Figure 46 and Figure 47.

Figure 46. Picture of 50 kW power block without controller

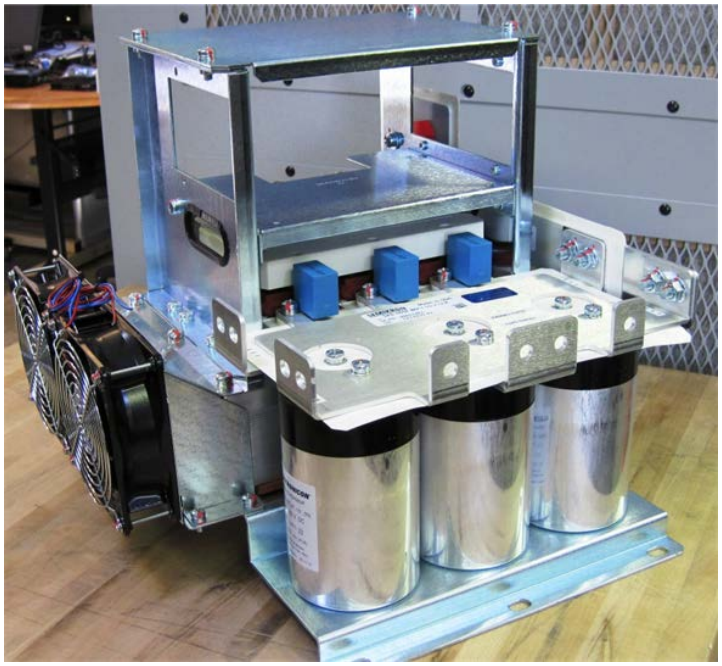

Figure 47. 50 kW power block with controller mounted on a backplane

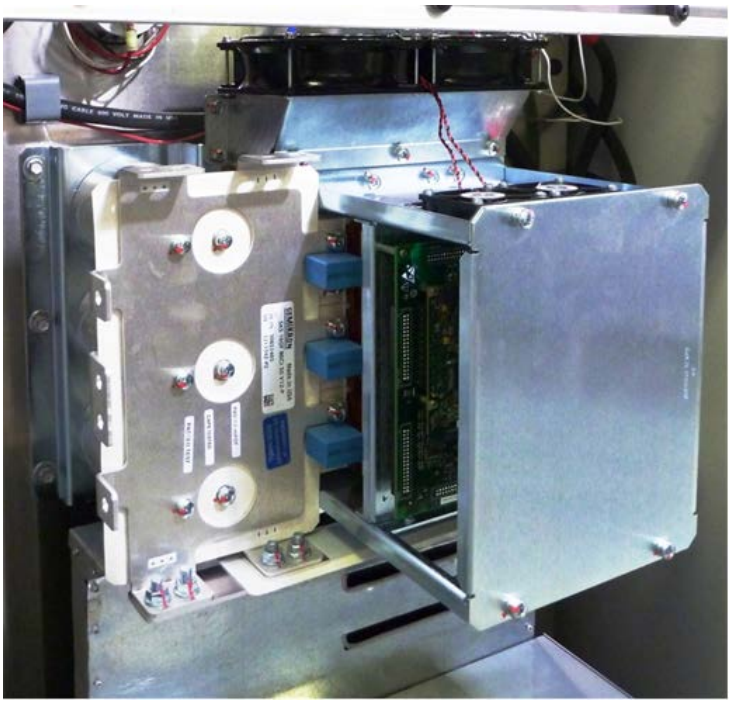

3.2 Advanced Controller Board Prototype

NREL worked with another vendor, National Instruments (NI), to develop a relatively low-cost yet state-of-the-art controller board for controlling the 50 kW power blocks. This new controller

board is based on NIs' single-board RIO (sbRIO) platform, which includes a 400 MHz PowerPC processor and Xilinx FPGA. The controller board consists of two parts: an off-the-shelf NI sbRIO used as the computation platform, and a newly designed FPGA mezzanine card (FMC) to provide input/ outputs. Though designed for the 50 kW power block, this new controller board is a deployment-ready, commercial embedded system for high-volume production of grid-tied inverter, DC-DC converter, and motor/ generator drives and will have input-output signal compatibility with most standard IGBT intelligent power modules. The design allows control algorithms can be developed either by using the on-board FPGA or the targetable real-time processor, thus providing programming flexibility, and will help users to reutilize their already-generated IPs. The new controller board provides advanced programming capability so that the 50 kW power blocks can be used in various Smart Grid applications. The new controller board is shown in Figure 48.

Figure 48. Advanced controller board for 50 kW power block (a) sbRIO side, (b) connector side

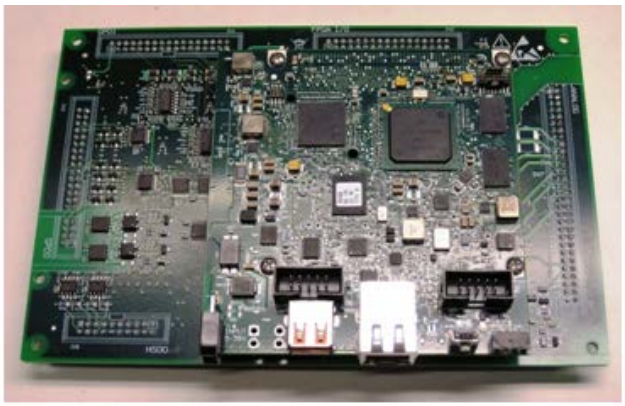

(a)

(b)

3.3 Graphical User Interface

NREL developed a wireless user interface so that the power block-based inverter system can be monitored and controlled through a wireless Apple iPad application. Through the application,

an operator can view real-time measurements, control the mode of operation and other settings, and export customized data. This iPad application demonstrated how the modular power block based power electronics could blend into the Smart Grid monitoring and control framework. Various pictures of the native iPad application and the user interface screens are shown in Figures 49 through Figure 51.

Figure 49. (a) NREL developed native iPad application for power block-based inverter system, (b) screen showing system status

(a)

(b)

Figure 50. (a) Password-protected control mode change screen, (b) screen showing different control modes and set points

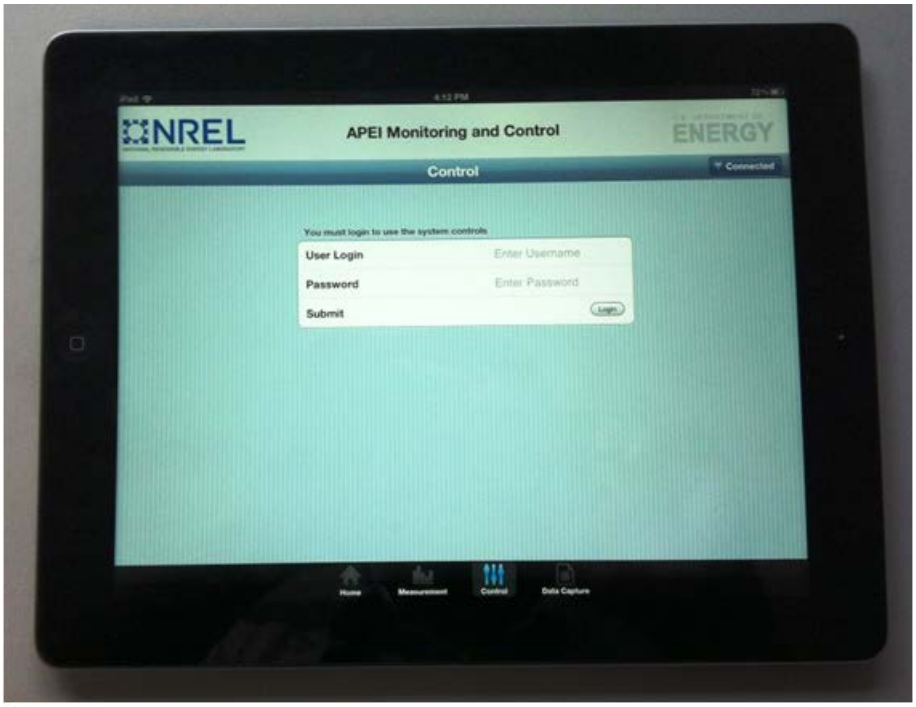
NREL
APEI Monitoring and Control
ENERGY
Control
Connected
You must login to use the system controls
User Login
Enter Username
Password
Enter Password
Submit
Login
Home
Measurement
Control
Data Capture

(a)

NREL
APEI Monitoring and Control
ENERGY
Control
Connected
System Power
ON
System Log
Inverter Power is: ON
Mode Request
VAR Mode
Power Factor Mode
Advanced Functions
kVAR Request (kVAR)
25
Lead/Lag
Lead
Update Settings
Home
Measurement
Control
Data Capture

(b)

Figure 51. (a) Screen showing various measurements, (b) screen showing data storing options

(a)

(b)

3.4 Connector Board

NREL also developed a PCB that would interface between the inverter controller board and the 50 kW power block driver circuit. This PCB stacks directly on the controller board and allows the user to easily connect to the power block and to other external devices such as sensors, relays, contactors etc. The proposed PCB will also provide easy connection of voltage and current sensors that output currents proportional to the measured quantities. Finally the interface PCB will provide option for the users to incorporate a unipolar DC supply for the gate drivers and bipolar power supply for external sensors. Pictures of the initial prototype connector board are given in Figure 52.

Figure 52. Connector board (a) controller board side, (b) user connector side

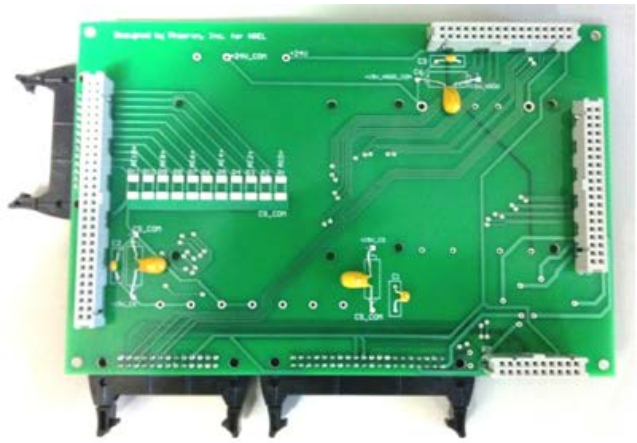

(a)

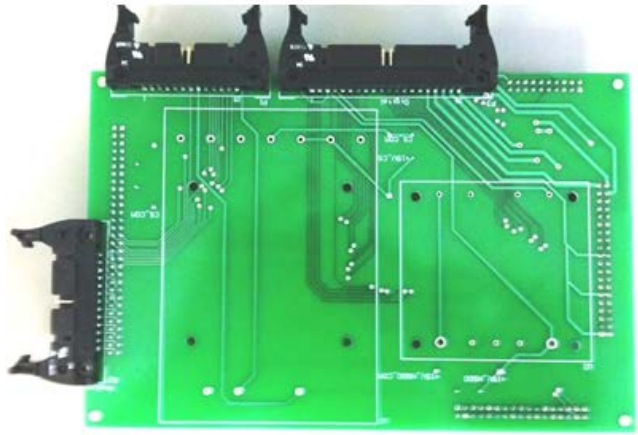

(b)

3.5 Test Setup

3.5.1 Three-Phase Inverter

NREL acquired preproduction prototype power blocks and the controller boards from the vendors, and designed a three-phase inverter platform to test these prototypes. The design utilizes the NREL-developed 50 kW modular power block as the main power electronics component. The NREL-developed power electronics controller board is used to implement control algorithms for the PV inverter. The inverter design packages the 50 kW power block along with other inverter components in a 60" (H) x30" (W) x30" (D) cabinet.

In addition to the power block, the inverter consists of three-phase filter inductors, three-phase filter capacitors, external voltage and current sensors, a DC contactor, a three-phase AC contactor, and auxiliary power supply. Various protection devices such as a DC disconnect, an AC circuit breaker, DC and AC surge suppressors, ground fault protection, and an emergency power-off (EPO) is included in the design. The inverter generates 208 VAC and ties to the 480 VAC grid through a common three-phase, 208 V delta–480 V wye, 60 Hz isolation transformer located outside of the cabinet. The cabinet is designed with forced air-cooling.

Given below are a few design features of the new grid-tied PV inverter:

- The design is based on the modular, scalable, and highly integrated 50 kW power block.
- The size and weight of the cabinet is smaller than commercial ones due to the exterior placement of the transformer. This will give user the flexibility to use outdoor pads for installing the transformer.
- Multiple inverters can be paralleled at the transformer provides scalability and redundancy.
- All capacitors used in this design are film capacitors, which will significantly improve the reliability.
- Several voltage relays are used as a backup to the software based protection in case of wrong operation of the input DC and/ or output AC contactors.
- Various levels of electrical protection are included in the design to protect the inverter electronics in case of a power system transient or malfunction. An EPO switch is included that will open all DC and AC connections in case of emergency shutdown needed the user.
- The cabinet layout is made in such a way that the high- power electrical terminals are properly insulated from accidental touch. In addition, the DC disconnect and the AC circuit breaker have door integrated interlock, thus preventing inverter operation when the front door is opened.
- The new controller board used in the design provides the advanced programming and communication capabilities so that the PV inverter can be used in emerging Smart Grid applications.

Various pictures of the NREL-designed three-phase inverter test system with power blocks are shown in Figures 53 through Figure 55.

Figure 53. Front side of the NREL-developed inverter

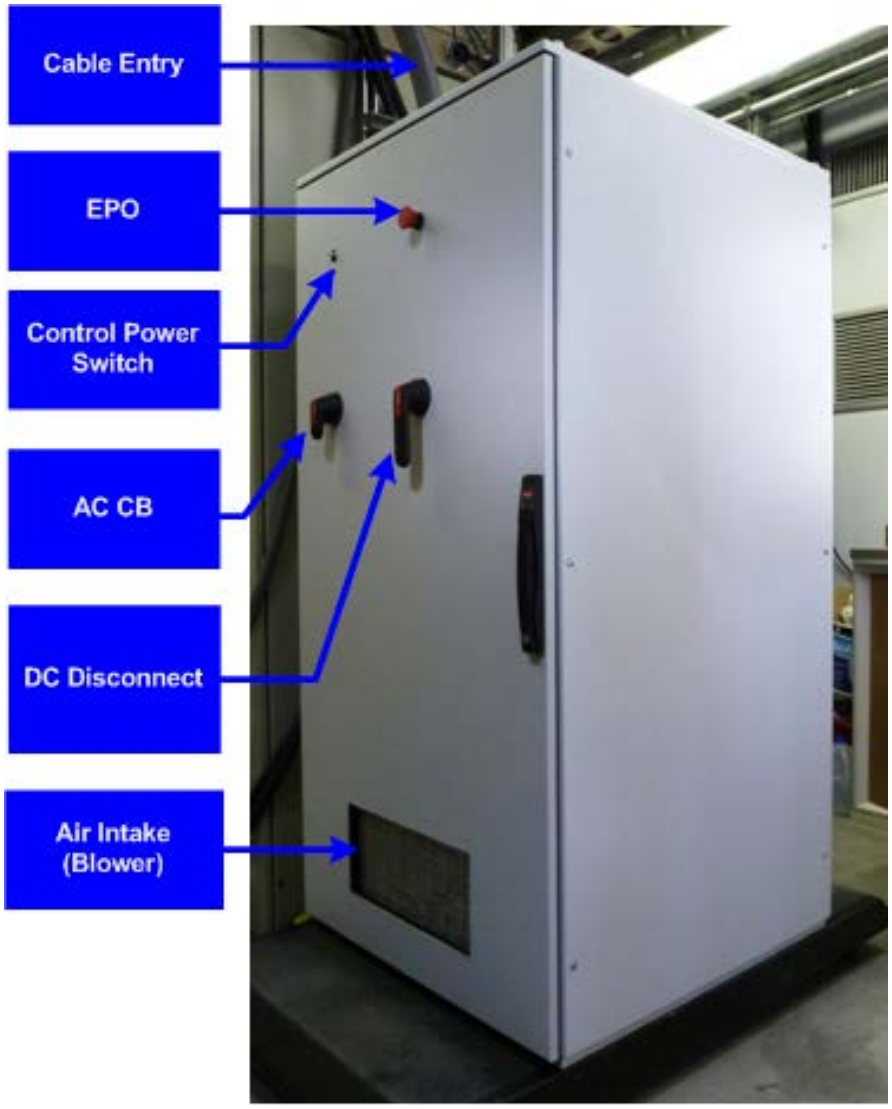

Figure 54. Front side of the inverter cabinet – inside view

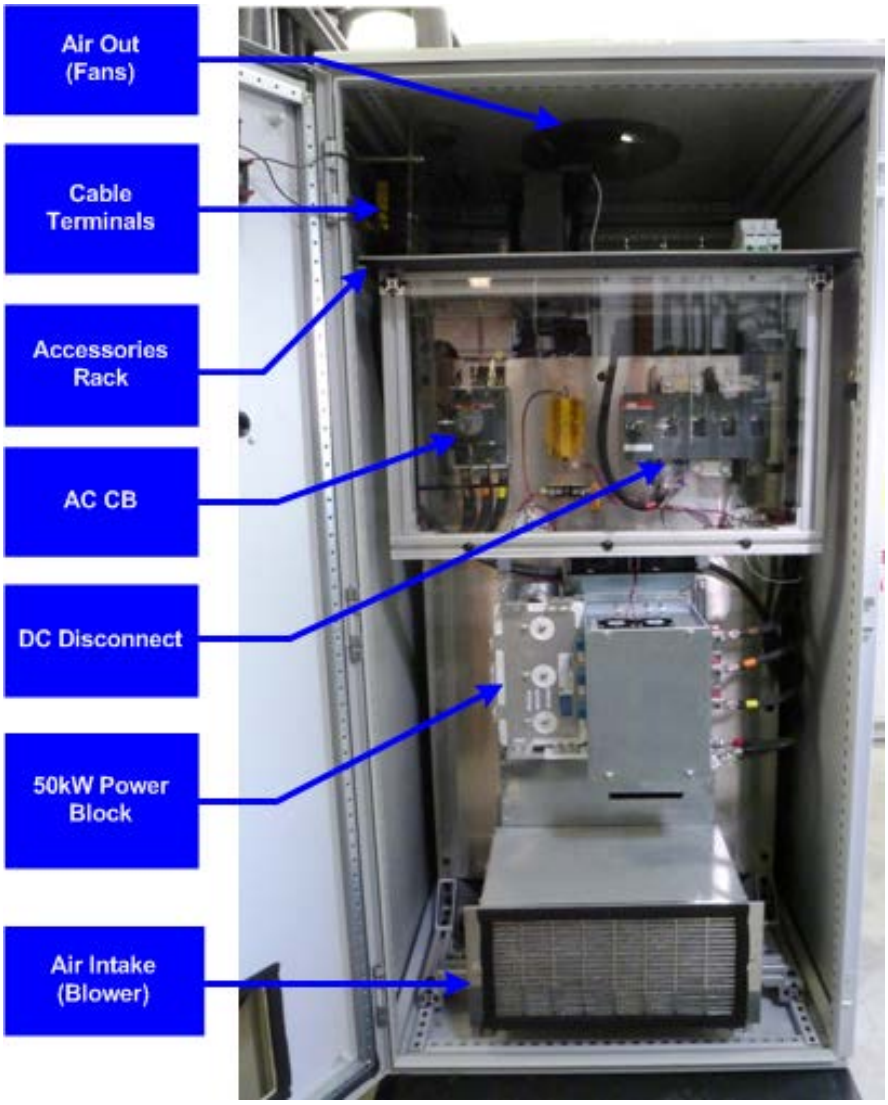

Figure 55. Back side of the inverter cabinet – inside view

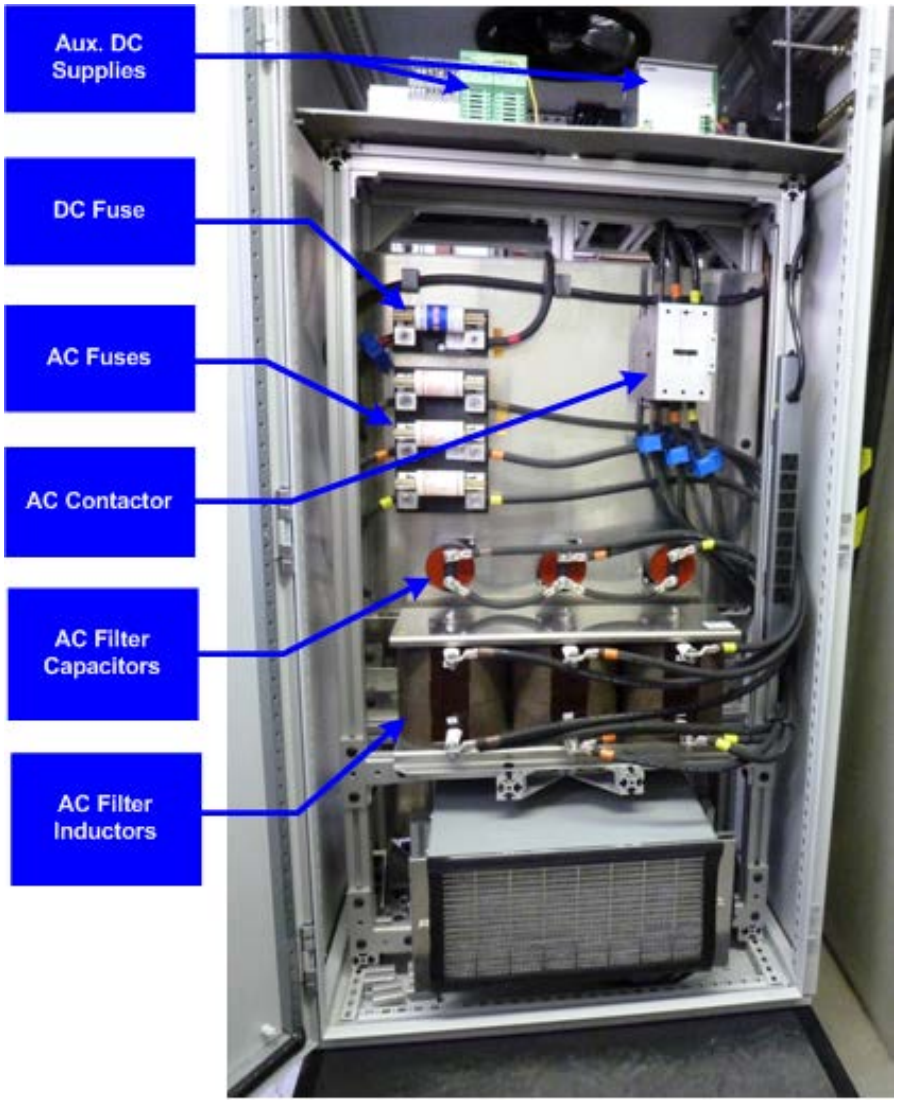

3.5.2 Inverter Test Setup

In addition to the inverter platform, other equipment such as a DC voltage source, an AC grid simulator, and a controllable RLC load bank were connected in the inverter test setup as shown in Figure 56.

The dual-channel DC supply used for the inverter setup was AV-900 from Aerovironment. The AV-900 can source/ sink DC power up to 250 kW, with a voltage range of 8 to 900 VDC and a current range of ±1000 ADC. For this setup, AV-900 was used as a voltage source and the DC voltage between 400-500 V was used. For the grid simulator, a Pacific Power AC source was used. An array of four grid simulators are available that can be controlled to generate three-phase programmed voltage up to 480 V at 200 kW. In this test setup, the grid simulator output was set at 480V, 60Hz. The load bank used for the setup was a customized version of the

Simplex Titan model, shown in Figure 56. This load bank can sink 165 kW real and 404 kVAR inductive and capacitive powers in step sizes as small as 125 W and 312.5 VAR. The test results, as shown in the next section, were collected using a Yokogawa DL 750 scopecorder.

As discussed before, the output of the inverter was tied to the grid simulator through a three-phase, 150 kVA, 208 V delta-480 V wye, 60 Hz transformer. This transformer provides electrical isolation between the inverter and the grid as well as gives a way to connect single-phase loads. In the present setup, the inverter generates 208 VAC. The secondary voltage of the transformer is 480 VAC and it is connected to the grid simulator. Depending on the customer requirement, the 208 V, delta-208 V, wye transformer can also be used in the future to connect to a 208 V grid.

Figure 56. Diagram of the inverter test setup at NREL

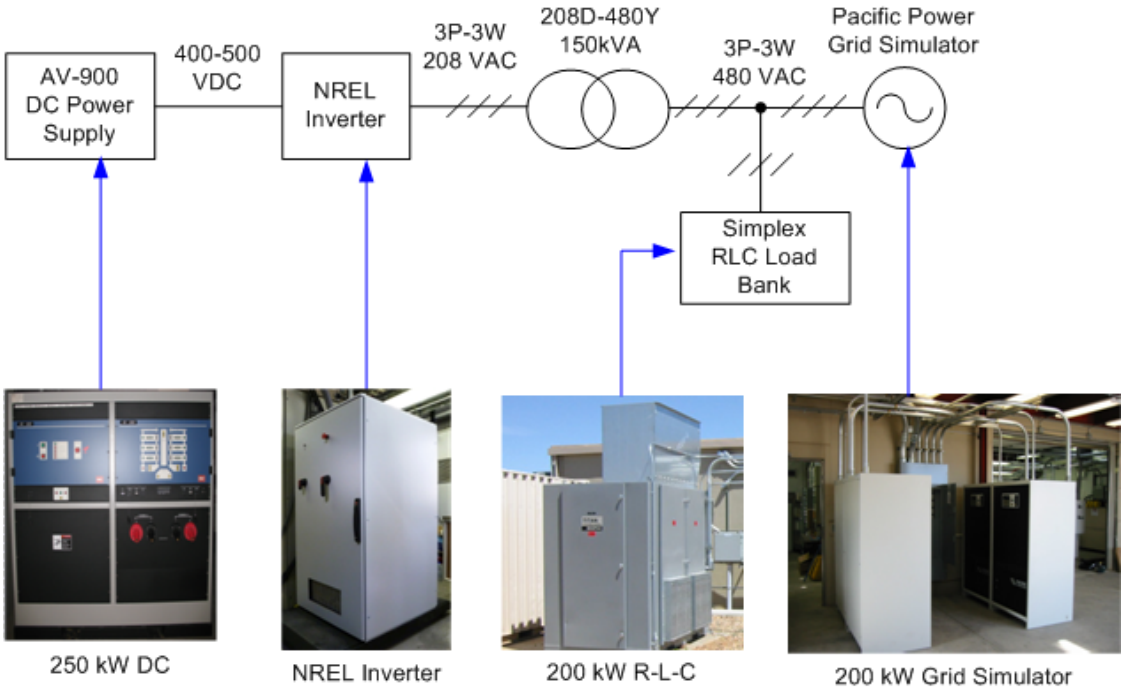

3.6 Test Results

Various tests were conducted on the components as well as on the power block itself to evaluate communications, control, and power operation. System acceptance tests were conducted at the Semikron USA facility. Semikron performed multiple tests to validate safe and proper operation of the 50 kW power block. The Semikron personnel conducted the operating limit tests. The advanced controller board was tested at the NI's facility for all the required input-output functionalities. In addition, NREL engineers performed tests on the controller board to evaluate functionality.

Once all the component level testing was completed, NREL proprietary control algorithms were implemented and verified in the advanced controller board using the NREL HIL system in which the actual controller board was put into the loop with the HIL based inverter model. Finally the algorithms were implemented for the actual inverter hardware. The focus of these tests was to verify the basic grid-tied inverter operation followed by some of the IEEE STD 1547

interconnection functionalities and some advanced functionalities. In order to maintain NREL's code as confidential, NREL staff maintained sole control of the software code and software integration efforts were performed by NREL staff on NREL computational resources.

3.6.1 Basic Grid-tied Inverter Operation

In these tests, the NREL-developed inverter was operated as basic grid-tied connected to the utility grid and sharing load with the grid. The inverter was controlled in current-control mode. The output current of the inverter was controlled based on the current reference values provided by the user. A phase-locked-loop was used to synchronize the inverter output voltage with the grid voltage. The PWM switching frequency was kept at 10 kHz with a dead time of 3 µs. In these tests, AV-900 was regulating DC bus at 400 VDC (except for higher currents when the DC voltage was set to 500 VDC) and the Pacific Power grid simulator regulating AC bus at three-phase 60 Hz, 480 Vrms line-line.

Various test results for the basic grid tied operation were performed. Figures 57 (a)-(e), demonstrate test results during grid-tied operation of the inverter at various current reference amplitudes. In each of these tests, the inverter output current output phase was set to unity power factor (UPF). The test results showed that the inverter output current is following the reference current with considerable accuracy.

Start-up transients test results for the inverter are shown Figures 58 (a)-(c). In these figures, the inverter was started with three different current reference values. The inverter start-up current transients were found to operate within acceptable limits. It is typically common to start the inverter with zero current value to minimize the transients.

The waveform traces shown in Figures 57 (a)-(e) and 58 (a)-(c) are labeled as follows:

Cyan: DC voltage

Yellow: DC current

Purple: Phase A line-neutral voltage

Magenta: Phase A line current

Green: Phase B line current

Blue: Phase C line current

Figure 57. Grid-tied inverter at UPF with different peak current reference set points (a) 0 A pk, (b) 20 Apk, (c) 40 Apk, (d) 60 Apk, (e) 80 Apk, (f) 118 Apk

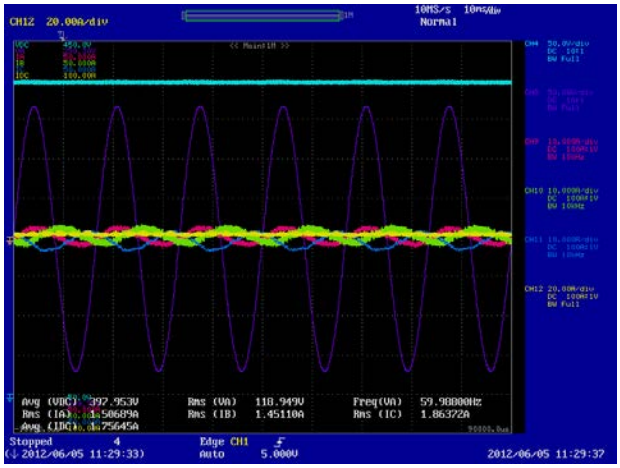

(a)

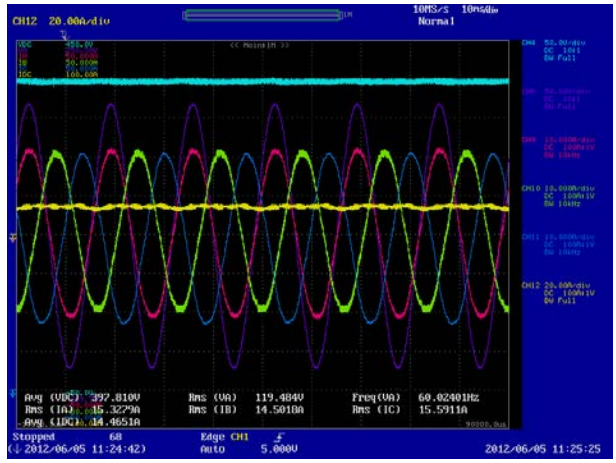

(b)

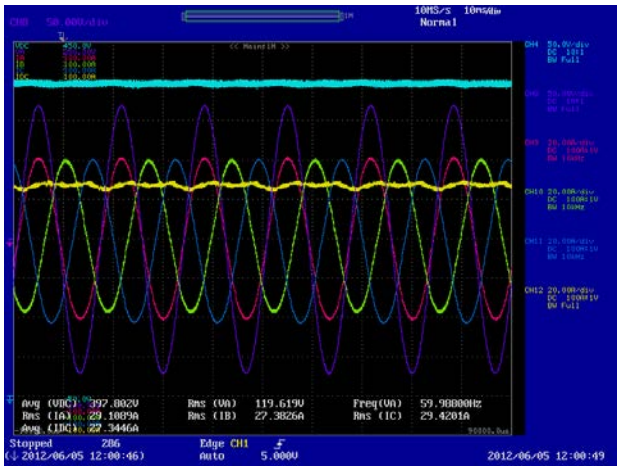

(c)

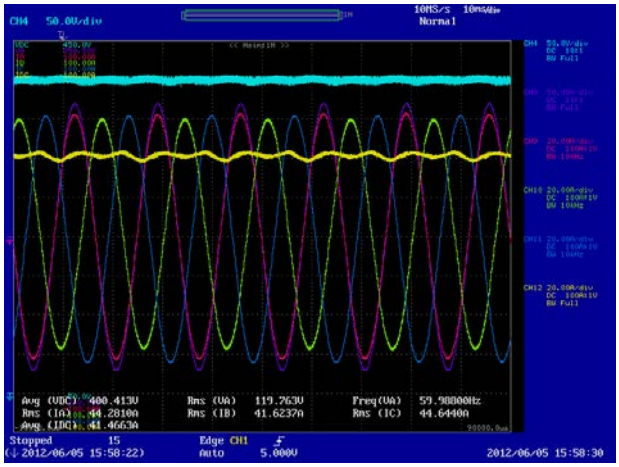

(d)

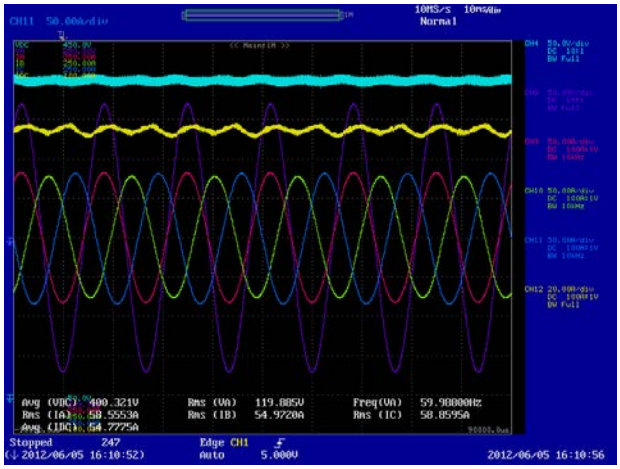

(e)

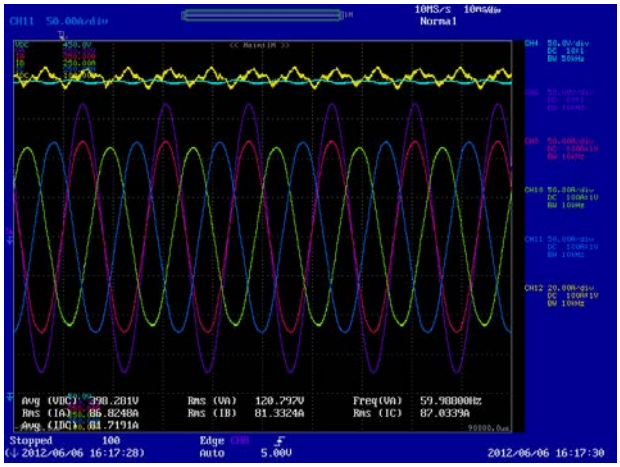

(f)

Figure 58. Start-up current transients for different peak current reference set points (a) 0 A pk, (b) 20 Apk, (c) 50 Apk

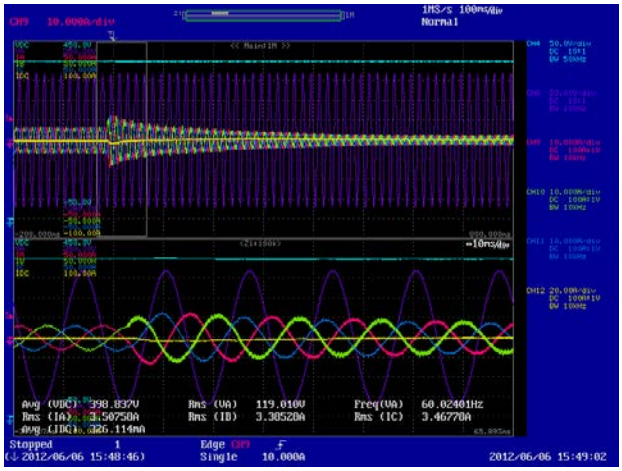

(a)

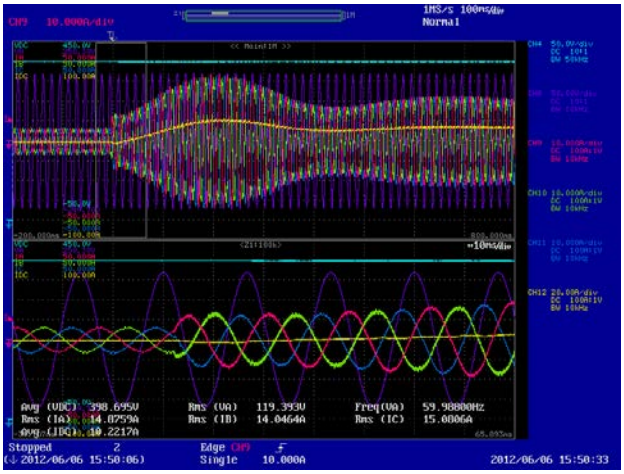

(b)

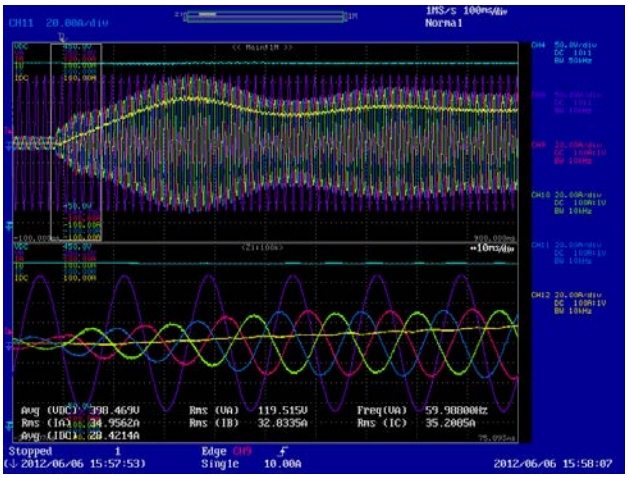

(c)

3.6.2 IEEE 1547 Interconnection

Sample IEEE 1547 tests were conducted to verify inverter operation for the grid disturbance. To determine the accuracy of the PLL frequency measurement, over and under frequency time tests were conducted. The tests were operated with an inverter output current set point of 100 Apk at UPF. For the over frequency tests, inverter over frequency trip limit was set to 60.4 Hz and a step change of grid frequency to 60.5 Hz was applied. For the under frequency tests, the inverter trip limit was set to 59.6 Hz and a step change of grid frequency to 59.5 Hz was applied. The NREL controller algorithm allows the user to set variable trip limit and trip delay for such frequency disturbance events. The effect of the delay parameter over the trip time was also verified. The results of over frequency trip tests are given in Figures 59 (a)-(c) and the results for under frequency trip tests are given in Figures 60 (a)-(c). It can be observed that the trip times can be varied by the user controllable trip delay. The trip time can easily be set within IEEE STD 1547 specified range as the frequency disturbance detection and interruption of the current only takes around 20ms. The waveform traces for Figures 59 (a)-(c) and 60 (a)-(c) are labeled as follows:

Cyan: DC voltage

Yellow: DC current

Red: Phase AB line-line voltage

Magenta: Phase A line current

Light blue: Grid frequency

The NREL island detection algorithm was implemented and tested to demonstrate its effectiveness to initiate a trip when an unintentional island condition was present. The active islanding detection method used for these tests were performed by driving the inverter output frequency out of bounds during islanded operation. Testing was performed by keeping the inverter on-line while it was connected to both the grid simulator and a resonant load. The load is configured as closely as possible to absorb the same amount of real power as being delivered the inverter, to have a resonant frequency of 60 Hz, and to have a quality factor of 1. A shunt trip signal is then sent to the grid simulator circuit breaker to cause an island. The testing is first conducted with island detection disabled, showing that the inverter remains on-line with output voltage near 60 Hz and 208 Vrms (before transformer) as shown in Figures 61 (a)-(b). The test was then repeated with island detection algorithms enabled. Since the purpose of these tests was to demonstrate the effectiveness of the island detection algorithms, not the actual IEEE Std 1547 disconnection compliance, the frequency limits were set at 55 and 65 Hz so that the frequency instability could be observed. The time delay was set to 10ms. The result with the island detection enabled is given in Figure 62. The waveform traces for Figures 61 (a)-(b) and Figure 62 are as labeled as follows:

Cyan: DC voltage

Yellow: DC current

Purple: Phase A line-neutral voltage

Magenta: Phase A line current

Green: Phase B line current

Blue: Phase C line current

Light blue: Grid frequency and Pink: Trip signal (5V/ div)

Figure 59. Over frequency trip times for different trip delays (a) trip time 30.2ms for a trip delay of 10ms, (b) trip time 54.3ms for a trip delay of 33ms, (c) trip time 100.1ms for a trip delay of 80ms

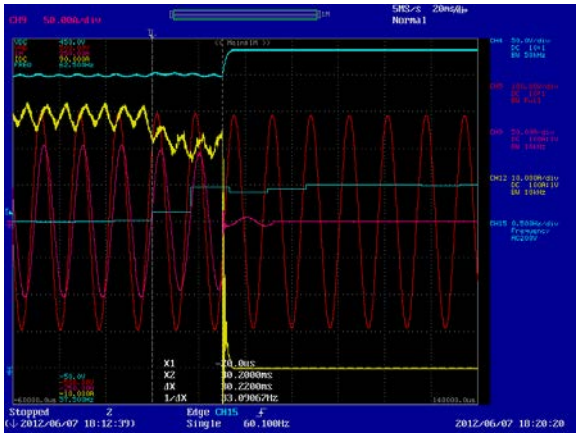

(a)

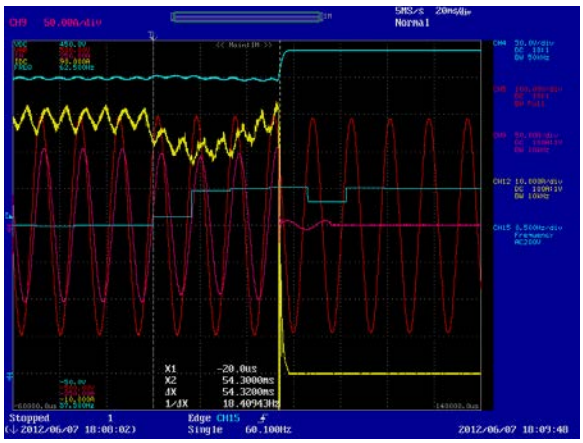

(b)

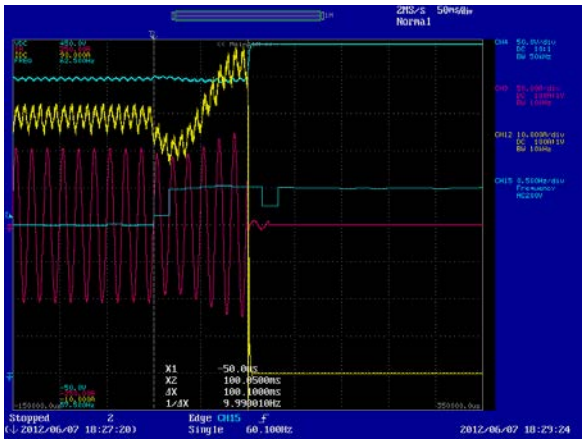

(c)

Figure 60. Under frequency trip times for different trip delays (a) trip time 29.8ms for a trip delay of 10ms, (b) trip time 53.1ms for a trip delay of 33ms, (c) trip time 99.8ms for a trip delay of 80ms

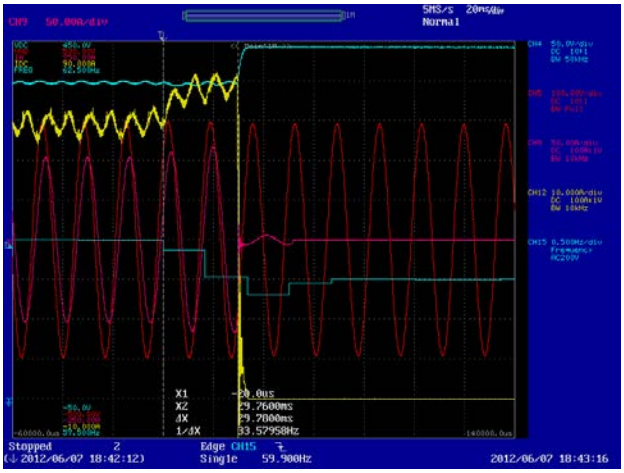

(a)

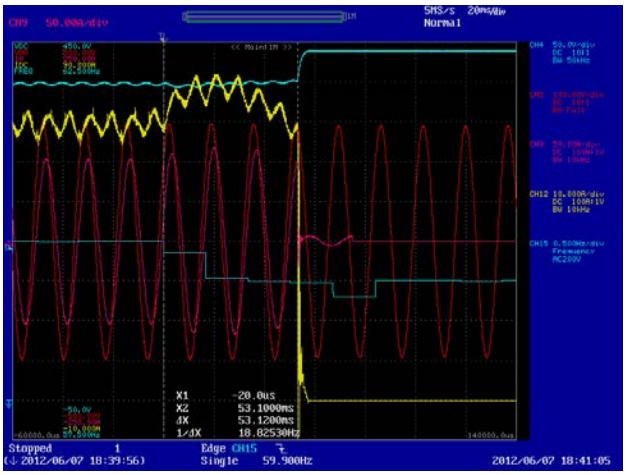

(b)

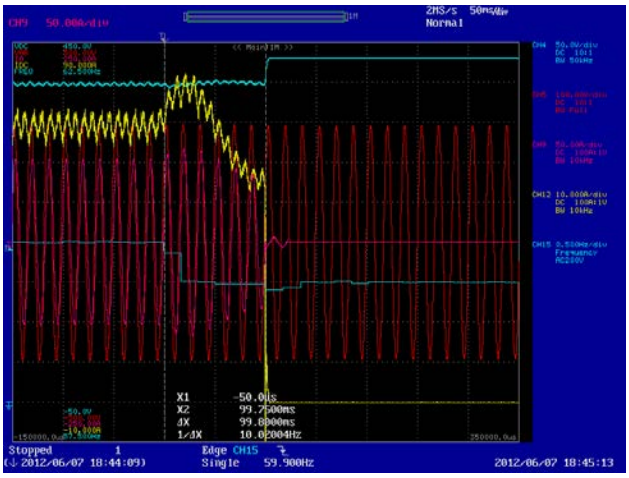

(c)

Figure 61. Islanded condition without any active island detection (a) zoomed at the time of grid trip, (b) zoomed at the end of window showing island continues 4 seconds after grid trip

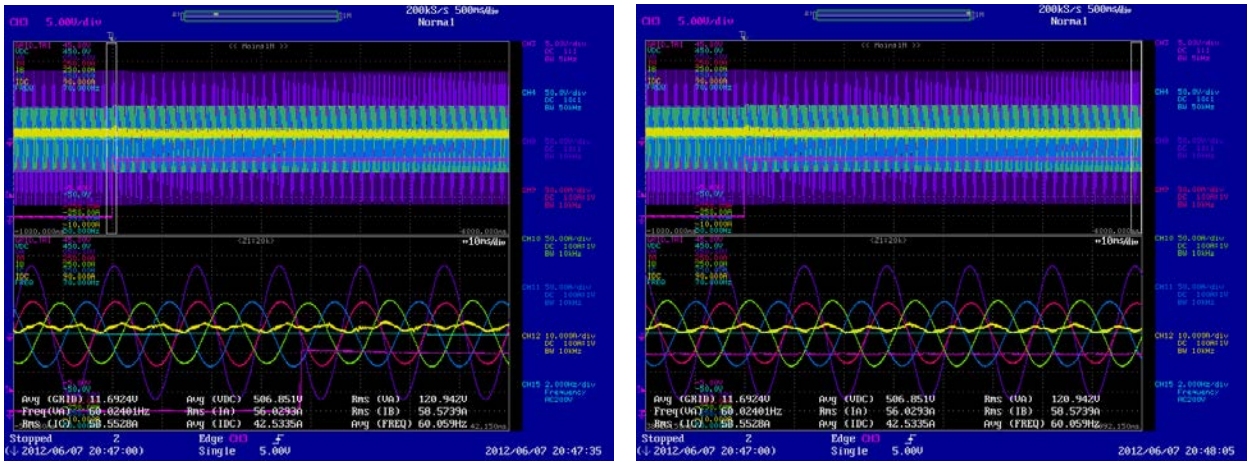

(a) (b)

Figure 62. Detection of island condition using island detection algorithm and subsequent inverter tripping

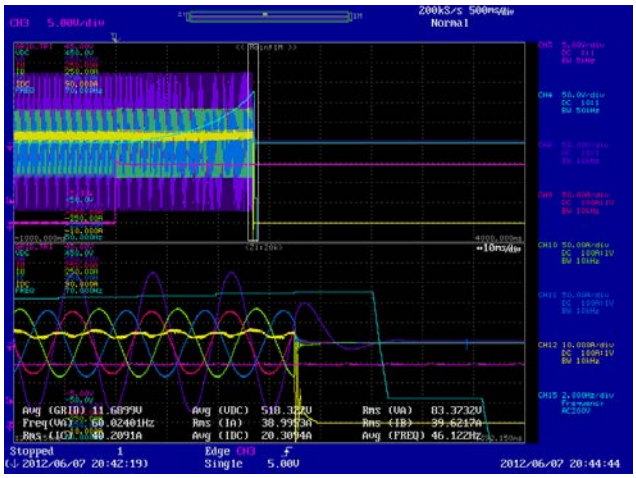

3.6.3 Advanced Functionalities

The power block based three-phase inverter system was tested to evaluate advanced inverter functionalities. In the first set of tests, the inverter was operated at different leading and lagging phase angles covering all four quadrants in the active and reactive power (P-Q) plane. Four-quadrant operation is the ability to produce real power or absorb real power along with the ability to produce lagging or leading VARs in any combination (McGranaghan, 2008). The ability of an inverter system to absorb real power provides advantages in some situations to assist to mitigate excess generation or to provide damping of power transients. This function also enables an inverter to do various advanced services such as VAR support, dynamic voltage regulation, and energy storage charge/ discharge. Figures 63 (a)-(h) show the results of the inverter operating in all four quadrants with a peak current amplitude of 40 Apk. The positive phase angle indicates that the line current leads the line-neutral voltage, and the negative phase angle indicates that the line current lags the line-neutral voltage. The results show that the controller operated in saturation for the angle of -45° for 40 Apk. By increasing the DC bus

voltage from 400 VDC to 500 VDC, tests showed that the inverter could operate in all four P-Q quadrant operations at an output current of 100 Apk.

The waveform traces for the Figures 63 (a)-(h) are labeled as follows:

Cyan: DC voltage

Yellow: DC current

Purple: Phase A line-neutral voltage

Magenta: Phase A line current

Green: Phase B line current

Blue: Phase C line current

Inverter was tested to demonstrate how the system would respond during a low-frequency ride-through (LFRT) event. In this case, the inverter low frequency trip limit was set at 59.6 Hz and the trip delay was set to 2.5s. This implies that that the inverter will be on for 2.5 seconds for a low frequency event. During the tests, grid simulator frequency was varied in step from 60 Hz to 59.5 Hz and then the grid simulator was set to run at 59.5 Hz for 2s before stepping back to 60 Hz. The results of the LFRT event are given in Figures 64 (a)-(c). A simplified LVRT control algorithm was used for the testing. Production LFRT capable inverter would require additional time delays depending on the magnitudes of the frequency disturbances.

The waveform traces for the Figures 64 (a)-(c) are as labeled as follows:

Cyan: DC voltage

Yellow: DC current

Red: Phase AB line-line voltage

Magenta: Phase A line current

Light blue: Grid frequency

Figure 63. Grid-tied inverter with current reference set at 40 Apk with different phase angles (a) 0°, (b) 45°, (c) 90°, (d) 135°, (e) 180°, (f) -135°, (g) -90°, (h) -45°

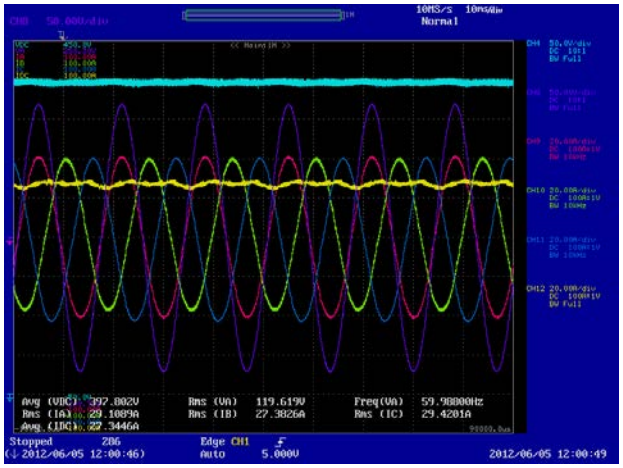

(a)

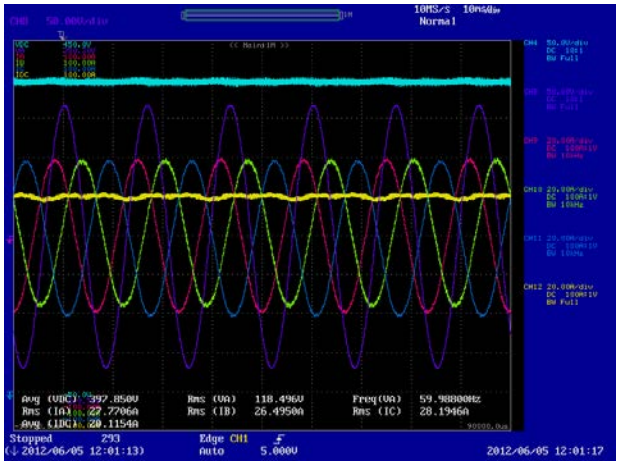

(b)

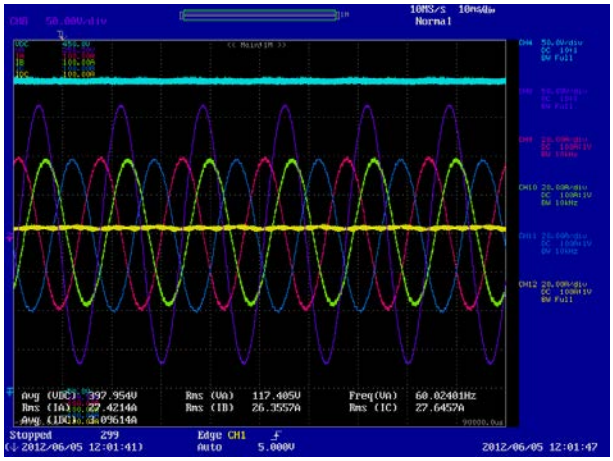

(c)

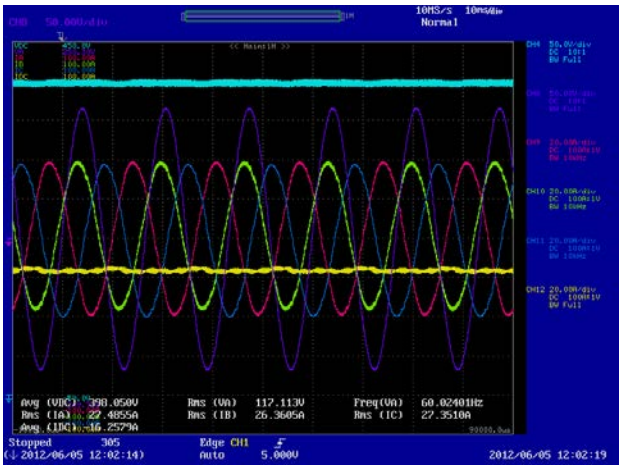

(d)

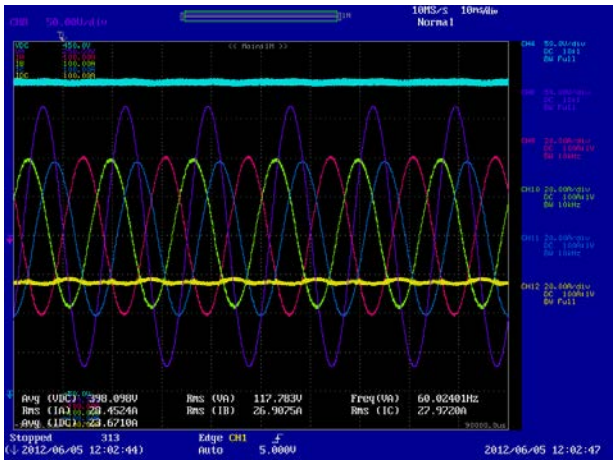

(e)

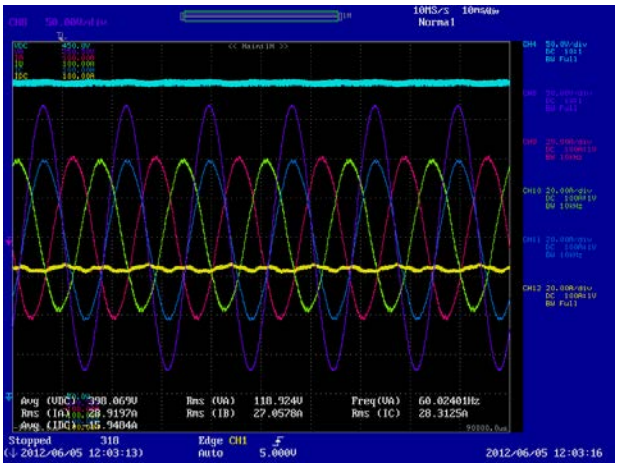

(f)

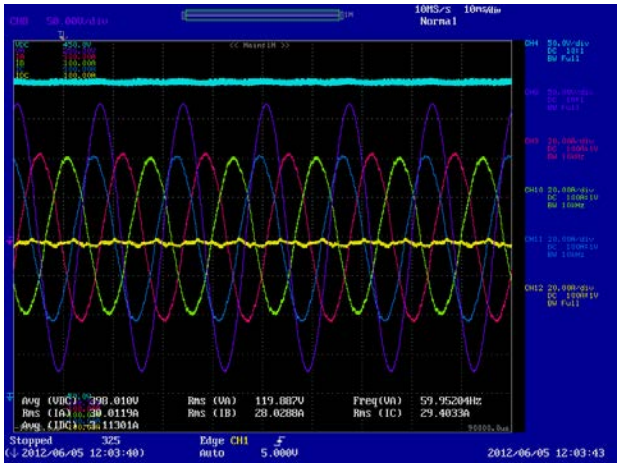
10MS/s 10ms/div
Normal
Avg (VDC) 398.010V
Rms (VA) 119.887V
Freq(VA) 59.95204Hz
Rms (IA) 30.0119A
Rms (IB) 28.0288A
Rms (IC) 29.4033A
Avg (IDC) 0.11301A
Stopped 325
Edge CH1
Auto 5.000V
2012/06/05 12:03:40
2012/06/05 12:03:43

(g)

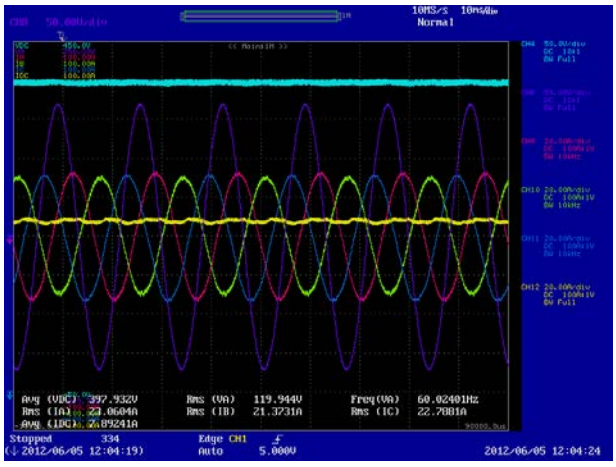
10MS/s 10ms/div
Normal
Avg (VDC) 397.932V
Rms (VA) 119.944V
Freq(VA) 60.02401Hz
Rms (IA) 22.0604A
Rms (IB) 21.3731A
Rms (IC) 22.7001A
Avg (IDC) 0.09241A
Stopped 334
Edge CH1
Auto 5.000V
2012/06/05 12:04:19
2012/06/05 12:04:24

(h)

Figure 64. Inverter's continued operation during a LFRT event (a) response of the inverter, (b) zoomed at the time of step change from 60 Hz to 59.5 Hz (c) zoomed at the time of step change back to 60 Hz

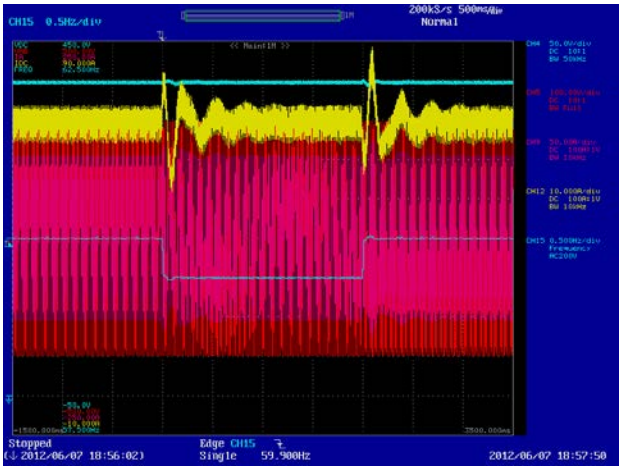

(a)

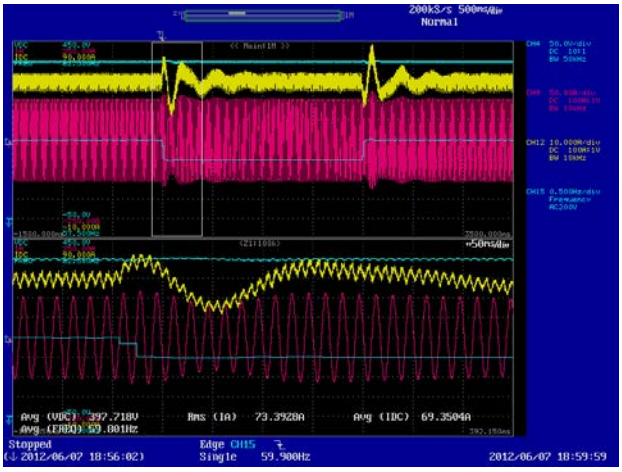

(b)

(c)

3.7 Cost Analysis

Power electronics accounts for a significant part of the distributed energy systems cost. One of the goals for the APEI initiative project was to reduce the cost of power electronics. In the mid-power APEI subtask, it was envisioned that developing a modular power electronic system that can be used in multiple applications would result in a lower cost due to economies of scale. NREL worked with Semikron to develop a 50 kW power block and worked with NI to develop the advanced controller board. Both of the systems use off-the-shelf parts and already-proven integration methods used in other applications, reducing development cost. Also the flexibility included in the design of the power block and the controller board made them suitable for multiple applications. According to the price quote received from the vendor Semikron, for the volume of one thousand the price for each 50 kW power block will be $2,200. The price of the controller board for the volume of one thousand will be $605. Therefore the total price of the power block and controller will be $2,805; which translates to $0.06/ Watt. This cost is lower than the cost of similar power blocks used in transportation and other applications.

In addition to the power block, a typical 50 kW inverter consists of the output power filter, high power isolation transformer, protection, high power contactors, sensors, auxiliary power, cabinet, and miscellaneous mechanical and electrical components. During the course of the project, NREL built a couple of prototype inverters. The prices of such prototype inverters were much higher due to the higher component costs for smaller volume purchases. Manufacturers can typically reduce the price of a component if they buy the components in bulk. The labor necessary for a single device will be greater than the labor needed per device when the device is bought in large quantities. As the high volume production was the main basis of this project's cost goal, the volume price of one thousand is used as the basis of cost calculations. The high volume costs of the NREL-developed inverter were calculated based on the quotes received from the vendors/ distributors for such quantities. For very few of the components, actual volume pricing could not be obtained. Approximate pricing was used for such components.

The materials cost of the NREL-developed inverter in quantities of one and one thousand is compared in Figure 65. In addition to that, two commercially available inverters' retail costs are also shown in the same figure. It can be seen from the figure that in quantities of one thousand, the NREL-developed inverter will cost around $0.30/ W which is slightly higher than the project cost goal of $0.25/ W. It is important to note that all these calculations are estimates from single vendors/ distributors, without considering competing vendors. Actual production cost will most likely be lower than the estimated cost after getting competitive quotes. The cost breakdown of the NREL-developed inverter in a quantity of one thousand is shown in Figure 66.

Figure 65. NREL-developed inverter material price with varying quantities

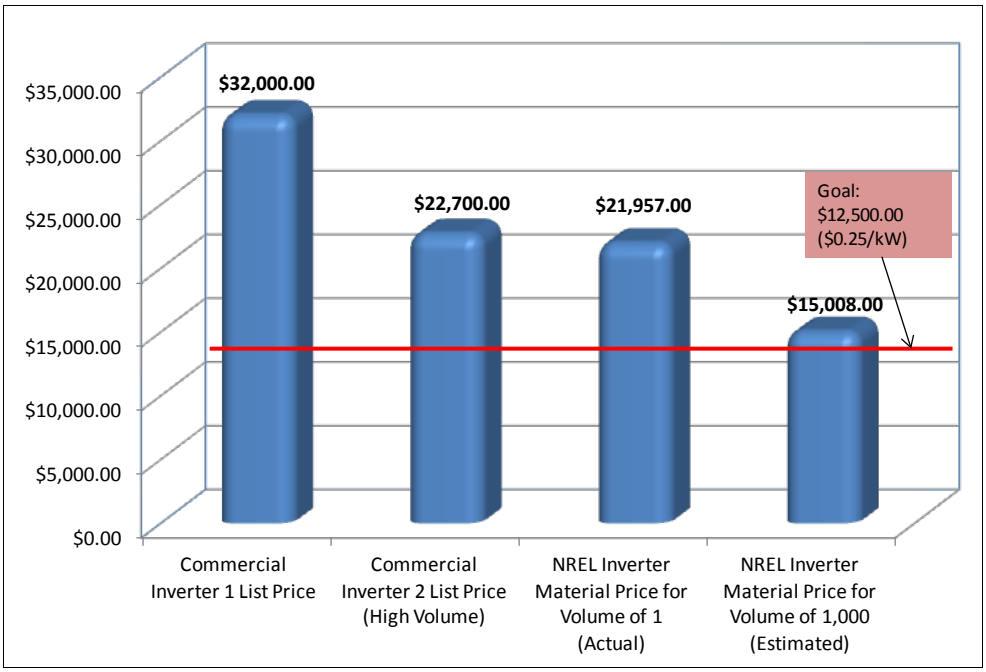

Figure 66. Estimated single inverter cost breakdown for quantities of one thousand (estimates assume using same parts as in NREL prototype inverters)

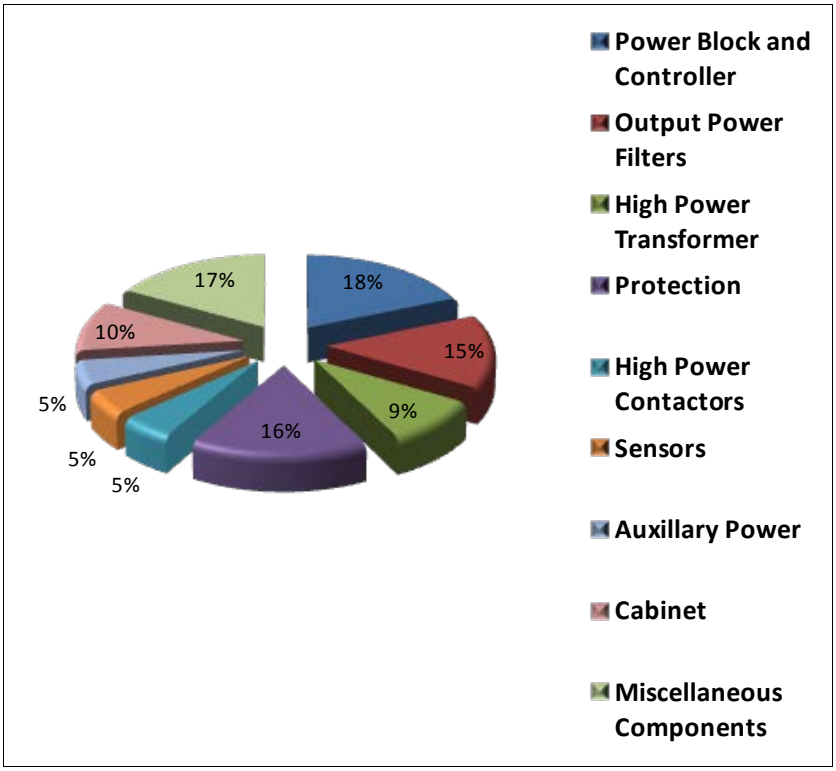

3.8 Field Demonstration

The purpose of this subtask was to provide the pre-production prototype power blocks to manufacturers that develop power electronics for the distributed energy market. The task was to include a request for proposal (RFP) solicitation where selected manufacturers would then be required to utilize the power blocks in their prototypes. Under the contract, these power block users would have to compare the engineering and manufacturing costs, efficiency, and reliability to their typical designs with the new 50 kW power block design.

During testing of the power block prototype developed under Task 2.3, additional design changes were implemented to make the power block more robust. For example, tests of earlier prototypes showed that the DC bus design created high stray inductances thus overheating the pole snubber capacitors. A new DC bus design and implemented to and testing showed that the new design eliminated the overheating problems. Semikron delivered preproduction power blocks to NREL in mid-April, 2012. Also during the Task 2.3, it was found that the generic controller board that came with the Semikron power block prototype was not flexible enough for the APEI project. As a result, NREL searched for other controller board options and in mid-2011, partnered with NI to develop a new controller board based on NI's sbRIO platform. The initial prototype controller board was delivered in late March and programming changes were made for the new platform. Further design changes were made to the NREL inverter so the power block could be integrated with new controller board. Only limited field-testing could be accomplished at NREL laboratory facilities prior to the end of the project's period of performance. As such, RFP to evaluate the pre-production prototypes in a full-scale field test could not be completed as proposed.

3.9 Conclusion

Under the mid-power APEI subtask, NREL successfully demonstrated a new 50 kW APEI system utilizing highly reliable, high volume sub systems for both the switching and control hardware. The APEI was designed to be modular for parallel power block applications and the controller board can be easily programmed using both the National Instruments and Mathworks Simulink control development platforms. Pre-production prototypes of both the Semikron Power Block and the NI controller board were provided to NREL with a design that is expected to reduce cost, improve performance, and at the same time provide advanced functionality. Both the power block and controller designs can be used for not only grid-tied PV systems but can also be used for grid-tied battery systems and variable speed motor control systems. Also as part of this work NREL developed a wireless user interface to demonstrate how the APEI can be monitored and controlled through a wireless Apple iPad application. NREL also developed a printed circuit board design that provides an electrical interface between the NI inverter controller board and the Semikron 50 kW power block driver circuit. Using a systems integration design approach, a mid-power APEI is ready to be manufactured that will a low cost, reliable and flexible advanced power electronics design up to 100 kW.

NREL successfully implemented grid-tied inverter control algorithms using the 50kW APEI power block platform and conducted demonstrated advanced functionality. Test results showed the APEI can be operated in full four-quadrants of active and reactive power (PQ) plane as an inverter. The inverter platform can be used in multiple applications such as power transient damping, VAR support, dynamic voltage regulation, and energy storage charge/ discharge. The use of the same power block in various applications is very important to achieve cost reduction goals through larger economies of scale.

The power block and controller board contractors are ready to manufacture their respective APEI components. Future work could include further hardware and software development and re-design as necessary to conduct field-testing of the mid-power APEI before moving the mid-power APEI technology to full-scale production.

Chapter 4:
Energy Technologies – Moving Forward

4.1. Renewable Electricity

Renewable electricity sources are inherently variable—not intermittent. For example, a wind turbine installed in a reasonably good wind resource will generate electricity about 80 percent of its lifetime (assuming a typical Rayleigh distribution). However, the same system is not always operating at its rated capacity so the average annual capacity factor can range from 25 percent – 45 percent depending on the wind resource. It therefore seems reasonable and fair to describe the natural power production of renewable electricity sources as variable. Whereas describing their operation as intermittent is likely to conjure up images of a system alternating between functioning properly and improperly; akin to an intermittent light switch or power cord.

PV and wind energy are by nature distributed generation technologies, whereas concentrating solar power (CSP) takes advantage of economies of scale in a centralized plant. Therefore, small wind and PV are unique among generation technologies in that their distributed nature allows them to be integrated at very small scales. CSP is a proven technology and today's silicon-based and thin-film PV technologies are steadily advancing.

In 2010, the International Energy Agency (IEA) suggested that PV and CSP (more or less evenly split) could provide about 20 percent – 25 percent of global electricity production by 2050. The Energy Commission estimates that PV alone accounts for 17 million megawatts (MW) of potential out of a theoretical 18.2 million MW from all renewable energy technologies (Staff Draft, 2011). To develop the roughly 1 million MW (theoretical maximum) of CSP potential, transmission expansion will be required in remote areas of the California desert where direct sunshine is most abundant.

As retail electricity rates continue to rise and PV costs maintain their current descent, it seems reasonable that electricity from these home-based systems may no longer need incentives to be cost competitive. It is worth noting that some PV technologies require rare elements like silver, indium, cadmium and tellurium, which may become limited in the next 20 years due to material shortages. It is encouraging, however, that a variety of emerging PV technologies (e.g., advanced thin-film, organic and polymer solar cells) are at various levels of maturation that will provide opportunities to continue cost reductions expected in the coming decade.

Today, power purchasing agreements for renewable electricity projects are beginning to show lower levelized costs than traditional generation. Since the Public Utility Regulatory Policies Act (PURPA) of 1978 and California policy incentives of the early 1980s, renewably generated electricity has been growing at impressive rates. California is on track to achieve 20 percent of its energy by 2013 to meet their renewable portfolio standard. Furthermore, there are 13 significant transmission upgrades at various levels of completion to deliver the renewable generation to meet California's goal of 33 percent by 2020 (Staff Draft, 2011).

4.2 Distributed Energy

DER refers to a variety of smaller (typically 1 – 2 MW), modular power-generating technologies that can be combined with load management and energy storage systems to improve the

quality and/ or reliability of the electricity supply. They are also described as distributed because they are placed at or near the point of energy consumption, unlike traditional centralized systems, where electricity is generated at a remotely located, large-scale power plant and then transmitted down power lines to the consumer.

Energy systems once designed for bulk production of electricity and fuels are becoming much more distributed and interconnected. As new technologies are integrated into the energy system infrastructure, the pathways between production and end use are becoming more complex and interrelationships are forming between electrical, thermal, and fuel systems.

Implementing distributed energy can be as simple as installing a small, stand-alone electricity generator to provide backup power at an electricity consumer's site. Or it can be a more complex system, highly integrated with the electricity grid and consisting of electricity and thermal generation, energy storage, and energy management systems. Consumers sometimes own the small-scale, on-site power generators, or they may be owned and operated by the utility or a third party. Federal-level R&D is encouraging novel home-scale energy storage systems that will provide additional support and stability to the distribution system.

The focus is on design and performance of energy systems that are optimized at different but interrelated scales, ranging from individual homes and businesses to communities and cities to regional and national infrastructures, and can be aggregated to optimize energy pathways at any scale. By considering the relationships among transportation and fuel production systems, the built environment, electricity generation systems, and integrated energy systems, we can accelerate an energy system transformation.

4.3 Energy Storage

Emerging challenges in integrating renewable generation and highly variable loads with the existing electrical grid has motivated the development of low-cost stationary energy storage technology which could transform the U.S. electric power grid industry (Boston Consulting, 2011). Electric energy storage separates generation capacity and variable demand in space and time, with potential applications ranging from long-duration bulk energy storage to short-duration power quality and frequency regulation balancing (Electric Power, 2010).

To date, R&D on energy storage has focused on electricity due to its obvious and urgent role in multiple energy markets. Traditionally, electric energy storage was developed to increase base load demand by shifting bulk energy produced when loads are low at night to when demand is high during the day. Energy storage will provide flexibility and control at the transmission level, while also being capable of storing excess or otherwise curtailed renewable energy.

The incumbent technology for storage is pumped hydropower, which increases generation asset utilization from base load resources, such as nuclear or coal generators. New opportunities for the application of electrical energy storage have emerged with high-penetration variable non-dispatchable renewable generation sources such as wind and solar, and changes in distribution feeder load profiles, such as local clusters of high-throughput electric vehicle charging stations.

In addition, the increase in deployment of distributed renewable generation enabled by low-cost PV creates a potential need for storage resources at the perimeter of the grid, including low-cost storage on the consumer side of the meter to convert variable distributed generation assets into reliable low-cost power, and to avoid peak loads on the centralized grid.

4.4 Transportation

A shift to sustainable and low-carbon energy sources is also required by the transportation sector. The widespread deployment of cost-effective electrified light-duty vehicles represents a tremendous opportunity for dramatic reductions in U.S. oil imports by shifting the U.S. transportation energy supply from petroleum to electricity. In 2008, the transportation sector alone represented 70 percent of all U.S. petroleum consumption, 57 percent of which came from foreign sources. At the same time, nearly 95 percent of the nation's transportation energy came from petroleum, with light-duty vehicles accounting for more than 60 percent of this total (U.S. Department of Energy, EIA).

In addition to economic benefits, electric vehicles have the potential to dramatically reduce greenhouse gas emissions as the makeup of our electricity shifts towards carbon neutrality. The U.S. transportation sector is the single greatest contributor to the nation's greenhouse gas emissions, accounting for roughly 30 percent of all U.S. CO_2 emissions (Inventory, 2009). On a well-to-wheel basis, electric vehicles produce about 38 percent less CO_2 emissions than gasoline-powered vehicles, assuming the national average for electrical energy sources (50 percent coal, 18 percent gas, and 3 percent oil) (U.S. Department of Energy, 2011). Further reductions in CO_2 emissions are anticipated from electric vehicle adoption as the U.S. electrical grid continues to de-carbonize.

In order to realize the economic and environmental benefits of widespread electric vehicle adoption, batteries should provide for a driving range of at least 300 miles on a single charge and be competitively priced with conventional gasoline-powered vehicles. Despite recent progress in both cost and performance, chemistry-based energy density limitations may prevent current lithium-ion battery technology from achieving these goals. Widespread adoption of electric vehicles will require battery cells with more than double the current state-of-the-art energy densities at one-third of the cost.

The vast majority of drivers will require a vehicle to deliver driving ranges similar to those of modern gasoline and diesel vehicles. One all-electric vehicle that is already capable of greater than a 300-mile range is the hydrogen-powered fuel cell electric vehicle (FCEV). Another competitive advantage of the FCEV is its ability to completely refuel in about 5 minutes. Combined, these two advantages are helping to move FCEVs from auto manufacturer pilot fleets into California showrooms in the 2015 – 2017 timeframe.

Another opportunity for storing energy with high volumetric energy density for transportation is to combine renewable hydrogen and recycled carbon dioxide. A renewably produced synthetic liquid hydrocarbon would take advantage of the existing distribution infrastructure while helping transform our carbon-intensive transportation sector — which is a major contributor to net greenhouse gas emissions. Beyond land-based systems, the majority of the earth's wind resources is located in the deep, open ocean and is essentially inaccessible to current technology.

4.5 Smart Grid

Successful Smart Grid implementation and demand-side management require utilities and electricity customers to have access to advanced control tools and real-time market information. Development of interoperable, intelligent technology devices such as advanced power electronics technology will improve and accelerate the use of DER systems and act as an enabler

to the success of Smart Grid implementation. The future Smart Grid requires investment now to reduce investment risk that can hinder progress as it has with renewable energy sources.

4.6 Systems Integration

It will not be possible to develop an advanced energy system simply by incrementally improving the existing system. An integrated approach with optimized sub-systems will be required to realize the environmental, economic, and national security benefits of this transformation. Optimized sub-systems extend from energy production, energy carrier options, and distribution to customers and efficient end use. Smart grids will bridge electricity production and enable end users to help balance the future energy system by shifting demand in time.

Energy systems integration R&D is being pursued by the Energy Commission within the PIER Program to obtain a higher degree of performance optimization, robustness, and reliability from energy systems than would be possible with the traditional system view. While traditional systems engineering seeks to optimize an individual system, a system of systems approach seeks to optimize the design and performance of multiple systems. California currently utilizes vast hydrogen power resources to provide support services required to increase the penetration of distributed renewable electricity sources.

Improved integration of wind- and solar-generated electricity will rely on continuing to improve the forecasting of these varying renewable sources. Forecast error reduction will reduce standby capacity and enable transmission and generation dispatchers to better compensate for these naturally varying systems.

Currently, most power electronic devices are only developed for specific technology markets that may disqualify them from the cost advantages that larger market economies of scale can realize. For example, an inverter used to connect a solar array with the utility grid was designed exactly for that purpose. It contained only the components and controls necessary for that application, and is not compatible with any other renewable energy sources. The short-term advantage of this approach is a least-cost option for the specific application.

The long-term disadvantage, however, is that the narrow market opportunity for such a device disqualifies it from the cost advantages that larger economies of scale would realize. In other words, making a device that is acceptable to more technologies will likely bring down its overall cost because of higher production. Another disadvantage of the application-specific approach is higher lifetime maintenance costs because of less availability of replacement parts and less expertise of maintenance personnel. The APEI initiative is a coordinated plan to develop a modular architecture for standardized, highly integrated power electronics interconnection technologies for DER platforms and Smart Grid interoperability. The technical performance objectives support the PIER's primary program objectives that included the improvement of energy cost and value, and the reliability and quality of California's electricity system.

The underlying metric for a sustainable energy system with low CO_2 emissions is economics. It is also fair to recognize that fossil fuel-generated electricity externalizes a significant cost burden on society by not capturing and storing the CO_2 emissions from their process. Renewable technologies, on the other hand, are not given economic credit for the value of reduced risk against natural gas price volatility, reduced emissions leading to improved air quality, and

reduced medical costs due to reduced asthma complications—all while helping to avert the consequences and costs of severe climate change. In order to save our planet from the catastrophic effects of severe climate change while providing fair treatment of people of all incomes will require R&D, thoughtful policies, and investment in a diverse, flexible and reliable energy system. Finally, bringing about the future transformational energy system also requires a sense of urgency.

REFERENCES

Liserre, M.; Sauter, T.; Hung, J.Y. (March 2010). "Future Energy Systems: Integrating Renewable Energy Sources into the Smart Power Grid Through Industrial Electronics". IEEE Industrial Electronics Magazine.

Kramer, W.: Chakraborty, S.; Kroposki, B.; Thomas, H. (March 2008). "Advanced power electronic interfaces for distributed energy systems. Part 1. Systems and Topologies". National Renewable Energy Laboratory Report TP-581-42672.

McGranaghan, M.; Ortmeyer, T.; Crudele, D.; Key, T.; Smith, J.; Barker, P. (February 2008). Sandia Report SAND2008-0944 P.

AC120-5KL DC-AC Inverter Specification Sheet, UQM Technologies.

Boston Consulting Group, "Revisiting Energy Storage: There is a Business Case" (2011), www.bcg.com/ documents/ file72092.pdf.

Electric Power Research Institute, "Electricity Energy Storage Technology Options: A White Paper Primer on Applications, Costs and Benefits", Product ID: 1020676 (2010), www.epri.com.

"Inventory of Greenhouse Gas Emissions and Sinks: 1990-2007", Environmental Protection Agency, Report No: EPA 430-R-09-004 (2009).

U.S. Department of Energy, Advanced Fuels & Advanced Vehicles Data Center, "Emissions from Hybrid and Plug-In Electric Vehicles" (2011), http:/ / www.afdc.energy.gov/ afdc/ vehicles/ electric_emissions.php.

U.S. Department of Energy, Energy Information Agency, http:/ / www.eia.doe.gov.

Staff Draft Report on Renewable Power in California: Status and Issues. California Energy Commission, August 2011, Publication No. CEC-150-2011-002.

GLOSSARY

APEI	advanced power electronics interface
CIL	controller-in-the-loop
CRADA	cooperative research and development agreement
CSP	concentrating solar power
DAC	digital-to-analog converter
DER	distributed energy resources
DERTF	Distributed Energy Resources Test Facility
DSP	digital signal processor
EPO	emergency power-off
FCEV	fuel cell electric vehicle
FPGA	field programmable gate array
GIU	grid interconnection unit
HIL	hardware-in-the-loop
HMI	human machine interface
IEA	International Energy Agency
LFRT	low-frequency ride-through
MPPT	maximum power point tracking
NI	national instruments
NREL	National Renewable Energy Laboratory
PCB	printed circuit board
PID	proportional-integral-derivative
PLL	phase-locked loop
PQ	active and reactive power
PV	photovoltaics
RFP	request for proposal
RLC	resistive-inductive-capacitive
SBRIO	single board reconfigurable input/ output controller
UPF	unity power factor
UQM	UQM Technologies Inc.

USH USHybrid Corporation